

# Unstructured Adiabatic Quantum Optimization

Thesis submitted in partial fulfillment  
of the requirements for the degree of

*Master of Science in Computer Science and Engineering by Research*

by

Alapan Chaudhuri  
2019111023  
[alapan.chaudhuri@research.iiit.ac.in](mailto:alapan.chaudhuri@research.iiit.ac.in)



Centre for Quantum Science and Technology (CQST)  
International Institute of Information Technology (IIIT)  
Hyderabad - 500032, India  
February 2026

Public Domain  
Alapan Chaudhuri, 2026  
No Rights Reserved

International Institute of Information Technology  
Hyderabad, India

## CERTIFICATE

It is certified that the work contained in this thesis, titled “Unstructured Adiabatic Quantum Optimization” by Alapan Chaudhuri, has been carried out under my supervision and is not submitted elsewhere for a degree.

---

Date

Adviser: Prof. Indranil Chakrabarty

---

Date

Co-Adviser: Prof. Shantanav Chakraborty

To a world that feels like it's splitting apart.  
May we keep repairing what we can.

“Computers are more forgiving than bare-bone nature or mathematics  
— both of which are infinitely more forgiving than academia.”

# Abstract

[TODO]

# Acknowledgement

# Contents

<b>1</b>	<b>Introduction</b>	<b>1</b>
<b>2</b>	<b>Physics and Computation</b>	<b>2</b>
<b>3</b>	<b>Quantum Computation</b>	<b>3</b>
<b>4</b>	<b>Adiabatic Quantum Computation</b>	<b>4</b>
<b>5</b>	<b>Adiabatic Quantum Optimization</b>	<b>5</b>
5.1	From Cost Function to Adiabatic Path . . . . .	6
5.2	Spectral Parameters . . . . .	7
5.3	Symmetry Reduction . . . . .	8
5.4	The Avoided Crossing . . . . .	10
5.5	Gap Structure . . . . .	12
5.6	What Remains . . . . .	13
<b>6</b>	<b>Spectral Analysis</b>	<b>14</b>
6.1	Gap to the Left of the Crossing . . . . .	14
6.2	Gap to the Right of the Crossing . . . . .	16
6.3	The Complete Gap Profile . . . . .	20
<b>7</b>	<b>Optimal Schedule</b>	<b>22</b>
7.1	How Theorem Choice Sets Runtime . . . . .	22
7.2	The Adiabatic Error Bound . . . . .	23
7.3	The Adaptive Schedule . . . . .	26
7.4	Runtime of Adiabatic Quantum Optimization . . . . .	28
<b>8</b>	<b>Hardness of Optimality</b>	<b>31</b>
8.1	NP-Hardness of Estimating $A_1$ . . . . .	31
8.2	#P-Hardness of Computing $A_1$ Exactly . . . . .	34
8.3	The Intermediate Regime . . . . .	35
<b>9</b>	<b>Information Gap</b>	<b>40</b>
9.1	The Cost of Ignorance . . . . .	40
9.2	Partial Knowledge and Hedging . . . . .	42
9.3	Quantum Bypass . . . . .	43
9.4	Gap Geometry and Schedule Optimality . . . . .	46
9.5	Anatomy of the Barrier . . . . .	49
9.6	Computational Nature of $A_1$ . . . . .	51
9.7	The Complexity Landscape . . . . .	53
<b>10</b>	<b>Formalization</b>	<b>57</b>
<b>11</b>	<b>Conclusion</b>	<b>58</b>

# List of Theorems

5.2.1 Definition (Spectral parameters) . . . . .	7
5.2.2 Definition (Spectral condition) . . . . .	8
5.3.1 Lemma (Eigenvalue equation) . . . . .	9
5.4.1 Lemma (Validity of approximation) . . . . .	10
5.4.2 Lemma (Gap within the crossing window) . . . . .	11
5.5.1 Lemma (Gap to the left of the crossing) . . . . .	12
5.5.2 Lemma (Gap to the right of the crossing) . . . . .	12
6.1.1 Lemma (Gap to the left of the crossing) . . . . .	14
6.2.1 Lemma (Gap to the right of the crossing) . . . . .	17
6.3.1 Theorem (Complete gap profile) . . . . .	20
7.2.1 Lemma (Adiabatic error bound [15, 25]) . . . . .	24
7.2.2 Lemma (Projector derivative bounds [15]) . . . . .	24
7.2.3 Theorem (Constant-rate runtime) . . . . .	25
7.3.1 Theorem (Adaptive rate [15]) . . . . .	26
7.3.2 Corollary . . . . .	27
7.3.3 Lemma (Grover gap integral) . . . . .	28
7.4.1 Theorem (Runtime of AQO: Main Result 1 [15]) . . . . .	30
8.1.1 Lemma (Disambiguation [15]) . . . . .	32
8.1.2 Theorem (NP-hardness of $A_1$ estimation [15]) . . . . .	33
8.2.1 Lemma (Exact degeneracy extraction [15]) . . . . .	34
8.2.2 Lemma (Paturi [33]) . . . . .	35
8.2.3 Lemma (Approximate degeneracy extraction [15]) . . . . .	35
8.2.4 Theorem (#P-hardness of $A_1$ estimation [15]) . . . . .	35
8.3.1 Theorem (Interpolation barrier) . . . . .	36
8.3.2 Theorem (Generic extrapolation barrier) . . . . .	36
8.3.3 Theorem (Quantum algorithm for $A_1$ ) . . . . .	37
8.3.4 Theorem (Classical lower bound for $A_1$ estimation) . . . . .	38
8.3.5 Corollary (Quadratic quantum-classical separation) . . . . .	38
9.1.1 Definition (Gap class) . . . . .	40
9.1.2 Definition (RC-admissible fixed schedules) . . . . .	40
9.1.3 Lemma (Adversarial gap construction) . . . . .	41
9.1.4 Lemma (Velocity bound for uninformed schedules) . . . . .	41
9.1.5 Theorem (Separation (uniformly RC-admissible class)) . . . . .	41
9.1.6 Corollary (Constant-width uncertainty family) . . . . .	41
9.2.1 Lemma ( $A_1$ -to- $s^*$ precision propagation) . . . . .	42
9.2.2 Theorem (Interpolation) . . . . .	42
9.2.3 Theorem (Hedging) . . . . .	43
9.3.1 Definition (Binary decision probe) . . . . .	44
9.3.2 Definition (Adaptive adiabatic protocol) . . . . .	44
9.3.3 Lemma (Decision-probe cost) . . . . .	44
9.3.4 Lemma (Phase 1 cost) . . . . .	44
9.3.5 Theorem (Adaptive adiabatic optimality in the decision-probe model) . . . . .	45
9.3.6 Theorem (Measurement lower bound) . . . . .	45

9.3.7 Proposition ( $A_1$ -blindness) . . . . .	45
9.4.1 Theorem (Geometric characterization) . . . . .	46
9.4.2 Lemma (Gap integral) . . . . .	46
9.4.3 Theorem (Scaling spectrum) . . . . .	47
Remark . . . . .	47
9.4.4 Proposition (Structural $\alpha = 1$ ) . . . . .	47
9.4.5 Theorem (Measure condition for the rank-one gap profile) . . . . .	48
9.4.6 Corollary (Grover measure constant) . . . . .	48
9.4.7 Theorem (Constant comparison) . . . . .	48
Remark . . . . .	48
9.5.1 Theorem (Product ancilla invariance) . . . . .	49
Remark . . . . .	49
9.5.2 Theorem (Universality of uniform superposition) . . . . .	49
9.5.3 Corollary . . . . .	49
9.5.4 Theorem (Coupled ancilla limitation) . . . . .	49
9.5.5 Theorem (Multi-segment rigidity) . . . . .	50
9.5.6 Theorem (No-go) . . . . .	50
9.5.7 Proposition (Rank- $k$ two-level obstruction) . . . . .	50
9.5.8 Proposition (Trace no-go) . . . . .	50
Remark . . . . .	50
9.5.9 Proposition (Constant-control optimality on two-level family) . . . . .	51
9.5.10 Proposition (Normalized-control lower bound) . . . . .	51
9.6.1 Proposition ( $A_1$ hardness is counting hardness) . . . . .	52
9.6.2 Proposition (Bounded treewidth tractability) . . . . .	52
9.6.3 Proposition (Reverse bridge obstruction) . . . . .	52
9.6.4 Proposition (Unique solution does not imply easy $A_1$ ) . . . . .	53
9.6.5 Proposition (Bounded degeneracy is vacuous) . . . . .	53
9.6.6 Proposition (Hard optimization does not imply hard $A_1$ ) . . . . .	53
9.7.1 Theorem (Tight quantum query complexity at schedule precision) . . . . .	53
9.7.2 Proposition (Precision phase diagram) . . . . .	54
9.7.3 Theorem (ETH computational complexity) . . . . .	54
9.7.4 Corollary (Quantum pre-computation cost) . . . . .	54
9.7.5 Proposition (Two-level worst-case reduction) . . . . .	54
9.7.6 Theorem (Bit-runtime information law) . . . . .	55

# List of Algorithms

## List of Figures

# Chapter 1

## Introduction

## Chapter 2

# Physics and Computation

## Chapter 3

# Quantum Computation

## Chapter 4

# Adiabatic Quantum Computation

## Chapter 5

# Adiabatic Quantum Optimization

In the circuit model, unstructured optimization is already understood. Given a black-box cost function on  $N = 2^n$  bit-strings, Grover's algorithm and its generalizations find a minimizer in  $O(\sqrt{N/d_0})$  queries, where  $d_0$  is the number of optima [1, 2]. The algorithm needs no prior spectral knowledge of the cost function. Amplitude amplification gathers the required information adaptively, one oracle query at a time. No spectral parameter must be computed in advance, no schedule must be tuned to a gap profile, and no pre-computation rivals the search cost itself.

Adiabatic quantum computation is polynomially equivalent to the circuit model [3], so the same speedup exists in principle. The obstruction is different. The evolution Hamiltonian  $H(s)$  interpolates continuously between an initial Hamiltonian  $H_0$  and the problem Hamiltonian  $H_z$ , and the runtime is controlled by the spectral gap of  $H(s)$  along the entire path. The location of the avoided crossing, the sharpness of the minimum gap, and the reopening rate all matter. Matching the Grover speedup now requires controlling spectral features that depend on the full degeneracy structure of  $H_z$ .

The adiabatic version of Grover's algorithm, due to Roland and Cerf [4], finds a single marked item among  $N = 2^n$  by slowly interpolating between a uniform superposition and a problem Hamiltonian that penalizes all unmarked items. The crossing between the two lowest energy levels occurs at  $s = 1/2$ , its position independent of the Hamiltonian's spectrum. The minimum spectral gap scales as  $1/\sqrt{N}$ , and a schedule that slows near the crossing achieves the optimal  $O(\sqrt{N})$  runtime.

Consider a cost function encoded in an  $n$ -qubit Hamiltonian diagonal in the computational basis, with  $M$  distinct energy levels, arbitrary degeneracies, and a spectral gap that may vary with the number of qubits. The ground states encode solutions to a combinatorial optimization problem. Can the adiabatic approach still match the  $\Theta(\sqrt{N})$  lower bound for unstructured search [5]?

The bound applies directly to our setup. Farhi et al. proved that when  $H_0$  is a rank-one projector onto the uniform superposition, no schedule can find the ground state in time  $o(\sqrt{N/d_0})$ , regardless of the cost function. Their proof constructs  $N$  equivalent Hamiltonians related by Fourier shifts and applies a continuous-time analogue of the BBBV argument [6]. Partial answers came first. Žnidarič and Horvat [7] showed via analytical and heuristic arguments that the minimum gap scales as  $\sqrt{d_0/2^n}$  for 3-SAT instances and identified the crossing position, but did not rigorously bound the runtime. Hen [8] proved a quadratic speedup for a random Hamiltonian whose energy distribution makes the crossing position spectrum-independent, sidestepping the central difficulty.

The answer in full generality is yes, but with a sharp caveat. The spectrum of the interpolated Hamiltonian is much richer than in the Grover case. Instead of a two-level system plus a degenerate bulk, one gets  $M$  interacting energy levels in a symmetric subspace, with higher-state avoided crossings that obscure the lowest gap. The ground-state crossing position depends nontrivially on the degeneracy structure of  $H_z$ . The minimum gap still scales as  $\Theta(1/\sqrt{N})$  up to spectral factors, but it occurs at a position that must be known to exponential precision for the schedule to be correct.

For a general diagonal problem Hamiltonian,  $H(s)$  has a single avoided crossing at position  $s^* = A_1/(A_1+1)$ , where  $A_1$  is a spectral parameter determined by the degeneracy structure. The minimum spectral gap at the crossing scales as  $\Theta(\sqrt{d_0/(NA_2)})$ , and the gap grows linearly on both sides. Chapter 6 proves the gap bounds outside the crossing window, and Chapter 7 derives the optimal runtime. Chapter 8 then shows the catch: computing  $s^*$  is NP-hard.

## 5.1 From Cost Function to Adiabatic Path

We now formalize the optimization setting and the interpolation path. Consider an  $n$ -qubit Hamiltonian  $H_z$  that is diagonal in the computational basis:

$$H_z = \sum_{z \in \{0,1\}^n} E_z |z\rangle\langle z|, \quad (5.1.1)$$

where  $E_z$  is the energy assigned to bit-string  $z$ . Since  $H_z$  acts diagonally, it encodes a classical cost function. The energy  $E_z$  is the cost of configuration  $z$ , and the ground states are the optimal solutions. Without loss of generality, we rescale and shift so that all eigenvalues lie in  $[0, 1]$ .

Suppose  $H_z$  has  $M$  distinct energy levels with eigenvalues

$$0 \leq E_0 < E_1 < \dots < E_{M-1} \leq 1. \quad (5.1.2)$$

For each level  $k$ , the set of bit-strings at that energy is

$$\Omega_k = \{z \in \{0,1\}^n : H_z |z\rangle = E_k |z\rangle\}, \quad (5.1.3)$$

with degeneracy  $d_k = |\Omega_k|$ . The degeneracies partition the full Hilbert space:  $\sum_{k=0}^{M-1} d_k = 2^n = N$ . The spectral gap of the problem Hamiltonian is  $\Delta = E_1 - E_0$ , the energy difference between the ground state and the first excited level.

NP-hard optimization problems such as MaxCut and QUBO encode directly as ground states of the 2-local Ising Hamiltonian [9, 10].

$$H_\sigma = \sum_{\langle i,j \rangle} J_{ij} \sigma_z^i \sigma_z^j + \sum_{j=1}^n h_j \sigma_z^j, \quad (5.1.4)$$

where  $J_{ij}, h_j \in \{-m, -m+1, \dots, m\}$  for some constant positive integer  $m$ . Since each eigenvalue is an integer linear combination of at most  $\binom{n}{2} + n$  couplings bounded by  $m$ , the eigenvalues lie in  $\{-L, -L+1, \dots, L\}$  for  $L = O(mn^2)$ , giving at most  $2L+1 \in \text{poly}(n)$  distinct energy levels. After normalization to unit operator norm, consecutive eigenvalues differ by at least  $1/(2L) \geq 1/\text{poly}(n)$ , so the spectral gap satisfies  $\Delta \geq 1/\text{poly}(n)$ .

Unstructured search also fits this framework. It has  $M = 2$  energy levels, a single ground state ( $d_0 = 1$ ) with energy  $E_0 = 0$ , and  $N - 1$  excited states ( $d_1 = N - 1$ ) at energy  $E_1 = 1$ . The ground state is the “marked item.” Classical search requires  $\Theta(N)$  queries, while Grover’s circuit algorithm requires  $\Theta(\sqrt{N})$  [1, 6].

The adiabatic Hamiltonian interpolates between a rank-one projector and  $H_z$ . The initial Hamiltonian is

$$H_0 = -|\psi_0\rangle\langle\psi_0|, \quad |\psi_0\rangle = |+\rangle^{\otimes n} = \frac{1}{\sqrt{N}} \sum_{z \in \{0,1\}^n} |z\rangle. \quad (5.1.5)$$

Every computational basis state receives equal amplitude, so  $|\psi_0\rangle$  introduces no bias toward any particular solution.

The adiabatic Hamiltonian is the linear interpolation

$$H(s) = -(1-s)|\psi_0\rangle\langle\psi_0| + sH_z, \quad s \in [0, 1]. \quad (5.1.6)$$

At  $s = 0$ , the ground state is  $|\psi_0\rangle$  with energy  $-1$ , and all other states have energy  $0$ . At  $s = 1$ , the Hamiltonian is  $H_z$  itself, and its ground states encode the solutions. The adiabatic theorem guarantees that if the schedule  $s(t)$  traverses  $[0, 1]$  slowly enough, the evolved state remains close to the instantaneous ground state throughout, arriving at the end in a state with high overlap with the ground space of  $H_z$ .

A rank-one  $H_0$  produces exactly one avoided crossing between the two lowest energy levels. That single crossing is the structural reason the spectral analysis in Chapters 5–7 is possible at all. At  $s = 0$ , the spectrum has a non-degenerate ground state at  $-1$  and an  $(N-1)$ -fold degenerate level at  $0$ . As  $s$  increases, the degeneracy splits according to  $H_z$ . Because  $H_0 = -|\psi_0\rangle\langle\psi_0|$  has rank one, all coupling between eigenstates of  $sH_z$  factors through  $|\psi_0\rangle$ . The matrix element  $\langle k|H_0|j\rangle = -\sqrt{d_k d_j}/N$  is nonzero for all pairs, yet the perturbation has only one degree of freedom, so eigenvalues repel through a single channel. Generic AQC Hamiltonians may exhibit multiple crossings requiring qualitatively different techniques [11, 12, 13]. Here, there is one.

The standard alternative to the rank-one projector is the transverse-field driver  $H_0 = -\sum_{j=1}^n \sigma_x^j$ , which is the default in quantum annealing hardware and in much of the AQC literature [11]. It couples every pair of computational basis states that differ in a single qubit, producing a dense web of avoided crossings throughout the interpolation. For random instances of NP-complete problems, Altshuler, Krovi, and Roland [14] showed

that the resulting spectrum exhibits Anderson localization. One then gets exponentially many avoided crossings with exponentially small gaps, and no known analytical technique yields tight gap bounds in that regime. The rank-one projector avoids this entirely. Because  $|\psi_0\rangle\langle\psi_0|$  has a single non-zero eigenvalue, all coupling between eigenstates of  $sH_z$  flows through one channel, producing one crossing that can be analyzed exactly. The tractability of Chapters 5–7 is a direct consequence of this choice. Whether comparable results can be obtained for the transverse-field driver remains open. The Discussion of [15] identifies this as a central challenge.

In the unstructured case,  $H(s) = -(1-s)|\psi_0\rangle\langle\psi_0| + s(I - |w\rangle\langle w|)$ , where  $|w\rangle$  is the marked item. Up to a global energy shift of  $s$ , this is the Roland-Cerf Hamiltonian [4]. The spectrum has  $N - 2$  states at energy  $s$  (degenerate, orthogonal to both  $|\psi_0\rangle$  and  $|w\rangle$ ) and two states whose energies depend on  $s$  and undergo an avoided crossing near  $s = 1/2$ .

## 5.2 Spectral Parameters

In the Roland-Cerf setting, the crossing position ( $s^* = 1/2$ ), its width, and the minimum gap are all determined by a single quantity,  $N$ . For a general problem Hamiltonian  $H_z$  with  $M$  energy levels and arbitrary degeneracies, no single number suffices. The crossing position depends on the full eigenvalue structure of  $H_z$ , not only on  $E_0$  and  $E_1$ . We therefore need quantities that compress this  $M$ -dimensional information into parameters that directly control the algorithm, namely the crossing location, the sharpness of the minimum gap, and the reopening rate.

**Definition 5.2.1** (Spectral parameters). *For the problem Hamiltonian  $H_z$  with eigenvalues  $E_0 < E_1 < \dots < E_{M-1}$  and degeneracies  $d_k$ , define*

$$A_p = \frac{1}{N} \sum_{k=1}^{M-1} \frac{d_k}{(E_k - E_0)^p}, \quad p \in \mathbb{N}. \quad (5.2.1)$$

Each excited level contributes its degeneracy  $d_k$  weighted by the inverse  $p$ -th power of its distance to the ground energy. Larger  $p$  gives more weight to near-ground levels. Concretely,  $A_1$  uses weight  $1/(E_k - E_0)$ , while  $A_2$  uses  $1/(E_k - E_0)^2$ . A level at energy  $E_0 + \varepsilon$  therefore contributes  $O(1/\varepsilon)$  to  $A_1$  but  $O(1/\varepsilon^2)$  to  $A_2$ . The parameter  $A_1$  determines the crossing position, and  $A_2$  determines how sharp the crossing is. Normalization by  $N = 2^n$  makes  $A_p$  an average over the full Hilbert space.

When  $M = 2$ ,  $d_0 = 1$ ,  $d_1 = N - 1$ ,  $E_0 = 0$ ,  $E_1 = 1$ :

$$A_p = \frac{N-1}{N} \approx 1 \quad \text{for all } p, \quad (5.2.2)$$

since  $E_1 - E_0 = 1$ . The spectral parameters are trivial in this case, which is precisely why the Roland-Cerf analysis is simple.

For a general Ising Hamiltonian with  $\Delta \geq 1/\text{poly}(n)$  and  $M \in \text{poly}(n)$ , the bound  $A_1 \leq (1 - d_0/N)/\Delta$  gives  $A_1 = O(\text{poly}(n))$ , while  $A_2 \geq 1 - d_0/N$  ensures  $A_2 = \Theta(1)$  at minimum.

$A_1$  determines the crossing position,  $s^* = A_1/(A_1 + 1)$ . The parameter  $A_2$  enters the minimum spectral gap,  $g_{\min} = \Theta(\sqrt{d_0/(NA_2)})$ . The gap scales as  $\sqrt{d_0/N}$ , so more ground states strengthen the coupling and widen the crossing. Both parameters appear in the runtime:

$$T = O\left(\frac{\sqrt{A_2}}{A_1(A_1 + 1)\Delta^2} \sqrt{\frac{N}{d_0}}\right).$$

Since every eigenvalue gap satisfies  $E_k - E_0 \leq 1$  and the total excited degeneracy is  $\sum_{k \geq 1} d_k = N - d_0$ , we have

$$A_2 \geq \frac{1}{N} \sum_{k=1}^{M-1} d_k = 1 - \frac{d_0}{N}. \quad (5.2.3)$$

For  $d_0 \ll N$  (few solutions),  $A_2 \geq 1 - 1/N$  is close to 1. We also have  $A_1 \leq (1 - d_0/N)/\Delta$ , since  $(E_k - E_0)^{-1} \leq \Delta^{-1}$  for all  $k \geq 1$ . A lower bound follows by the same comparison: because  $E_k - E_0 \geq \Delta$ , termwise comparison gives  $A_1 \geq A_2\Delta$ . Since  $E_k - E_0 \leq 1$ , we also have  $A_1 \leq A_2$ . Hence

$$A_2\Delta \leq A_1 \leq A_2.$$

The two-level approximation near the crossing is accurate only when the crossing window  $\delta_s = O(\sqrt{d_0 A_2 / N})$  is narrow compared to  $[0, 1]$ . Since  $\delta_s/s^* = O((1/\Delta)\sqrt{d_0/(A_2 N)})$ , this requires the spectral parameters to be polynomially bounded relative to  $N$ .

**Definition 5.2.2** (Spectral condition). *The problem Hamiltonian  $H_z$  satisfies the spectral condition if there exists a constant  $c \ll 1$  such that*

$$\frac{1}{\Delta} \sqrt{\frac{d_0}{A_2 N}} < c. \quad (5.2.4)$$

The quantity on the left is, up to constants, the ratio between crossing-window width and local spectral scale. When this ratio is small, the two-level approximation near the crossing is accurate. Higher levels stay perturbative, and the window occupies only a small part of  $[0, 1]$ . The appendix of [15] shows that  $c \approx 0.02$  is sufficient. When the condition fails, the argument breaks in a specific place. The eigenvalue equation is still valid, but the quadratic truncation in  $\delta$  (Eq. (5.4.3)) requires  $|\delta| \ll s\Delta$ . That fails when many excited levels crowd near  $E_0$ . The result is a genuine multi-crossing regime, exemplified by transverse-field dynamics on random NP-complete instances [14]. The spectral condition therefore marks the boundary between the single-crossing regime of Chapters 5–7 and a regime that remains analytically intractable [12].

For any  $H_z$  with  $\Delta > (1/c)\sqrt{d_0/N}$ , the condition holds, using  $A_2 \geq 1 - d_0/N$ . For the Ising Hamiltonian with  $\Delta \geq 1/\text{poly}(n)$  and  $d_0$  not scaling with  $N$ , the left side is exponentially small in  $n$ , so the condition is easily satisfied. With  $\Delta = 1$  and  $d_0 = 1$  (unstructured search), the left side is  $1/\sqrt{N}$ , well below any constant  $c$  for  $N \geq 2$ .

### 5.3 Symmetry Reduction

The Hilbert space of  $H(s)$  has dimension  $N = 2^n$ , exponentially large in the number of qubits. Direct spectral analysis is intractable. But the problem Hamiltonian  $H_z$  has only  $M$  distinct energy levels, and the initial state  $|\psi_0\rangle$  treats all bit-strings at the same energy identically. This permutation symmetry within each degenerate subspace reduces the eigenvalue problem from  $N$  dimensions to  $M$ .

For each energy level  $k$ , define the symmetric state

$$|k\rangle = \frac{1}{\sqrt{d_k}} \sum_{z \in \Omega_k} |z\rangle, \quad 0 \leq k \leq M-1. \quad (5.3.1)$$

These  $M$  states are orthonormal:  $\langle j|k\rangle = \delta_{jk}$ . They span the  $M$ -dimensional symmetric subspace

$$\mathcal{H}_S = \text{span}\{|k\rangle : 0 \leq k \leq M-1\}. \quad (5.3.2)$$

In this basis, the problem Hamiltonian has  $M$  non-degenerate eigenvalues:

$$H_z = \sum_{k=0}^{M-1} E_k |k\rangle \langle k| \quad \text{on } \mathcal{H}_S, \quad (5.3.3)$$

and the initial state decomposes as

$$|\psi_0\rangle = \sum_{k=0}^{M-1} \sqrt{\frac{d_k}{N}} |k\rangle. \quad (5.3.4)$$

Since  $|\psi_0\rangle \in \mathcal{H}_S$  and both  $H_z$  and  $|\psi_0\rangle \langle \psi_0|$  map  $\mathcal{H}_S$  to itself, the adiabatic Hamiltonian  $H(s)$  leaves  $\mathcal{H}_S$  invariant. The time evolution starting from  $|\psi_0\rangle$  remains in  $\mathcal{H}_S$  for all  $s$ .

The complement  $\mathcal{H}_S^\perp$  has dimension  $N-M$  and is spanned by states orthogonal to  $|\psi_0\rangle$  within each degenerate subspace. For each level  $k$ , order the bit-strings in  $\Omega_k$  as  $z_k^{(1)}, \dots, z_k^{(d_k)}$  and define the Fourier basis

$$|k^{(\ell)}\rangle = \frac{1}{\sqrt{d_k}} \sum_{\ell'=1}^{d_k} \exp\left[\frac{i2\pi\ell\ell'}{d_k}\right] |z_k^{(\ell')}\rangle, \quad 1 \leq \ell \leq d_k-1. \quad (5.3.5)$$

Note that  $|k^{(0)}\rangle = |k\rangle$  is the symmetric state already in  $\mathcal{H}_S$ . The remaining  $d_k-1$  states for each level  $k$  form a basis for  $\mathcal{H}_S^\perp$ :

$$\mathcal{H}_S^\perp = \text{span}\{|k^{(\ell)}\rangle : 0 \leq k \leq M-1, 1 \leq \ell \leq d_k-1\}. \quad (5.3.6)$$

Each  $|k^{(\ell)}\rangle$  is an eigenstate of  $H(s)$  with eigenvalue  $sE_k$ :

$$H(s) |k^{(\ell)}\rangle = -(1-s) |\psi_0\rangle \underbrace{\langle \psi_0|}_{=0} k^{(\ell)} + sE_k |k^{(\ell)}\rangle = sE_k |k^{(\ell)}\rangle. \quad (5.3.7)$$

The inner product vanishes because  $|k^{(\ell)}\rangle$  is orthogonal to  $|k\rangle = |k^{(0)}\rangle$  by construction, and  $|\psi_0\rangle$  is a linear combination of the  $|k\rangle$  states. Thus, out of the full  $2^n$ -dimensional Hilbert space, only  $M$  dimensions participate in the adiabatic evolution. The remaining  $N - M$  states are spectators: they are exact eigenstates with known eigenvalues  $sE_k$  and have zero overlap with the initial state. For Ising Hamiltonians,  $M = O(\text{poly}(n))$ , so the full dynamics lives in a polynomial-dimensional subspace.

Henceforth,  $H(s)$  denotes its restriction to the symmetric subspace  $\mathcal{H}_S$ :

$$H(s) = -(1-s)|\psi_0\rangle\langle\psi_0| + s \sum_{k=0}^{M-1} E_k |k\rangle\langle k|. \quad (5.3.8)$$

This is a rank-one perturbation of the diagonal matrix  $sH_z$ , the setting of the Golub eigenvalue interlacing results [16].

**Lemma 5.3.1** (Eigenvalue equation). *Let  $H(s)$  be the adiabatic Hamiltonian restricted to  $\mathcal{H}_S$  as in Eq. (5.3.8). Then  $\lambda(s)$  is an eigenvalue of  $H(s)$  if and only if*

$$\frac{1}{1-s} = \frac{1}{N} \sum_{k=0}^{M-1} \frac{d_k}{sE_k - \lambda(s)}. \quad (5.3.9)$$

*Proof.* Let  $|\psi\rangle = \sum_{k=0}^{M-1} \alpha_k |k\rangle$  be an eigenstate of  $H(s)$  with eigenvalue  $\lambda$ , and set  $\gamma = \langle\psi_0\rangle\psi$ . Acting with  $H(s)$  on  $|\psi\rangle$ :

$$H(s)|\psi\rangle = s \sum_{k=0}^{M-1} E_k \alpha_k |k\rangle - (1-s)\gamma |\psi_0\rangle = \lambda \sum_{k=0}^{M-1} \alpha_k |k\rangle. \quad (5.3.10)$$

Comparing coefficients of  $|k\rangle$  and using  $\langle\psi_0\rangle k = \sqrt{d_k/N}$  gives

$$\alpha_k = \frac{(1-s)\gamma\sqrt{d_k/N}}{sE_k - \lambda}. \quad (5.3.11)$$

Since  $\gamma = \langle\psi_0\rangle\psi = (1/\sqrt{N}) \sum_k \alpha_k \sqrt{d_k}$ , substituting Eq. (5.3.11) yields

$$1 = \frac{1-s}{N} \sum_{k=0}^{M-1} \frac{d_k}{sE_k - \lambda}, \quad (5.3.12)$$

which is equivalent to Eq. (5.3.9). Each step is reversible: given a solution  $\lambda$  of Eq. (5.3.9), the coefficients in Eq. (5.3.11) define an eigenstate (after normalization), provided  $\gamma \neq 0$ . The case  $\gamma = 0$  corresponds to  $\lambda = sE_k$  for some  $k$ , which are the eigenvalues in  $\mathcal{H}_S^\perp$  already accounted for.  $\square$

Viewed as a function of  $\lambda$ , the right-hand side of Eq. (5.3.9) is a sum of  $M$  terms, each decreasing with a vertical asymptote at  $\lambda = sE_k$ . Between consecutive poles  $sE_{k-1}$  and  $sE_k$ , the function decreases monotonically from  $+\infty$  to  $-\infty$ , producing exactly one root per interval. Below the lowest pole  $sE_0$ , there is one additional root. The total count is  $M$  eigenvalues in  $\mathcal{H}_S$ , consistent with the dimension.

The two lowest eigenvalues are  $\lambda_0(s) < sE_0$  (ground state) and  $\lambda_1(s) \in (sE_0, sE_1)$  (first excited state). The spectral gap is  $g(s) = \lambda_1(s) - \lambda_0(s) > 0$ . However, this ordering information alone does not yield a useful quantitative upper bound on  $g(s)$  uniformly over  $s \in [0, 1]$ . Extracting tight bounds requires analyzing the eigenvalue equation in the vicinity of the crossing.

For  $M = 2$ , Eq. (5.3.9) becomes

$$\frac{1}{1-s} = \frac{1}{N} \cdot \frac{1}{-\lambda} + \frac{N-1}{N} \cdot \frac{1}{s-\lambda}, \quad (5.3.13)$$

where we set  $E_0 = 0$  and  $E_1 = 1$ . Clearing denominators produces the quadratic  $N\lambda^2 - N(2s-1)\lambda - s(1-s) = 0$ , whose two roots give the ground and first excited energies:

$$\lambda_\pm(s) = \frac{2s-1}{2} \pm \frac{1}{2} \sqrt{(2s-1)^2 + \frac{4s(1-s)}{N}}. \quad (5.3.14)$$

At  $s = 0$ , the ground energy is  $\lambda_- = -1$  and the first excited energy is  $\lambda_+ = 0$ , consistent with the spectrum of  $H(0) = -|\psi_0\rangle\langle\psi_0|$ . The gap  $g(s) = \lambda_+(s) - \lambda_-(s)$  simplifies to

$$g(s) = \sqrt{(2s-1)^2 + \frac{4s(1-s)}{N}}, \quad (5.3.15)$$

which is minimized at  $s = 1/2$  exactly, giving  $g_{\min} = 1/\sqrt{N}$ . This is the Roland-Cerf gap. The general theory of the next section reproduces this scaling as a special case.

## 5.4 The Avoided Crossing

The eigenvalue equation (Lemma 5.3.1) characterizes the spectrum of  $H(s)$  implicitly, but yields explicit formulas for  $s^*$ ,  $\delta_s$ , and  $g_{\min}$  when analyzed near the ground-state energy. Near the crossing, the ground and first excited states behave like a two-level system, with the higher levels acting as a perturbation controlled by the spectral condition.

The two lowest eigenvalues have the form  $\lambda(s) = sE_0 + \delta(s)$ , where  $\delta(s)$  is a correction to the trivial energy  $sE_0$ . Writing the eigenvalue as a perturbation of the nearest pole isolates the ground-state contribution and converts the implicit equation into an explicit power series, a standard technique for rank-one updates of diagonal eigenvalue problems [16]. Substituting into Eq. (5.3.9):

$$-\frac{d_0}{N\delta} + \frac{1}{N} \sum_{k=1}^{M-1} \frac{d_k}{s(E_k - E_0) - \delta} = \frac{1}{1-s}. \quad (5.4.1)$$

The first term has a pole at  $\delta = 0$ ; the sum has poles at  $\delta = s(E_k - E_0)$  for  $k \geq 1$ . When  $|\delta| \ll s\Delta$  (guaranteed by the spectral condition), the sum can be expanded in powers of  $\delta/(s(E_k - E_0))$ :

$$\frac{1}{N} \sum_{k=1}^{M-1} \frac{d_k}{s(E_k - E_0) - \delta} = \frac{1}{s} \left( A_1 + \frac{\delta}{s} A_2 + \frac{\delta^2}{s^2} A_3 + \dots \right). \quad (5.4.2)$$

Truncating at the  $A_2$  term and rearranging Eq. (5.4.1) gives a quadratic in  $\delta$  whose two roots are the corrections  $\delta_0^+(s)$  and  $\delta_0^-(s)$  for the first excited and ground states, respectively:

$$\delta_0^\pm(s) = \frac{s(A_1 + 1)}{2A_2(1-s)} \left[ (s - s^*) \pm \sqrt{(s^* - s)^2 + \frac{4A_2 d_0}{N(A_1 + 1)^2} (1-s)^2} \right], \quad (5.4.3)$$

Here  $\delta_0^+(s) > 0$  corresponds to the first excited state and  $\delta_0^-(s) < 0$  to the ground state: the superscript indicates the sign of the correction relative to  $sE_0$ . The crossing position is

$$s^* = \frac{A_1}{A_1 + 1}. \quad (5.4.4)$$

The problem Hamiltonian has  $M$  eigenvalues and  $M$  degeneracies, so in principle there are  $2M$  free spectral parameters. Yet the crossing location depends on one weighted average,  $A_1$ . This reduction is what makes a closed-form schedule possible despite rich spectral structure. For Ising Hamiltonians with  $\Delta \geq 1/\text{poly}(n)$ ,  $A_1$  is polynomially bounded above. In the hard-search regime  $d_0 \ll N$ , one also has  $A_1 = \Omega(1)$ , so  $s^*$  stays away from 0. As  $A_1 \rightarrow \infty$  (many levels close to the ground state),  $s^* \rightarrow 1$ ; for small  $A_1$ ,  $s^*$  moves toward 0.

The crossing position is the balance point in the eigenvalue equation,  $A_1/s^* = 1/(1-s^*)$ . The left side is the aggregate pull of the excited spectrum toward  $sE_0$ , and the right side is the projector contribution. At  $s = s^*$ , the linear coefficient in the quadratic for  $\delta$  (Eq. (5.4.3)) vanishes, so the roots  $\delta_0^\pm$  are symmetric about zero. The minimum gap is then set by the constant term  $d_0/N$ , which is why ground-state degeneracy controls the opening size.

How good is the truncation? The actual roots  $\delta_\pm(s)$  of the full equation differ from  $\delta_0^\pm(s)$  by a relative error controlled by the spectral condition. The following result, whose proof uses the intermediate value theorem on the full equation after bounding the remainder using  $A_3$  and the spectral condition, makes this precise. The technique was developed for optimal spatial search via continuous-time quantum walks [17], where the same rank-one perturbation structure arises with a graph Laplacian replacing the diagonal Hamiltonian; the adaptation to the AQO setting appears in [15].

**Lemma 5.4.1** (Validity of approximation). *Let  $H_z$  satisfy the spectral condition (Definition 5.2.2) with constant  $c \approx 0.02$ , and define*

$$\delta_s = \frac{2}{(A_1 + 1)^2} \sqrt{\frac{d_0 A_2}{N}}. \quad (5.4.5)$$

*Then for any  $s \in \mathcal{I}_{s^*} = [s^* - \delta_s, s^* + \delta_s]$ , there exists a constant  $\eta \ll 1$  such that the two lowest eigenvalues of  $H(s)$  satisfy*

$$\delta_+(s) \in ((1 - \eta) \delta_0^+(s), (1 + \eta) \delta_0^+(s)), \quad (5.4.6)$$

$$\delta_-(s) \in ((1 + \eta) \delta_0^-(s), (1 - \eta) \delta_0^-(s)), \quad (5.4.7)$$

where  $\delta_0^\pm(s)$  are given by Eq. (5.4.3).

The proof evaluates the full equation (5.4.1) at  $\delta_0^\pm(1 \pm \eta)$  and shows, using the spectral condition to bound the truncated Taylor remainder, that the full equation changes sign between these points. The intermediate value theorem then guarantees a root in the interval. The spectral condition enters through the bound  $|\delta_0^\pm(s)|/(s\Delta) \leq \kappa c < 1$ , where  $\kappa$  is a constant depending on  $c$ , ensuring the geometric series in the Taylor expansion converges. The constant  $c \approx 0.02$  is sufficient for  $\eta \leq 0.1$ . The complete calculation appears in the appendix of [15].

Since both corrections are approximated to within  $1 \pm \eta$ , the spectral gap  $g(s) = \delta_+(s) - \delta_-(s)$  is within a factor of  $1 \pm 2\eta$  of  $\delta_0^+(s) - \delta_0^-(s)$ , which evaluates to

$$g(s) = (1 \pm 2\eta) \cdot \frac{s(A_1 + 1)}{A_2(1-s)} \sqrt{(s^* - s)^2 + \frac{4A_2 d_0}{N(A_1 + 1)^2} (1-s)^2}. \quad (5.4.8)$$

At  $s = s^*$ , the first term under the square root vanishes, leaving only the second:

$$g_{\min} = g(s^*) \geq (1 - 2\eta) \cdot \frac{2A_1}{A_1 + 1} \sqrt{\frac{d_0}{NA_2}}. \quad (5.4.9)$$

The gap scales as  $\sqrt{d_0/N}$  with corrections from the spectral structure. The factor  $2A_1/(A_1 + 1)$  captures the position of the crossing: a crossing near the boundary ( $s^* \rightarrow 0$  or  $s^* \rightarrow 1$ ) reduces the gap. The factor  $\sqrt{d_0/N}$  is the Grover-like contribution: more solutions (larger  $d_0$ ) increase the gap and reduce the runtime. The factor  $1/\sqrt{A_2}$  encodes the spectral structure beyond the simplest two-level case.

An exact algebraic identity connects  $s^*$ ,  $\delta_s$ , and the leading-order minimum gap. Writing  $\hat{g} = \frac{2A_1}{A_1 + 1} \sqrt{\frac{d_0}{NA_2}}$  for the leading-order expression, direct substitution gives

$$\frac{s^*(A_1 + 1)^2}{A_2} \cdot \delta_s = \hat{g}, \quad (5.4.10)$$

and by Eq. (5.4.9),  $g_{\min} \geq (1 - 2\eta)\hat{g}$ . This relation will be used in Chapter 7 to verify the runtime calculation.

Three regions partition  $[0, 1]$  based on the crossing:

$$\mathcal{I}_{s^-} = [0, s^* - \delta_s], \quad \mathcal{I}_{s^*} = [s^* - \delta_s, s^* + \delta_s], \quad \mathcal{I}_{s^+} = (s^* + \delta_s, 1]. \quad (5.4.11)$$

**Lemma 5.4.2** (Gap within the crossing window). *Let  $H_z$  satisfy the spectral condition with constant  $c$ , and define*

$$\kappa' = \frac{(1 + 2\eta)(1 + 2c)}{(1 - 2\eta)(1 - 2c)} \sqrt{1 + (1 - 2c)^2}. \quad (5.4.12)$$

*Then for any  $s \in \mathcal{I}_{s^*}$ ,*

$$g_{\min} \leq g(s) \leq \kappa' \cdot g_{\min}. \quad (5.4.13)$$

*Proof.* The lower bound is immediate from the definition of  $g_{\min}$  as the minimum over  $\mathcal{I}_{s^*}$ . For the upper bound, start from Eq. (5.4.8) with  $|s - s^*| \leq \delta_s$ :

$$g(s) \leq \frac{s(A_1 + 1)}{A_2(1-s)} \sqrt{\delta_s^2 + \frac{4A_2 d_0}{N(A_1 + 1)^2} (1-s)^2}. \quad (5.4.14)$$

Factoring out  $(A_1 + 1)\delta_s(1-s)$  under the square root and using  $s/s^* \leq 1 + \delta_s/s^*$ :

$$g(s) \leq \frac{s^*(A_1 + 1)^2}{A_2} \delta_s \cdot \frac{s}{s^*} \cdot \sqrt{\frac{1}{(1-s)^2(A_1 + 1)^2} + 1}. \quad (5.4.15)$$

The first factor equals  $\hat{g}$  by Eq. (5.4.10). The spectral condition gives  $\delta_s/(1 - s^*) \leq 2c$  and  $\delta_s/s^* \leq 2c$ . To see the first, compute

$$\frac{\delta_s}{1 - s^*} = \frac{2}{1 + A_1} \sqrt{\frac{d_0 A_2}{N}} = \frac{2A_2 \Delta}{1 + A_1} \cdot \frac{1}{\Delta} \sqrt{\frac{d_0}{A_2 N}} \leq 2s^* c \leq 2c, \quad (5.4.16)$$

where we used  $A_2 \Delta / (1 + A_1) \leq A_1 / (1 + A_1) = s^*$ . The bound  $\delta_s/s^* \leq 2c$  follows similarly. Substituting into the upper bound:

$$g(s) \leq (1 + 2\eta)\hat{g} \cdot (1 + 2c) \sqrt{1 + (1 - 2c)^2} \leq \kappa' \cdot g_{\min}, \quad (5.4.17)$$

where the factor  $(1 + 2\eta)$  comes from the upper approximation in Eq. (5.4.8), and the last step uses  $\hat{g} \leq g_{\min}/(1 - 2\eta)$ .  $\square$

Inside  $\mathcal{I}_{s^*}$ , the gap is  $\Theta(g_{\min})$ ; outside, it is strictly larger, as the next section establishes. The avoided crossing is localized.

Specializing to unstructured search, with  $A_1 = A_2 = (N - 1)/N$ :

$$s^* = \frac{(N - 1)/N}{(N - 1)/N + 1} = \frac{N - 1}{2N - 1} \approx \frac{1}{2}, \quad (5.4.18)$$

$$g_{\min} = \frac{2(N - 1)/(2N - 1)}{\sqrt{N \cdot (N - 1)/N}} = \frac{2(N - 1)}{(2N - 1)\sqrt{N - 1}} \approx \frac{1}{\sqrt{N}}, \quad (5.4.19)$$

$$\delta_s = \frac{2N^2}{(2N - 1)^2} \sqrt{\frac{N - 1}{N^2}} \approx \frac{1}{2\sqrt{N}}. \quad (5.4.20)$$

The crossing is at  $s^* \approx 1/2$ , the minimum gap scales as  $1/\sqrt{N}$ , and the window width scales as  $1/\sqrt{N}$ . These agree asymptotically with the exact quadratic solution in Eq. (5.3.15), confirming the general theory reproduces the known scaling. The small discrepancy between  $s^* = (N - 1)/(2N - 1)$  and the exact minimum at  $s = 1/2$  is a higher-order effect of the two-level truncation, vanishing as  $O(1/N)$ .

## 5.5 Gap Structure

The adiabatic schedule requires the gap everywhere, not just near the crossing. The local adaptive schedule speeds up where the gap is large and slows where it is small, so the runtime depends on the gap profile across the full interval  $[0, 1]$ . Inside  $\mathcal{I}_{s^*}$ , the gap is  $\Theta(g_{\min})$ . Outside it, the gap grows linearly. Proving this requires different techniques for the two sides.

**Lemma 5.5.1** (Gap to the left of the crossing). *For any  $s \in \mathcal{I}_{s^-} = [0, s^* - \delta_s]$ , the spectral gap of  $H(s)$  satisfies*

$$g(s) \geq \frac{A_1(A_1 + 1)}{A_2}(s^* - s). \quad (5.5.1)$$

Why does this hold? One route uses the variational principle. An explicit ansatz  $|\phi\rangle$  gives an upper bound  $\lambda_0(s) \leq \langle \phi | H(s) | \phi \rangle$ , while the eigenvalue equation gives the lower bound  $\lambda_1(s) \geq sE_0$ . The ansatz is

$$|\phi\rangle = \frac{1}{\sqrt{A_2 N}} \sum_{k=1}^{M-1} \frac{\sqrt{d_k}}{E_k - E_0} |k\rangle, \quad (5.5.2)$$

This ansatz concentrates amplitude near the ground energy and yields a tight upper bound on  $\lambda_0(s)$ . A second route uses concavity. Because  $\lambda_0(s) = \min_{|\psi\rangle} \langle \psi | H(s) | \psi \rangle$  is the pointwise minimum of linear functions in  $s$ , it is concave. The tangent line at  $s^*$  therefore lies above  $\lambda_0(s)$ . Combining that tangent bound with  $\lambda_1(s) \geq sE_0$  reproduces Eq. (5.5.1). Chapter 6 develops both arguments in detail.

**Lemma 5.5.2** (Gap to the right of the crossing). *Assume  $A_1 \geq 1/2$  (equivalently  $s^* \geq 1/3$ ). Let  $k = 1/4$ ,  $a = 4k^2\Delta/3$ , and*

$$s_0 = s^* - \frac{k g_{\min}(1 - s^*)}{a - k g_{\min}}. \quad (5.5.3)$$

*Then for all  $s \geq s^*$ , the spectral gap of  $H(s)$  satisfies*

$$g(s) \geq \frac{\Delta}{30} \cdot \frac{s - s_0}{1 - s_0}. \quad (5.5.4)$$

This bound is linear in  $s - s_0$ , with slope proportional to  $\Delta$ . The proof strategy differs from the left side. One places a line  $\gamma(s) = sE_0 + \beta(s)$  between the two lowest eigenvalues and then uses Sherman-Morrison [18] to control the resolvent norm  $\|R_{H(s)}(\gamma)\|$ . This yields  $g(s) \geq 2/\|R_{H(s)}(\gamma)\|$ . The constants  $k = 1/4$  and  $a = 4k^2\Delta/3$  are chosen so that the auxiliary function  $f(s)$  decreases monotonically on  $[s^*, 1]$ , producing the clean slope constant  $\Delta/30$ .

At the window boundary, both bounds match  $g_{\min}$  in order. At  $s = s^* - \delta_s$ , the left bound gives

$$g(s^* - \delta_s) \geq \frac{A_1(A_1 + 1)}{A_2} \cdot \delta_s = \frac{2A_1}{A_1 + 1} \sqrt{\frac{d_0}{NA_2}} = \hat{g}, \quad (5.5.5)$$

which satisfies  $\hat{g} = \Theta(g_{\min})$  by Eq. (5.4.9). At  $s = s^*$  (right boundary start),  $\beta(s^*) \geq k g_{\min}$ , so  $g(s^*) \geq 2k g_{\min}/(1 + f(s^*)) = O(g_{\min})$  since  $f(s^*) = \Theta(1)$ . The gap profile is therefore continuous across region boundaries: it dips to  $g_{\min}$  at  $s^*$  and rises linearly on both sides.

With the gap profile in hand, runtime follows from the optimal local adaptive schedule [19, 4], where  $ds/dt \propto g(s)^2$ . Evolution therefore slows quadratically as the gap decreases. The total runtime is

$$T \propto \int_0^1 \frac{ds}{g(s)^2}, \quad (5.5.6)$$

split across the three regions. In the left and right regions, linear gap growth gives  $1/g(s)^2 \propto 1/(s - s^*)^2$ , so each outer contribution scales like  $1/\delta_s$  at the window boundary. Inside the window, the gap is approximately constant at  $g_{\min}$  and contributes  $2\delta_s/g_{\min}^2$ . This window term dominates. The bottleneck is therefore a  $\Theta(1/\sqrt{N})$ -wide interval around  $s^*$ :

$$\frac{\delta_s}{g_{\min}^2} \propto \frac{\sqrt{A_2}}{A_1(A_1 + 1)\Delta^2} \sqrt{\frac{N}{d_0}}, \quad (5.5.7)$$

yielding the optimal runtime [15]. For the Ising Hamiltonian with  $A_1, A_2 = O(\text{poly}(n))$  and  $\Delta \geq 1/\text{poly}(n)$ , this gives  $T = \tilde{O}(\sqrt{N/d_0})$ , matching the Grover lower bound up to polylogarithmic factors. Chapter 7 carries out this calculation rigorously.

## 5.6 What Remains

At this point, the structure is in place and the remaining steps are focused. Chapter 6 proves the outer-region gap bounds. Chapter 7 converts those bounds into the optimal runtime. Chapter 8 accounts for the pre-computation cost required to realize that schedule.

Given the complete gap profile, the optimal runtime is

$$T = O\left(\frac{1}{\varepsilon} \cdot \frac{\sqrt{A_2}}{A_1(A_1 + 1)\Delta^2} \cdot \sqrt{\frac{N}{d_0}}\right), \quad (5.6.1)$$

where  $\varepsilon$  is the target error. For Ising Hamiltonians, this is  $\tilde{O}(\sqrt{N/d_0})$ , matching the lower bound of Farhi, Goldstone, and Gutmann [5]. Adiabatic quantum optimization achieves the Grover speedup. Chapter 7 derives this rigorously.

The local adaptive schedule requires  $s^*$  to precision  $O(\delta_s) = O(2^{-n/2})$ , so  $A_1$  must be known at comparable precision. Approximating  $A_1$  is already hard much earlier on this scale. At additive error  $1/\text{poly}(n)$ , two oracle queries suffice to solve 3-SAT, so the task is NP-hard. Exact computation of  $A_1$ , or approximation to  $O(2^{-\text{poly}(n)})$ , is #P-hard because polynomial interpolation recovers all degeneracies  $d_k$  from  $O(\text{poly}(n))$  exact queries. Chapter 8 proves both statements and quantifies the resulting precision gap.

In the circuit model, Grover's algorithm reaches  $\tilde{O}(\sqrt{N/d_0})$  without pre-computing any spectral parameter. Oracle queries gather the needed information during execution. In the adiabatic framework, by contrast, the schedule is fixed before evolution starts, which forces NP-hard pre-computation. This asymmetry is not a proof artifact. It reflects a genuine model-level difference. The adiabatic speedup is real, but it is conditional on solving a hard preprocessing problem first [15]. Chapter 9 makes this tradeoff explicit through an uninformed-schedule separation, an interpolation theorem for partial information, and an adaptive measurement protocol that bypasses classical hardness.

In the unstructured case, the limitation vanishes:  $A_1 = (N-1)/N \approx 1$  is trivially known, so  $s^* \approx 1/2$  requires no hard computation. The complexity arises only for problem Hamiltonians with rich spectral structure, where the degeneracies  $d_k$  and energy gaps  $E_k - E_0$  are not known in advance. The Ising Hamiltonian encoding an NP-hard problem is precisely such a case.

# Chapter 6

## Spectral Analysis

Chapter 5 established the crossing window  $\mathcal{I}_{s^*}$  where the spectral gap satisfies  $g(s) = \Theta(g_{\min})$ , and it stated the outer-region bounds. The left side has a linear lower bound ([Lemma 5.5.1](#)), and so does the right side ([Lemma 5.5.2](#)). This chapter proves both lemmas.

The two proofs use different tools because the spectrum behaves differently on the two sides of the crossing. To the left of  $s^*$ , the ground energy  $\lambda_0(s)$  sits below  $sE_0$  while the first excited energy  $\lambda_1(s)$  sits above it. A variational argument then gives a sharp linear gap bound. To the right of  $s^*$ , eigenvalues of  $sH_z$  crowd the interval  $[sE_0, sE_1]$ , and that variational strategy loses traction. There we switch to a resolvent argument plus Sherman-Morrison for rank-one perturbations. The combined result is the piecewise profile needed in Chapter 7: steep on the left, flatter on the right, and nearly flat inside the window.

### 6.1 Gap to the Left of the Crossing

The eigenvalue equation ([Lemma 5.3.1](#)) places the ground state energy at  $\lambda_0(s) < sE_0$  and the first excited energy at  $\lambda_1(s) \in (sE_0, sE_1)$ . The gap  $g(s) = \lambda_1(s) - \lambda_0(s)$  is therefore positive, but this ordering alone does not provide a useful quantitative bound for the runtime integral. We need a tight lower bound that captures the linear growth of the gap as  $s$  decreases away from  $s^*$ .

The strategy is to tighten the upper bound on  $\lambda_0(s)$ . Two approaches give the same result. The first uses the variational principle. For any normalized state  $|\phi\rangle$ , the ground energy satisfies  $\lambda_0(s) \leq \langle \phi | H(s) | \phi \rangle$ , so a well-chosen ansatz gives a quantitative bound. The second uses concavity. Since  $\lambda_0(s) = \min_{|\psi\rangle} \langle \psi | H(s) | \psi \rangle$  is the pointwise minimum of affine functions in  $s$ , it is concave, and any tangent line lies above it. The variational route is more direct, so we present it first.

**Lemma 6.1.1** (Gap to the left of the crossing). *For any  $s \in \mathcal{I}_{s^-} = [0, s^* - \delta_s]$ , the spectral gap of  $H(s)$  satisfies*

$$g(s) \geq \frac{A_1(A_1 + 1)}{A_2} (s^* - s). \quad (6.1.1)$$

*Proof.* We upper-bound  $\lambda_0(s)$  via the variational principle and lower-bound  $\lambda_1(s)$  from the eigenvalue equation.

The ansatz must live in the span of  $\{|k\rangle : k \geq 1\}$ , orthogonal to the ground-state component  $|0\rangle$ , and should concentrate amplitude on levels close to  $E_0$  where the energy expectation is lowest. The natural weighting is the inverse energy gap: levels near  $E_0$  receive more amplitude. Requiring unit norm fixes the overall scale, giving

$$|\phi\rangle = \frac{1}{\sqrt{A_2 N}} \sum_{k=1}^{M-1} \frac{\sqrt{d_k}}{E_k - E_0} |k\rangle. \quad (6.1.2)$$

This weighting arises naturally in first-order perturbation theory: the correction to the ground state  $|E_0\rangle$  of  $sH_z$  due to the perturbation  $-(1-s)|\psi_0\rangle\langle\psi_0|$  has coefficients proportional to  $\langle E_k | \psi_0 \rangle / (E_k - E_0) = \sqrt{d_k} / (E_k - E_0)$ , which is exactly the form above up to normalization. Normalization is immediate:

$$\langle \phi | \phi \rangle = \frac{1}{A_2 N} \sum_{k=1}^{M-1} \frac{d_k}{(E_k - E_0)^2} = \frac{A_2}{A_2} = 1. \quad (6.1.3)$$

To compute  $\langle \phi | H(s) | \phi \rangle$ , decompose  $H(s) = -(1-s)|\psi_0\rangle\langle\psi_0| + s(H_z - E_0) + sE_0$ . Each term contributes separately.

The projector term gives

$$-(1-s) |\langle \psi_0 | \phi \rangle|^2 = -(1-s) \left( \frac{1}{\sqrt{A_2 N}} \sum_{k=1}^{M-1} \frac{d_k}{(E_k - E_0) \sqrt{N}} \right)^2 = -(1-s) \frac{A_1^2}{A_2}, \quad (6.1.4)$$

where  $\langle \psi_0 | \phi \rangle = A_1 / \sqrt{A_2}$  follows from  $\langle \psi_0 | k = \sqrt{d_k/N}$  and the definition of  $A_1$ .

The shifted diagonal term gives

$$s \langle \phi | (H_z - E_0) | \phi \rangle = \frac{s}{A_2 N} \sum_{k=1}^{M-1} \frac{d_k}{(E_k - E_0)^2} \cdot (E_k - E_0) = \frac{s}{A_2 N} \sum_{k=1}^{M-1} \frac{d_k}{E_k - E_0} = \frac{s A_1}{A_2}. \quad (6.1.5)$$

The constant term contributes  $s E_0 \langle \phi | \phi \rangle = s E_0$ . Combining:

$$\lambda_0(s) \leq \langle \phi | H(s) | \phi \rangle = s E_0 - (1-s) \frac{A_1^2}{A_2} + s \frac{A_1}{A_2} = s E_0 + \frac{A_1}{A_2} (s(1+A_1) - A_1). \quad (6.1.6)$$

Since  $s^*(1+A_1) = A_1$ , we have  $s(1+A_1) - A_1 = (1+A_1)(s-s^*) = (s-s^*)/(1-s^*)$ , so

$$\lambda_0(s) \leq s E_0 + \frac{A_1}{A_2} \cdot \frac{s-s^*}{1-s^*}. \quad (6.1.7)$$

For  $s < s^*$ , the second term is negative, confirming  $\lambda_0(s) < s E_0$ .

For the first excited state, the eigenvalue equation (Lemma 5.3.1) confines  $\lambda_1(s)$  to the interval  $(s E_0, s E_1)$ , so

$$\lambda_1(s) \geq s E_0. \quad (6.1.8)$$

The gap is therefore

$$g(s) = \lambda_1(s) - \lambda_0(s) \geq s E_0 - s E_0 - \frac{A_1}{A_2} \cdot \frac{s-s^*}{1-s^*} = \frac{A_1}{A_2} \cdot \frac{s^*-s}{1-s^*}. \quad (6.1.9)$$

Since  $1/(1-s^*) = A_1 + 1$ , we obtain  $g(s) \geq A_1(A_1+1)(s^*-s)/A_2$ .  $\square$

At the left boundary of the crossing window,  $s = s^* - \delta_s$ , the bound gives

$$g(s^* - \delta_s) \geq \frac{A_1(A_1+1)}{A_2} \cdot \delta_s = \hat{g}, \quad (6.1.10)$$

using  $A_1(A_1+1)\delta_s/A_2 = \hat{g}$  from Eq. (5.4.10). Since  $g_{\min} = (1 \pm O(\eta))\hat{g}$  from Eq. (5.4.9), the gap at the window boundary is  $\Theta(g_{\min})$ , so the three-region decomposition is tight: the left bound meets the window bound at the boundary rather than leaving a gap between them.

An alternative derivation uses concavity. Since  $\lambda_0(s) = \min_{|\psi\rangle} \langle \psi | H(s) | \psi \rangle$  is the pointwise minimum of affine functions in  $s$ , it is concave. The Hellmann-Feynman theorem [20] gives the second derivative explicitly:

$$\ddot{\lambda}_0(s) = -2 \sum_{j \geq 1} \frac{|\langle \phi_j(s) | \dot{H} | \phi_0(s) \rangle|^2}{\lambda_j(s) - \lambda_0(s)} \leq 0,$$

where  $\dot{H} = H_z + |\psi_0\rangle \langle \psi_0|$  and  $|\phi_j(s)\rangle$  are the instantaneous eigenstates. Concavity implies that every tangent line lies above the function. In particular, the tangent at  $s^*$  gives  $\lambda_0(s) \leq \lambda_0(s^*) + \lambda'_0(s^*)(s-s^*)$ , an upper bound of the same form as (6.1.7), though the variational approach gives slightly sharper constants.

When  $M = 2$  ( $d_0 = 1$ ,  $d_1 = N-1$ ,  $E_0 = 0$ ,  $E_1 = 1$ ), the ansatz reduces to  $|\phi\rangle = |1\rangle$ , and the bound becomes

$$g(s) \geq \frac{(N-1)/N \cdot (2N-1)/N}{(N-1)/N} \left( \frac{1}{2} - s \right) = \frac{2N-1}{N} \left( \frac{1}{2} - s \right) \approx 2 \left( \frac{1}{2} - s \right). \quad (6.1.11)$$

The exact gap  $g(s) = \sqrt{(2s-1)^2 + 4s(1-s)/N}$  at  $s = 1/4$  equals  $\sqrt{1/4 + 3/(4N)} \approx 1/2$ , while the bound gives  $(2N-1)/(4N) \approx 1/2$ . The bound is tight near  $s^*$  and only becomes loose as  $s$  approaches 0, where the true gap approaches 1 while the bound continues growing.

## 6.2 Gap to the Right of the Crossing

The variational principle cannot bound the gap to the right of  $s^*$ . It bounds ground energies from above, not excited energies from below, and what we need on the right is a lower bound on  $\lambda_1(s) - \lambda_0(s)$  that captures the linear reopening of the gap.

The obstacle is structural. On the left,  $\lambda_1(s)$  is bounded below by  $sE_0$  from the eigenvalue equation, which gives a clean anchor point. On the right,  $\lambda_1(s)$  still lies between  $sE_0$  and  $sE_1$ , but now many higher branches pass through the same interval and generate their own avoided crossings. We need a method that controls spectral distance without tracking individual branches one by one. The eigenvalue equation (Lemma 5.3.1) characterizes the full spectrum implicitly, but it does not directly give the linear-in- $(s - s^*)$  lower bound we need.

The resolvent provides exactly this. For a self-adjoint operator  $A$  with spectrum  $\sigma(A)$  and any  $\lambda \notin \sigma(A)$ , the resolvent

$$R_A(\lambda) = (\lambda I - A)^{-1} \quad (6.2.1)$$

is a bounded operator whose norm equals the inverse distance from  $\lambda$  to the spectrum:

$$\|R_A(\lambda)\| = \frac{1}{\text{dist}(\lambda, \sigma(A))}. \quad (6.2.2)$$

This follows from the spectral theorem. In the eigenbasis of  $A$  with eigenvalues  $\{\lambda_j\}$ , the resolvent is diagonal with entries  $1/(\lambda - \lambda_j)$ , so its operator norm is  $\max_j |1/(\lambda - \lambda_j)| = 1/\min_j |\lambda - \lambda_j|$ . If a point  $\gamma$  lies between two consecutive eigenvalues  $\lambda_0$  and  $\lambda_1$ , then  $\text{dist}(\gamma, \sigma(A)) = \min(\gamma - \lambda_0, \lambda_1 - \gamma) \leq g/2$ , since the minimum of two non-negative numbers summing to  $g$  is at most  $g/2$ . Therefore  $\|R_A(\gamma)\| = 1/\text{dist}(\gamma, \sigma(A)) \geq 2/g$ , and the useful contrapositive is

$$g(s) \geq \frac{2}{\|R_{H(s)}(\gamma)\|}. \quad (6.2.3)$$

The spectral-gap problem has become a norm problem. A lower bound on the gap is now an upper bound on a resolvent norm.

This resolvent approach to rank-one perturbations has precedent in spatial search. Childs and Goldstone [21] used it to prove  $O(\sqrt{N})$  search time on the complete graph. The algebra is the same as in our Hamiltonian  $H(s) = sH_z - (1-s)|\psi_0\rangle\langle\psi_0|$ , with a graph Laplacian replaced by a diagonal cost Hamiltonian. Chakraborty, Novo, and Roland [22, 17] then extended the method to broad graph families via Sherman-Morrison. Here we import that same mechanism, with graph parameters replaced by  $A_1$  and  $A_2$ .

Spatial search via continuous-time quantum walks solves the following problem. Given a graph  $G$  on  $N$  vertices with a subset  $S$  of marked vertices, one seeks a marked vertex by evolving the initial state  $|s\rangle = (1/\sqrt{N})\sum_v|v\rangle$  under  $H_{\text{search}} = -\gamma L - \sum_{v \in S}|v\rangle\langle v|$ , where  $L$  is the graph Laplacian and  $\gamma > 0$  is tunable [21]. When  $|S| = 1$ , the oracle term is rank one (and low rank more generally). The correspondence with our setting is straightforward:  $L$  plays the role of  $sH_z$ , the oracle projector plays the role of  $(1-s)|\psi_0\rangle\langle\psi_0|$ , the graph spectral gap corresponds to  $\Delta$ , and the effective resistance plays the role of  $A_2$ . In both settings, one places a line  $\gamma(s)$  between the two lowest eigenvalues, applies Sherman-Morrison to split the resolvent into a known diagonal part and a correction term, then bounds that correction. The method works because rank-one perturbations of diagonal operators always admit this inversion step, reducing the gap problem to one rational bound.

The constants  $k = 1/4$  and  $f(s^*) = 4$  are not accidents of this particular Hamiltonian. They are artifacts of the line-placement optimization, balancing the denominator's positivity against the numerator's growth in the function  $f(s)$ , and depend only on the rank-one structure, not on whether the underlying operator is a graph Laplacian or a problem Hamiltonian. Any future application of this technique to a new rank-one perturbation will face the same optimization, with the same constants serving as a starting point.

Since  $H(s) = sH_z - (1-s)|\psi_0\rangle\langle\psi_0|$  is a rank-one perturbation of  $sH_z$ , we can invert its resolvent explicitly. The Sherman-Morrison identity [18] states that for an invertible operator  $A$  and vectors  $|u\rangle, \langle v|$ ,

$$(A + |u\rangle\langle v|)^{-1} = A^{-1} - \frac{A^{-1}|u\rangle\langle v|A^{-1}}{1 + \langle v|A^{-1}|u\rangle}, \quad (6.2.4)$$

provided  $1 + \langle v|A^{-1}|u\rangle \neq 0$ . Applying this to the resolvent of  $H(s)$  decomposes it into the resolvent of  $sH_z$  (whose spectrum is known explicitly) and a correction from the rank-one term  $-(1-s)|\psi_0\rangle\langle\psi_0|$ . The triangle inequality then yields an upper bound on  $\|R_{H(s)}(\gamma)\|$ .

Choose a line  $\gamma(s)$  between  $\lambda_0(s)$  and  $\lambda_1(s)$  for all  $s \geq s^*$ , apply the Sherman-Morrison decomposition, bound each piece using the spectral parameters  $A_1$  and  $A_2$ , and convert the resulting bound on  $\|R_{H(s)}(\gamma)\|$  into a linear lower bound on  $g(s)$ .

The simplest choice for  $\gamma(s)$  starts at  $sE_0$  when  $s = s^*$  and ends between  $E_0$  and  $E_1$  at  $s = 1$ . Take  $\beta(s) = a(s - s^*)/(1 - s^*)$  with  $a < \Delta$ , and set  $\gamma(s) = sE_0 + \beta(s)$ . With  $a = \Delta/6$ , one can show  $f(s) \leq 1$  for all  $s \geq s^*$ , which gives  $g(s) \geq \beta(s) = (\Delta/6)(s - s^*)/(1 - s^*)$ . This is too weak near the crossing. At the window boundary  $s = s^* + \delta_s$ , it yields  $g(s^* + \delta_s) \geq (\Delta/6) \cdot \delta_s/(1 - s^*) = (\Delta A_2)/(6A_1) \cdot g_{\min}$ . Since  $\Delta A_2 \leq A_1$ , this is at most  $g_{\min}/6$ , and it can be polynomially smaller when  $\Delta A_2 \ll A_1$ . At  $s = s^*$ , the same bound gives only  $g(s^*) \geq 0$ , missing the true minimum gap.

The failure has a geometric explanation. At  $s^*$ , the ground energy  $\lambda_0(s^*)$  is not at  $s^*E_0$  but rather  $g_{\min}/2$  below it. The line  $\gamma(s)$  passes through  $s^*E_0$  at  $s = s^*$ , so it sits between the two eigenvalues but with zero margin below. The resolvent norm at a point equidistant from two eigenvalues has norm  $2/g$ , but at a point touching one eigenvalue, the norm diverges. The line must start with  $O(g_{\min})$  separation from both eigenvalues at  $s^*$ .

The fix is to shift the line's origin from  $s^*$  to a point  $s_0 < s^*$  so that  $\beta(s^*) = k g_{\min}$  for a constant  $k < 1$ . With  $\beta(s) = a(s - s_0)/(1 - s_0)$ , the constraint  $\beta(s^*) = k g_{\min}$  determines

$$s_0 = s^* - \frac{k g_{\min}(1 - s^*)}{a - k g_{\min}}. \quad (6.2.5)$$

The line now passes through  $\gamma(s^*) = s^*E_0 + k g_{\min}$ , which lies between  $\lambda_0(s^*)$  and  $\lambda_1(s^*)$  when  $k$  is chosen appropriately. The price is that  $s_0 < s^*$  introduces additional terms in the monotonicity analysis for  $f(s)$ , requiring a careful choice of  $a$ .

**Lemma 6.2.1** (Gap to the right of the crossing). *Assume  $A_1 \geq 1/2$ . Let  $k = 1/4$ ,  $a = 4k^2\Delta/3 = \Delta/12$ , and  $s_0$  as in Eq. (6.2.5). Then for all  $s \geq s^*$ , the spectral gap of  $H(s)$  satisfies*

$$g(s) \geq \frac{\Delta}{30} \cdot \frac{s - s_0}{1 - s_0}. \quad (6.2.6)$$

*Proof.* Set  $\gamma(s) = sE_0 + \beta(s)$  with  $\beta(s) = a(s - s_0)/(1 - s_0)$ . We bound  $\|R_{H(s)}(\gamma)\|$  from above using the Sherman-Morrison formula.

Since  $H(s) = sH_z - (1 - s)|\psi_0\rangle\langle\psi_0|$ , the resolvent of  $H(s)$  at  $\gamma$  satisfies, via Eq. (6.2.4) and the triangle inequality,

$$\|R_{H(s)}(\gamma)\| \leq \|R_{sH_z}(\gamma)\| + (1 - s) \frac{\|R_{sH_z}(\gamma)|\psi_0\rangle\langle\psi_0|R_{sH_z}(\gamma)\|}{1 + (1 - s)\langle\psi_0|R_{sH_z}(\gamma)|\psi_0\rangle}. \quad (6.2.7)$$

The unperturbed resolvent  $R_{sH_z}(\gamma)$  is diagonal in the  $|k\rangle$  basis with entries  $1/(\gamma - sE_k) = 1/(\beta - s(E_k - E_0))$  for  $k \geq 1$  and  $1/\beta$  for  $k = 0$ . The nearest eigenvalue of  $sH_z$  to  $\gamma$  is  $sE_0$ , at distance  $\beta$ , so  $\|R_{sH_z}(\gamma)\| = 1/\beta$ .

We bound the numerator and denominator of the second term separately. Both require that  $\beta(s) \leq s(E_k - E_0)/2$  for all  $k \geq 1$ , which ensures the Taylor expansion in powers of  $\beta/(s(E_k - E_0))$  converges rapidly. Since  $\beta(s) \leq a = \Delta/12$  and  $s(E_k - E_0) \geq s^*\Delta \geq \Delta/3$  (using  $s^* = A_1/(A_1 + 1) \geq 1/3$ , which holds when  $A_1 \geq 1/2$ ), we have  $\beta \leq \Delta/12 < \Delta/6 \leq s(E_k - E_0)/2$ . The condition  $A_1 \geq 1/2$  requires that the spectral gaps  $E_k - E_0$  are not too large relative to  $d_0$ ; when  $A_1 < 1/2$ , the crossing occurs at  $s^* < 1/3$  and the ground-state degeneracy  $d_0$  is large enough that random sampling finds a solution with constant probability, making the adiabatic approach unnecessary.

**Numerator bound.** The squared norm of  $R_{sH_z}(\gamma)|\psi_0\rangle$  expands as

$$\|R_{sH_z}(\gamma)|\psi_0\rangle\|^2 = \frac{d_0}{N\beta^2} + \frac{1}{N} \sum_{k=1}^{M-1} \frac{d_k}{(s(E_k - E_0) - \beta)^2}. \quad (6.2.8)$$

Using  $s(E_k - E_0) - \beta \geq s(E_k - E_0)/2$ , each term in the sum is at most  $4d_k/(Ns^2(E_k - E_0)^2)$ , giving

$$\|R_{sH_z}(\gamma)|\psi_0\rangle\langle\psi_0|R_{sH_z}(\gamma)\| \leq \|R_{sH_z}(\gamma)|\psi_0\rangle\|^2 \leq \frac{d_0}{N\beta^2} + \frac{4A_2}{s^2}. \quad (6.2.9)$$

**Denominator bound.** Expanding the expectation value:

$$\begin{aligned} 1 + (1 - s)\langle\psi_0|R_{sH_z}(\gamma)|\psi_0\rangle &= 1 + \frac{(1 - s)d_0}{N\beta} - \frac{1 - s}{N} \sum_{k=1}^{M-1} \frac{d_k}{s(E_k - E_0) - \beta} \\ &= 1 + \frac{(1 - s)d_0}{N\beta} - \frac{1 - s}{s} \sum_{k=1}^{M-1} \frac{d_k}{N(E_k - E_0)} \sum_{\ell=0}^{\infty} \left( \frac{\beta}{s(E_k - E_0)} \right)^\ell. \end{aligned} \quad (6.2.10)$$

Using  $\beta/(s(E_k - E_0)) \leq 1/2$  to bound the geometric series by  $1 + 2\beta/(s(E_k - E_0))$ :

$$1 + (1-s) \langle \psi_0 | R_{sH_z}(\gamma) | \psi_0 \rangle \geq 1 + \frac{(1-s)d_0}{N\beta} - (1-s) \left( \frac{A_1}{s} + \frac{2A_2\beta}{s^2} \right). \quad (6.2.11)$$

**Collecting terms.** Substituting the bounds (6.2.9) and (6.2.11) into (6.2.7) and factoring:

$$\|R_{H(s)}(\gamma)\| \leq \frac{1}{\beta} (1 + f(s)), \quad (6.2.12)$$

and

$$f(s) = \frac{\frac{d_0}{N} s^2(1-s) + 4A_2\beta^2(1-s)}{\frac{d_0}{N} s^2(1-s) + \beta s \frac{s-s^*}{1-s^*} - 2A_2\beta^2(1-s)}. \quad (6.2.13)$$

To obtain this form, multiply numerator and denominator of the second term in (6.2.7) by  $\beta$ , then multiply by  $s^2(1-s)$  to clear fractions. The key step is rewriting the denominator's constant-plus-linear terms. Using  $A_1 = s^*/(1-s^*)$ :

$$1 - \frac{(1-s)A_1}{s} + \frac{(1-s)d_0}{N\beta} = \frac{s-s^*}{s(1-s^*)} + \frac{(1-s)d_0}{N\beta}, \quad (6.2.14)$$

since  $1 - A_1(1-s)/s = (s - A_1(1-s))/s = (s - s^*(1-s)/(1-s^*))/s = (s(1-s^*) - s^*(1-s))/(s(1-s^*)) = (s - s^*)/(s(1-s^*))$ . Multiplying through by  $\beta s^2(1-s)$  and collecting the Taylor-bounded terms into the  $A_2\beta^2$  contributions gives Eq. (6.2.13). The fraction  $d_0/N$  measures the density of ground states in the computational basis.

The numerator of  $f(s)$  measures the rank-one perturbation's effect on the resolvent: the  $d_0/N$  term comes from the  $|0\rangle$  component of  $|\psi_0\rangle$  (the ground-state overlap), while the  $A_2$  term comes from the excited components. The denominator captures the spectral rigidity: the term  $\beta s(s-s^*)/(1-s^*)$  grows as  $\gamma$  moves away from the crossing, stabilizing the resolvent against the perturbation. Near  $s^*$ , the denominator is small (the gap is small), so  $f(s^*)$  is  $O(1)$ . As  $s$  increases, the denominator grows and  $f(s) \rightarrow 0$ .

From (6.2.12) and (6.2.3), the spectral gap satisfies

$$g(s) \geq \frac{2\beta(s)}{1 + f(s)} \geq \frac{2\beta(s)}{1 + \max_{s \geq s^*} f(s)}. \quad (6.2.15)$$

If  $f$  is monotonically decreasing on  $[s^*, 1]$ , then  $\max_{s \geq s^*} f(s) = f(s^*)$ , and the bound becomes  $g(s) \geq 2\beta(s)/(1 + f(s^*))$ , which is linear in  $s - s_0$ .

**Monotonicity of  $f$ .** We show  $f'(s) < 0$  for  $s \in [s^*, 1]$ . Write  $f = u/v$ , so the sign of  $f'$  is the sign of  $u'v - uv'$ . After expansion and cancellation, three contributions remain. Two are manifestly negative. The third is positive and proportional to  $(d_0/N)s_0$ , which appears because the line origin is shifted below  $s^*$ . The key step is to prove the negative terms dominate. Write  $f = u/v$  with

$$\begin{aligned} u &= \frac{d_0}{N} s^2(1-s) + 4A_2\beta^2(1-s), \\ v &= \frac{d_0}{N} s^2(1-s) + \beta s \frac{s-s^*}{1-s^*} - 2A_2\beta^2(1-s). \end{aligned} \quad (6.2.16)$$

Then  $f' = (u'v - uv')/v^2$ , so the sign of  $f'$  is determined by  $u'v - uv'$ .

Computing  $u'$  and  $v'$  using  $\beta' = a/(1-s_0)$ :

$$\begin{aligned} u' &= \frac{4aA_2\beta}{1-s_0}(2+s_0-3s) + \frac{d_0}{N}s(2-3s), \\ v' &= \frac{a(3s^2-2s(s^*+s_0)+s^*s_0)}{(1-s_0)(1-s^*)} - \frac{2aA_2\beta}{1-s_0}(2+s_0-3s) + \frac{d_0}{N}s(2-3s). \end{aligned} \quad (6.2.17)$$

Expanding  $u'v$  and  $uv'$  and taking the difference, two terms cancel exactly: the  $(d_0/N)^2 s^3(2-3s)(1-s)$  term and the  $8aA_2^2\beta^3(1-s)(2+s_0-3s)/(1-s_0)$  term. The remaining expression has three terms [15]:

$$\begin{aligned} u'v - uv' &= -\frac{4aA_2\beta^2}{(1-s_0)(1-s^*)} \left( s^2(1+s_0-s^*) - 2s s_0 + s^* s_0 \right) \\ &\quad + \frac{12aA_2 \frac{d_0}{N} \beta}{1-s_0} s(1-s)^2 s_0 \end{aligned} \quad (6.2.18)$$

$$-\frac{\frac{d_0}{N} s^2 a}{(1-s_0)(1-s^*)} \left( -s^2(s^* + s_0 - 1) + 2s s_0 s^* - s^* s_0 \right).$$

The first and third terms are negative; the second is positive (it is the only term involving  $(d_0/N)s_0$ , which arises from the shift of  $s_0$  below  $s^*$ ). We must show the first negative term dominates the positive one.

Factor out  $-4aA_2\beta/(1-s_0)$  from the sum of the first two terms:

$$-\frac{4aA_2\beta}{1-s_0} \left( \frac{\beta}{1-s^*} (s^2(1+s_0-s^*) - 2s s_0 + s^* s_0) - \frac{3d_0}{N} s_0 s(1-s)^2 \right). \quad (6.2.19)$$

The quadratic  $s^2(1+s_0-s^*) - 2s s_0 + s^* s_0$  is convex in  $s$  because  $1+s_0-s^* > 0$  (recall  $s_0 < s^*$ ). Its minimizer lies at  $s_m < s^*$ , and the quadratic is positive for all  $s \geq s^*$ ; at  $s = s^*$  it equals  $s^*(1-s^*)(s^*-s_0) > 0$ . The cubic  $s(1-s)^2$  is maximized at  $s = 1/3 \leq s^*$ . Therefore, on  $[s^*, 1]$ , the bracket in (6.2.19) is bounded below by its value at  $s = s^*$ :

$$\frac{a(s^*-s_0)^2}{1-s_0} - \frac{3d_0}{N} s_0 (1-s^*)^2. \quad (6.2.20)$$

Using  $s_0 \leq s^*$  and  $s^* - s_0 = k g_{\min}(1-s^*)/(a - k g_{\min})$ , this is positive whenever

$$a < \frac{4}{3} k^2 \frac{A_1}{A_2}. \quad (6.2.21)$$

Since  $\Delta A_2 \leq A_1$  (because  $A_2 \leq \sum_{k \geq 1} d_k / (N(E_k - E_0)^2) \leq A_1/\Delta$ ), the choice  $a = (4/3)k^2\Delta$  satisfies (6.2.21). With this choice,  $u'v - uv' < 0$  on  $[s^*, 1]$ , so  $f$  is monotonically decreasing.

**Evaluating  $f(s^*)$ .** At  $s = s^*$ ,  $\beta(s^*) = k g_{\min}$ . The term  $\beta s(s-s^*)/(1-s^*)$  vanishes, so

$$f(s^*) = \frac{\frac{d_0}{N} s^{*2} (1-s^*) + 4A_2 k^2 g_{\min}^2 (1-s^*)}{\frac{d_0}{N} s^{*2} (1-s^*) - 2A_2 k^2 g_{\min}^2 (1-s^*)}. \quad (6.2.22)$$

Replacing  $g_{\min}$  by its leading-order expression  $\hat{g} = 2s^* \sqrt{d_0/(N A_2)}$  from Eq. (5.4.9) (valid up to a  $(1 \pm O(\eta))$  factor that does not affect the final constant), we have  $A_2 k^2 \hat{g}^2 = 4k^2 s^{*2} d_0 / N$ . Substituting:

$$f(s^*) = \frac{1+16k^2}{1-8k^2}. \quad (6.2.23)$$

For  $k = 1/4$ ,  $f(s^*) = (1+1)/(1-1/2) = 4$ , so  $1+f(s^*) = 5$ .

**Final bound.** From (6.2.15):

$$g(s) \geq \frac{2\beta(s)}{1+f(s^*)} = \frac{2a}{1+f(s^*)} \cdot \frac{s-s_0}{1-s_0}. \quad (6.2.24)$$

The prefactor evaluates to

$$\frac{2a}{1+f(s^*)} = \frac{2 \cdot (4/3)k^2\Delta}{1+(1+16k^2)/(1-8k^2)} = \frac{4}{3}k^2 \cdot \frac{1-8k^2}{1+4k^2} \cdot \Delta. \quad (6.2.25)$$

The function  $P(k) = (4/3)k^2(1-8k^2)/(1+4k^2)$  is maximized at  $k_{\text{opt}} = \frac{1}{2}\sqrt{\sqrt{3/2}-1} \approx 0.237$ , where  $P(k_{\text{opt}}) = \frac{1}{3}(5-2\sqrt{6}) \approx 0.034$ . For  $k = 1/4$ :

$$P(1/4) = \frac{4}{3} \cdot \frac{1}{16} \cdot \frac{1/2}{5/4} = \frac{1}{30}. \quad (6.2.26)$$

Therefore  $g(s) \geq (\Delta/30)(s-s_0)/(1-s_0)$ .  $\square$

Specializing to  $M = 2$  and  $\Delta = 1$ , the bound gives  $g(s) \geq (1/30)(s-s_0)/(1-s_0)$ , where  $s_0 = 1/2 - O(1/\sqrt{N})$  is close to  $s^* \approx 1/2$  for large  $N$ . Near  $s = 3/4$ , the exact gap from Eq. (5.3.15) is  $g(3/4) = \sqrt{1/4 + 3/(4N)} \approx 1/2$ , while the bound gives approximately  $(1/30)(1/4)/(1/2) = 1/60$ . The bound is conservative by a factor of approximately 30 but correctly captures the linear growth. This constant is the price of a clean, uniform bound valid for all problem Hamiltonians satisfying the spectral condition.

### 6.3 The Complete Gap Profile

Combining the results of this chapter with those of Chapter 5, the spectral gap  $g(s)$  is bounded below across all of  $[0, 1]$ .

**Theorem 6.3.1** (Complete gap profile). *Let  $H_z$  satisfy the spectral condition (Definition 5.2.2) and assume  $A_1 \geq 1/2$  (equivalently  $s^* \geq 1/3$ ). The spectral gap of  $H(s) = -(1-s)|\psi_0\rangle\langle\psi_0| + sH_z$  satisfies, for all  $s \in [0, 1]$ :*

$$g(s) \geq \begin{cases} \frac{A_1(A_1+1)}{A_2}(s^*-s), & s \in \mathcal{I}_{s^-} = [0, s^* - \delta_s], \\ g_{\min}, & s \in \mathcal{I}_{s^*} = [s^* - \delta_s, s^* + \delta_s], \\ \frac{\Delta}{30} \cdot \frac{s - s_0}{1 - s_0}, & s \in \mathcal{I}_{s^+} = (s^* + \delta_s, 1], \end{cases} \quad (6.3.1)$$

where  $s_0 = s^* - k g_{\min}(1 - s^*)/(a - k g_{\min})$  with  $k = 1/4$  and  $a = \Delta/12$ .

*Proof.* The three cases follow from Lemma 5.4.2 (window, proved in Chapter 5), Lemma 6.1.1 (left), and Lemma 6.2.1 (right). The right bound holds for all  $s \geq s^*$  and therefore covers  $\mathcal{I}_{s^+}$ . The window bound  $g(s) \geq g_{\min}$  is tighter than the right bound at  $s^*$  but weaker far from the crossing.  $\square$

The bounds match across region boundaries. At the left boundary  $s = s^* - \delta_s$ :

$$\frac{A_1(A_1+1)}{A_2} \cdot \delta_s = \hat{g} = \Theta(g_{\min}), \quad (6.3.2)$$

so the left bound at the window boundary is  $\Theta(g_{\min})$ , consistent with the window bound. At  $s = s^*$ , the right bound gives  $g(s^*) \geq 2\beta(s^*)/(1 + f(s^*)) = 2k g_{\min}/5 = g_{\min}/10$ , which is below  $g_{\min}$  by a constant factor but still  $O(g_{\min})$ . The window bound provides the tighter estimate  $g(s^*) = g_{\min}$ .

The piecewise bounds are intentionally asymmetric. The left arm is steep, while the right arm is shallower. The variational method tracks the left slope closely, whereas the resolvent method trades tightness for uniform validity in a congested spectral region. Geometrically, the profile is a broad V centered at  $s^*$  with a narrow rounded minimum of width about  $2\delta_s$ . The left slope is  $A_1(A_1+1)/A_2$ , which is  $O(\text{poly}(n))$  for Ising instances. The right slope is  $\Delta/(30(1-s_0))$ , set by the problem gap  $\Delta$ . At the endpoints,  $g(0) = 1$  for  $H_0$  and  $g(1) = \Delta$  for  $H_z$ .

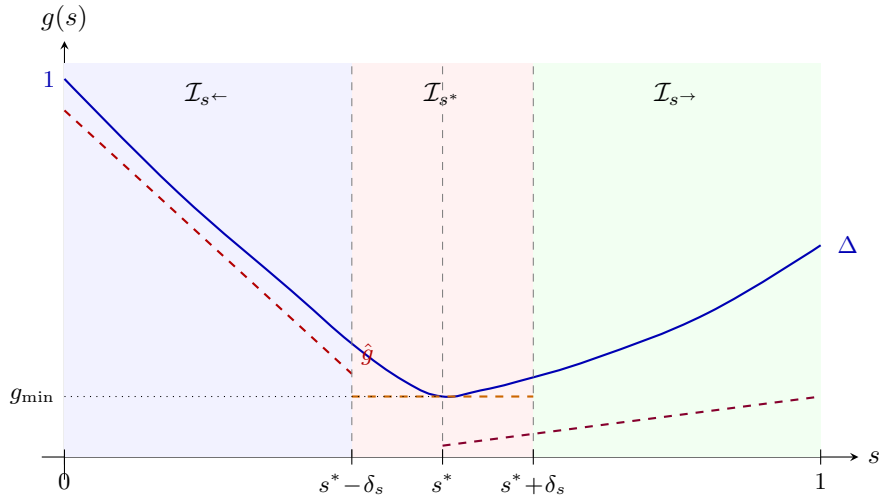


Figure 6.1: Schematic gap profile for  $H(s)$ . The solid curve shows the true spectral gap  $g(s)$ , which equals 1 at  $s = 0$ , dips to  $g_{\min}$  at  $s = s^*$ , and recovers to  $\Delta$  at  $s = 1$ . The left arm is steep (slope  $A_1(A_1+1)/A_2$ ); the right arm is shallower (slope controlled by  $\Delta$ ). Dashed lines show the piecewise lower bounds from Theorem 6.3.1: linear on the left, constant  $g_{\min}$  in the window, and linear on the right (reaching  $\Delta/30$  at  $s = 1$ ). The right bound is below  $g_{\min}$  at  $s^*$  but remains  $O(g_{\min})$ .

The gap depends on four parameters:  $A_1$ ,  $A_2$ ,  $d_0$ , and  $\Delta$ . For any problem Hamiltonian  $H_z$  satisfying the spectral condition, Theorem 6.3.1 bounds  $g(s)$  over all of  $[0, 1]$  up to constants. The minimum is  $g_{\min} =$

$\Theta(\sqrt{d_0/(NA_2)})$  at  $s^* = A_1/(A_1 + 1)$ , and it is exponentially small in  $n$  when  $d_0 = O(1)$ . The crossing location depends only on  $A_1$ . More solutions (larger  $d_0$ ) widen the gap, while richer near-ground spectral structure (larger  $A_2$ ) narrows it. At  $s = 1$ , the gap returns to  $\Delta$ , the spectral gap of  $H_z$  itself.

For unstructured search, the exact gap  $g(s) = \sqrt{(2s - 1)^2 + 4s(1 - s)/N}$  and the piecewise bound from [Theorem 6.3.1](#) can be compared directly. The left bound has slope  $(2N - 1)/N \approx 2$ , matching the asymptotic slope of the exact gap, which approaches  $2(1 - 1/N) \approx 2$  away from  $s^*$ . The window bound  $g_{\min} = 1/\sqrt{N}$  is exact. The right bound has slope approximately  $1/15$  near  $s^*$ , weaker than the true slope by a factor of 30, but sufficient for the runtime integral since the window dominates.

The window dominates the runtime integral.  $\int_0^1 g(s)^{-2} ds$  splits across the three regions. In the left and right regions,  $g(s) \sim C|s - s^*|$  for constants  $C$ , and

$$\int_{\delta_s}^{s^*} \frac{du}{(Cu)^2} = \frac{1}{C^2} \left( \frac{1}{\delta_s} - \frac{1}{s^*} \right) \leq \frac{1}{C^2 \delta_s}, \quad (6.3.3)$$

which is  $O(1/(C^2 \delta_s))$ . In the window,  $g(s) \geq g_{\min}$  gives  $\int_{s^* - \delta_s}^{s^* + \delta_s} g(s)^{-2} ds \leq 2\delta_s/g_{\min}^2$ . The window contribution  $\delta_s/g_{\min}^2 = \Theta(A_2^{3/2}/(A_1(A_1 + 1)) \cdot \sqrt{N/d_0})$  dominates the outer regions, and the full integral, including the  $\Delta$ -dependent right-arm contribution, yields the runtime  $T = O((\sqrt{A_2}/(A_1(A_1 + 1)\Delta^2))\sqrt{N/d_0})$  that Chapter 7 derives rigorously.

# Chapter 7

## Optimal Schedule

The spectral gap of  $H(s)$  is now bounded from below on all of  $[0, 1]$ . [Theorem 6.3.1](#) shows a piecewise form: the gap reaches  $g_{\min}$  at  $s^*$ , then reopens with slope  $A_1(A_1 + 1)/A_2$  on the left and  $\Delta/30$  on the right. Chapter 5 already identified the key runtime integral,  $\int_0^1 g(s)^{-2} ds$  (Eq. (5.5.6)), and showed that the crossing window dominates. The remaining issue is the adiabatic theorem itself: its error bound determines which power of  $g$  controls runtime.

With a constant-rate theorem, runtime is controlled by  $\int_0^1 g(s)^{-3} ds$ . For the profile of [Theorem 6.3.1](#), the crossing window contributes  $\delta_s/g_{\min}^3$ . In the two-level case  $M = 2$  with  $g_{\min} = 1/\sqrt{N}$ , this gives  $T = O(N)$  and no speedup over classical search. An adaptive schedule with  $K'(s)$  scaled to the gap replaces  $\int g^{-3} ds$  with  $\int g^{-p} ds$  for  $p \in (1, 2)$ . The resulting runtime

$$T = O\left(\frac{\sqrt{A_2}}{A_1(A_1 + 1)\Delta^2} \sqrt{\frac{N}{d_0} \frac{1}{\varepsilon}}\right)$$

matches Grover scaling up to explicit spectral prefactors.

### 7.1 How Theorem Choice Sets Runtime

The gap profile alone does not determine runtime. Translating spectral data into evolution time requires an adiabatic theorem, and different theorems permit different schedules. That choice changes the gap dependence and, in the running example, is exactly the difference between  $O(N)$  and  $O(\sqrt{N})$ .

The earliest rigorous bounds, due to Jansen, Ruskai, and Seiler [23], apply to a constant schedule  $K'(s) = T$  and give a transition probability of order  $O(1/T^2)$ . Their Theorem 3 states that for a state  $\psi \in P(0)$ , the probability of leaving the ground space satisfies

$$(\psi, [1 - P(s)]U_\tau(s)\psi) \leq A(s)^2, \quad (7.1.1)$$

where  $A(s) \leq (1/T)(\|H'\|/g^2)|_{\text{bdry}} + (1/T) \int_0^s (7\sqrt{m} \|H'\|^2/g^3 + \|H'\|/g^2) ds'$ , with  $m$  the multiplicity of the ground eigenvalue and the boundary term evaluated at  $s = 0$  and  $s$ . Setting  $A(s) = \varepsilon$  and solving for  $T$  gives

$$T = O\left(\frac{1}{\varepsilon} \int_0^1 \frac{\|H'\|^2}{g(s)^3} ds\right). \quad (7.1.2)$$

With  $M = 2$  and  $\|H'\| = O(1)$ , the integral  $\int_0^1 g^{-3} ds$  is dominated by the  $O(1/\sqrt{N})$ -wide window where  $g \approx 1/\sqrt{N}$ . Its contribution is  $(1/\sqrt{N}) \cdot N^{3/2} = N$ . Therefore the JRS bound gives  $T = O(N/\varepsilon)$ , which matches classical search. A constant schedule allocates the same physical time per unit of  $s$  whether the gap is  $O(1)$  or  $O(1/\sqrt{N})$ . That uniform allocation forces the  $g^{-3}$  dependence, so the narrow crossing window dominates and the quantum speedup disappears.

The resolution is to let the schedule depend on the gap. Roland and Cerf [4] introduced a *local* adiabatic condition. Instead of enforcing adiabaticity with one global timescale  $T$ , they enforce it infinitesimally on each segment  $[s, s + ds]$ . The standard criterion gives

$$\left| \frac{ds}{dt} \right| \leq \frac{\varepsilon g(s)^2}{|\langle e_1(s) | H'(s) | e_0(s) \rangle|},$$

where  $e_0, e_1$  are the ground and first excited states. Inverting this inequality yields

$$K'(s) = \frac{dt}{ds} \geq \frac{|\langle e_1 | H' | e_0 \rangle|}{\varepsilon g(s)^2}.$$

For the running example,  $|\langle e_1 | H' | e_0 \rangle| = O(1)$  because  $H'(s) = |\psi_0\rangle\langle\psi_0| + H_z$  is constant. Thus  $K'(s) \propto 1/g(s)^2$ , and the runtime becomes

$$T = \frac{C}{\varepsilon} \int_0^1 g(s)^{-2} ds. \quad (7.1.3)$$

The integral can be evaluated explicitly. Writing  $g(s)^2 = (2s - 1)^2 + 4s(1 - s)/N$  and substituting  $u = 2s - 1$ :

$$\int_0^1 g(s)^{-2} ds = \frac{1}{2} \int_{-1}^1 \frac{du}{u^2 + (1 - u^2)/N} = \frac{1}{2} \int_{-1}^1 \frac{N du}{1 + (N - 1)u^2}. \quad (7.1.4)$$

For large  $N$ , the substitution  $v = \sqrt{N-1}u$  gives  $\frac{N}{2\sqrt{N-1}} \int_{-\sqrt{N-1}}^{\sqrt{N-1}} \frac{dv}{1+v^2} = \frac{N}{2\sqrt{N-1}} \cdot 2 \arctan(\sqrt{N-1}) = O(\sqrt{N})$ , since  $\arctan(\sqrt{N-1}) \rightarrow \pi/2$ . Therefore  $T = O(\sqrt{N}/\varepsilon)$ , recovering the Grover speedup from a smooth, continuous-time evolution.

The Roland-Cerf construction requires exact knowledge of  $g(s)$  at every point. For the running example with  $M = 2$ , this is feasible because the gap has the closed form in Eq. (5.3.15). For a general  $M$ -level problem Hamiltonian, the exact gap is unknown and only the piecewise bounds of Theorem 6.3.1 are available. If one substitutes a lower bound  $g_0(s) \leq g(s)$ , the schedule slows down conservatively because  $1/g_0^2 \geq 1/g^2$ , so the runtime increases only by constants. The difficulty shifts to error control: derivative terms in the adiabatic bound become sensitive to corners in  $g_0$ . The adaptive schedule of section 7.3 addresses this through the exponent  $p \in (1, 2)$ .

Several later results sharpened this picture. Boixo, Knill, and Somma [24] introduced eigenpath traversal, which replaces continuous evolution with projections onto ground states of intermediate Hamiltonians  $H(s_0), H(s_1), \dots, H(s_L)$ . Their key ingredient is phase randomization between steps. It suppresses coherent accumulation of diabatic error, which otherwise recreates the usual  $O(1/g_{\min}^2)$  behavior. Under the condition  $\int g^{-p} ds = O(g_{\min}^{1-p})$ , this gives  $O(1/g_{\min})$  scaling. Cunningham and Roland [25] tightened constants and gave a continuous-time version that underlies section 7.2. Elgart and Hagedorn [26] followed a different route using Gevrey-smooth switching, obtaining superpolynomial suppression with runtime  $T \geq K g^{-2} |\ln g|^{6\alpha}$ . The schedule used here has a different practical advantage: it only needs a certified lower bound  $g_0(s) \leq g(s)$ , not the exact gap.

## 7.2 The Adiabatic Error Bound

The Schrödinger equation  $i d|\psi\rangle/dt = H(s(t))|\psi\rangle$  governs the evolution under the time-dependent Hamiltonian  $H(s)$ , with  $s : [0, T] \rightarrow [0, 1]$  parameterizing the interpolation. The density-matrix form  $d\rho/dt = -i[H, \rho]$  is more convenient for the error analysis and also covers mixed states. We reparameterize time by  $t = K(s)$ , where  $K : [0, 1] \rightarrow \mathbb{R}^+$  is differentiable and monotone increasing. The chain rule then gives

$$\frac{d\rho}{ds} = -iK'(s)[H(s), \rho(s)], \quad (7.2.1)$$

where  $K'(s) = dK/ds > 0$  controls the instantaneous evolution rate. The total runtime is  $T = K(1) = \int_0^1 K'(s) ds$ . A large  $K'(s)$  means slow evolution (long physical time per unit of  $s$ ), allowing the state to track the ground state through a small-gap region. A small  $K'(s)$  means fast evolution, appropriate where the gap is large and diabatic transitions are suppressed.

The error of the adiabatic evolution is the probability that the final state does not lie in the ground space of  $H(1)$ :

$$\varepsilon = 1 - \text{Tr}[P(1)\rho(1)], \quad (7.2.2)$$

where  $P(s)$  denotes the projector onto the ground eigenspace of  $H(s)$  and  $\rho(0) = P(0)$  (the system starts in the ground state of  $H(0)$ ). The projector  $P(s)$  and the ground energy  $\lambda_0(s)$  are both functions of  $s$ , varying as the Hamiltonian interpolates from  $H_0$  to  $H_z$ . The operator

$$(H(s) - \lambda_0(s))^+ = \sum_{j \geq 1} \frac{1}{\lambda_j(s) - \lambda_0(s)} |\phi_j(s)\rangle\langle\phi_j(s)| \quad (7.2.3)$$

is the pseudoinverse of  $H(s) - \lambda_0(s)$ : it acts as zero on the ground space and as  $(\lambda_j - \lambda_0)^{-1}$  on the  $j$ -th excited eigenspace. Its operator norm is  $1/g(s)$ , so a small spectral gap amplifies the pseudoinverse.

**Lemma 7.2.1** (Adiabatic error bound [15, 25]). *Let  $H(s)$  be a twice-differentiable path of Hamiltonians with a continuous ground energy  $\lambda_0(s)$  and a spectral gap  $g(s) > 0$  for all  $s \in [0, 1]$ . Let  $K : [0, 1] \rightarrow \mathbb{R}^+$  be a schedule with absolutely continuous derivative  $K'$ . Then the evolution (7.2.1) starting from  $\rho(0) = P(0)$  satisfies*

$$\varepsilon \leq \frac{1}{K'(1)} \| [P'(1), (H(1) - \lambda_0(1))^+] \| + \int_0^1 \frac{1}{K'} \| [P', (H - \lambda_0)^+]' \| ds + \int_0^1 \left| \left( \frac{1}{K'} \right)' \right| \| [P', (H - \lambda_0)^+] \| ds. \quad (7.2.4)$$

*Proof.* Since  $\rho(0) = P(0)$ , the error is  $\varepsilon = \text{Tr}[P(0)\rho(0)] - \text{Tr}[P(1)\rho(1)] = |\text{Tr}[P\rho]|_0^1$ , so it suffices to track  $\text{Tr}[P(s)\rho(s)]$ . Differentiating:

$$\frac{d}{ds} \text{Tr}[P\rho] = \text{Tr}[P'\rho] + \text{Tr}[P\rho']. \quad (7.2.5)$$

The second term vanishes. Substituting the evolution equation (7.2.1):  $\text{Tr}[P\rho'] = -iK' \text{Tr}[P[H, \rho]]$ . Since  $HP = \lambda_0 P$ , the cyclic property gives  $\text{Tr}[P[H, \rho]] = \text{Tr}[PH\rho - P\rho H] = \lambda_0 \text{Tr}[P\rho] - \text{Tr}[HP\rho] = 0$ .

For  $\text{Tr}[P'\rho]$ , write  $Q = I - P$  and use the decomposition  $P' = PP'Q + QP'P$ , which holds because  $PP'P = 0$  and  $QP'Q = 0$ .<sup>i</sup> Inserting  $Q = (H - \lambda_0)^+(H - \lambda_0)$  and using the identities  $(H - \lambda_0)\rho P = [H, \rho]P$  and  $P\rho(H - \lambda_0) = -P[H, \rho]$  (both consequences of  $HP = \lambda_0 P$ ), a cyclic rearrangement under the trace gives

$$\text{Tr}[P'\rho] = \text{Tr}[PP'(H - \lambda_0)^+[H, \rho]] - \text{Tr}[(H - \lambda_0)^+P'P[H, \rho]]. \quad (7.2.6)$$

Since  $(H - \lambda_0)^+P = P(H - \lambda_0)^+ = 0$  (the pseudoinverse annihilates the ground space),  $PP'(H - \lambda_0)^+$  reduces to  $P'(H - \lambda_0)^+$  and  $(H - \lambda_0)^+P'P$  reduces to  $(H - \lambda_0)^+P'$ , so the two terms combine into a commutator:

$$\text{Tr}[P'\rho] = \text{Tr}[[P', (H - \lambda_0)^+] [H, \rho]] = i(K')^{-1} \text{Tr}[[P', (H - \lambda_0)^+] \rho'], \quad (7.2.7)$$

where the last equality substitutes  $[H, \rho] = i(K')^{-1}\rho'$  from (7.2.1).

Integrating from 0 to 1 gives  $\text{Tr}[P\rho]|_0^1 = i \int_0^1 (K')^{-1} \text{Tr}[[P', (H - \lambda_0)^+] \rho'] ds$ . Integration by parts, with  $u = (K')^{-1}[P', (H - \lambda_0)^+]$  and  $dv = \rho' ds$ , transfers the derivative from  $\rho$  onto  $u$ :

$$\begin{aligned} \text{Tr}[P\rho]|_0^1 &= i(K'(1))^{-1} \text{Tr}[[P'(1), (H(1) - \lambda_0(1))^+] \rho(1)] \\ &\quad - i \int_0^1 \text{Tr}[\left( (K')^{-1} [P', (H - \lambda_0)^+]' + ((K')^{-1})' [P', (H - \lambda_0)^+] \right) \rho] ds. \end{aligned} \quad (7.2.8)$$

The boundary term at  $s = 0$  vanishes. Since  $\rho(0) = P(0)$ , the commutator trace expands as

$$\text{Tr}[[P', (H - \lambda_0)^+] P] = \text{Tr}[P'(H - \lambda_0)^+P] - \text{Tr}[(H - \lambda_0)^+P'P].$$

For the first summand,  $(H - \lambda_0)^+P = 0$  (the pseudoinverse annihilates the ground-space projector), so  $\text{Tr}[P'(H - \lambda_0)^+P] = 0$ . For the second, cyclicity of the trace gives  $\text{Tr}[(H - \lambda_0)^+P'P] = \text{Tr}[P(H - \lambda_0)^+P'] = 0$  by the same identity. Taking absolute values and bounding  $|\text{Tr}[A\rho]| \leq \|A\|$  for any density matrix  $\rho$  yields (7.2.4).  $\square$

The error bound depends on  $H(s)$  only through the commutator  $[P', (H - \lambda_0)^+]$  and its derivative. The following bounds express these in terms of the Hamiltonian derivatives  $H'$ ,  $H''$  and the spectral gap  $g$ , using the Riesz integral representation of the spectral projector introduced by Kato [20].

**Lemma 7.2.2** (Projector derivative bounds [15]). *Under the conditions of Lemma 7.2.1:*

$$\|P'(s)\| \leq \frac{2\|H'(s)\|}{g(s)}, \quad (7.2.9)$$

$$\|[P'(s), (H(s) - \lambda_0(s))^+]\| \leq \frac{4\|H'(s)\|}{g(s)^2}, \quad (7.2.10)$$

$$\|[P'(s), (H(s) - \lambda_0(s))^+]'\| \leq \frac{40\|H'(s)\|^2}{g(s)^3} + \frac{4\|H''(s)\|}{g(s)^2}. \quad (7.2.11)$$

*Proof of (7.2.9).* Let  $\Gamma$  be a circle in the complex plane centered at  $\lambda_0(s)$  with radius  $g(s)/2$ . The Riesz integral representation gives

$$P(s) = \frac{1}{2\pi i} \oint_{\Gamma} R_{H(s)}(z) dz, \quad (7.2.12)$$

<sup>i</sup>Differentiating  $P^2 = P$  gives  $P'P + PP' = P'$ . Left-multiplying by  $P$ :  $PP'P + PP' = PP'$ , so  $PP'P = 0$ . Then  $QP'Q = P' - PP' - P'P + PP'P = P' - P' = 0$ .

where  $R_{H(s)}(z) = (zI - H(s))^{-1}$  is the resolvent. Differentiating with respect to  $s$ :

$$P'(s) = \frac{1}{2\pi i} \oint_{\Gamma} R_{H(s)}(z) H'(s) R_{H(s)}(z) dz, \quad (7.2.13)$$

using the resolvent identity  $R'_H = R_H H' R_H$ . On the contour  $\Gamma$ , every point  $z$  lies at distance exactly  $g(s)/2$  from  $\lambda_0(s)$  and at distance at least  $g(s)/2$  from every other eigenvalue (since the nearest eigenvalue is  $\lambda_1(s)$  at distance  $g(s)$  from  $\lambda_0(s)$ ). Therefore  $\|R_{H(s)}(z)\| = 1/\text{dist}(z, \sigma(H(s))) \leq 2/g(s)$  on  $\Gamma$ . Bounding the integral:

$$\|P'(s)\| \leq \frac{1}{2\pi} \oint_{\Gamma} \|R_H(z)\| \cdot \|H'(s)\| \cdot \|R_H(z)\| |dz| \leq \frac{1}{2\pi} \left(\frac{2}{g}\right)^2 \|H'\| \cdot \pi g = \frac{2\|H'\|}{g}. \quad (7.2.14)$$

□

Bound (7.2.10) follows from (7.2.9):  $\|[A, B]\| \leq 2\|A\| \cdot \|B\|$  gives  $\|[P', (H - \lambda_0)^+]\| \leq 2 \cdot 2\|H'\|/g \cdot 1/g = 4\|H'\|/g^2$ .

Bound (7.2.11) requires two intermediate results. Write  $\tilde{H} = H - \lambda_0$  for the shifted Hamiltonian. Its pseudoinverse satisfies

$$(\tilde{H}^+)' = -\tilde{H}^+ \tilde{H}' \tilde{H}^+ + P' \tilde{H}^+ + \tilde{H}^+ P', \quad (7.2.15)$$

where  $\tilde{H}' = H' - \lambda'_0$ . To see this, split the difference quotient  $(\tilde{H}^+(s+h) - \tilde{H}^+(s))/h$  using  $Q = \tilde{H}^+ \tilde{H}$  and  $P = I - Q$ . The  $Q$ -part gives  $\lim_{h \rightarrow 0} \tilde{H}^+(s)(\tilde{H}(s) - \tilde{H}(s+h))\tilde{H}^+(s+h)/h = -\tilde{H}^+ \tilde{H}' \tilde{H}^+$ , while the  $P$ -part, after adding and subtracting  $P(s+h)\tilde{H}^+(s+h)$  and  $\tilde{H}^+(s)P(s)$ , yields  $P' \tilde{H}^+ + \tilde{H}^+ P'$ . Bounding the norm and using  $|\lambda'_0| = |\langle \phi_0 | H' | \phi_0 \rangle| \leq \|H'\|$  (Hellmann-Feynman):

$$\|(\tilde{H}^+)' \| \leq \frac{\|H'\| + |\lambda'_0|}{g^2} + \frac{4\|H'\|}{g^2} \leq \frac{6\|H'\|}{g^2}. \quad (7.2.16)$$

The second intermediate result bounds  $P''$ . Differentiating  $P' = (2\pi i)^{-1} \oint_{\Gamma} R_H H' R_H dz$  gives

$$P'' = \frac{1}{2\pi i} \oint_{\Gamma} (2R_H H' R_H H' R_H + R_H H'' R_H) dz, \quad (7.2.17)$$

where the two  $R_H H' R_H H' R_H$  terms arise from differentiating each resolvent factor. Bounding by  $\|R_H(z)\| \leq 2/g$  on  $\Gamma$  and integrating over the contour of length  $\pi g$ :

$$\|P''\| \leq \frac{1}{2\pi} \left(\frac{2}{g}\right)^3 2\|H'\|^2 \cdot \pi g + \frac{1}{2\pi} \left(\frac{2}{g}\right)^2 \|H''\| \cdot \pi g = \frac{8\|H'\|^2}{g^2} + \frac{2\|H''\|}{g}. \quad (7.2.18)$$

Now expand  $[P', (H - \lambda_0)^+]' = [P'', (H - \lambda_0)^+] + [P', ((H - \lambda_0)^+)']$  and bound each commutator:

$$\|[P'', (H - \lambda_0)^+]\| \leq \frac{2\|P''\|}{g} \leq \frac{16\|H'\|^2}{g^3} + \frac{4\|H''\|}{g^2}, \quad (7.2.19)$$

and, using (7.2.9) and (7.2.16):

$$\|[P', ((H - \lambda_0)^+)']\| \leq 2\|P'\| \cdot \|(\tilde{H}^+)' \| \leq 2 \cdot \frac{2\|H'\|}{g} \cdot \frac{6\|H'\|}{g^2} = \frac{24\|H'\|^2}{g^3}. \quad (7.2.20)$$

Summing gives  $40\|H'\|^2/g^3 + 4\|H''\|/g^2$ . A block-matrix decomposition of the commutator with respect to  $P$  and  $Q = I - P$ , tracking cross terms exactly rather than using submultiplicativity, replaces the coefficient 40 by  $\approx 4.77$  [15]; the asymptotic scaling is unchanged.

The simplest schedule is constant:  $K'(s) = T$ , evolving at a uniform rate regardless of the gap. Substituting the derivative bounds into the error bound (7.2.4) with  $(1/K')' = 0$  gives the constant-rate result.

**Theorem 7.2.3** (Constant-rate runtime). *Under the conditions of Lemma 7.2.1, a constant schedule  $K'(s) = T$  achieves error at most  $\varepsilon$  provided*

$$T \geq \frac{1}{\varepsilon} \left( \frac{4\|H'(1)\|}{g(1)^2} + \int_0^1 \frac{40\|H'(s)\|^2}{g(s)^3} ds + \int_0^1 \frac{4\|H''(s)\|}{g(s)^2} ds \right). \quad (7.2.21)$$

*Proof.* With constant  $K'$ , the third term in (7.2.4) vanishes. Substituting bounds (7.2.10) and (7.2.11) into the remaining two terms:

$$\varepsilon \leq \frac{1}{T} \left( \frac{4\|H'(1)\|}{g(1)^2} + \int_0^1 \frac{40\|H'(s)\|^2}{g(s)^3} ds + \int_0^1 \frac{4\|H''(s)\|}{g(s)^2} ds \right). \quad (7.2.22)$$

Setting the right side equal to  $\varepsilon$  and solving for  $T$  gives (7.2.21).  $\square$

Since  $H'' = 0$  for the linear interpolation  $H(s) = -(1-s)|\psi_0\rangle\langle\psi_0| + sH_z$ , and  $H'(s) = |\psi_0\rangle\langle\psi_0| + H_z$  is constant with  $\|H'\| = O(1)$ , the dominant term in (7.2.21) is  $\int_0^1 g(s)^{-3} ds$ . From the gap profile of Theorem 6.3.1, the crossing window contributes

$$\int_{s^* - \delta_s}^{s^*} g(s)^{-3} ds \leq \frac{\delta_s}{g_{\min}^3} = \frac{A_2}{A_1(A_1 + 1)} \cdot g_{\min}^{-2}, \quad (7.2.23)$$

using  $\delta_s = A_2 g_{\min} / (A_1(A_1 + 1))$  from Eq. (5.4.10). This gives  $T_{\text{constant}} = O(\delta_s / (\varepsilon g_{\min}^3))$ .

Specializing to  $M = 2$  with  $g_{\min} = 1/\sqrt{N}$ , the exact gap  $g(s) = \sqrt{(2s-1)^2 + 4s(1-s)/N}$  from Eq. (5.3.15) gives  $\int_0^1 g(s)^{-3} ds = O(N)$ . The dominant contribution comes from the  $O(1/\sqrt{N})$  window where  $g \approx 1/\sqrt{N}$ . Hence  $T_{\text{constant}} = O(N/\varepsilon)$ , matching classical search. A constant-rate schedule therefore gives no quantum speedup: it wastes time where the gap is large and still moves too quickly near  $s^*$ .

### 7.3 The Adaptive Schedule

The constant schedule fails because it treats every value of  $s$  the same. The error bound (7.2.4) suggests the opposite strategy: choose large  $K'(s)$  where the gap is small and small  $K'(s)$  where the gap is large. Since  $K'(s) = dt/ds$ , this means spending physical time where diabatic transitions are dangerous. The natural ansatz is  $K'(s) \propto 1/g(s)^p$  for some  $p \geq 1$ . Then runtime scales as  $T \propto \int_0^1 g(s)^{-p} ds$ , while the error terms involve integrals of the form  $\int g^{q-3} ds$ .

The exponent  $p$  controls the runtime-error tradeoff. The family  $K'(s) \propto 1/g_0(s)^p$  extends Roland-Cerf ( $p = 2$ ) to a continuum of schedules. At  $p = 1$ ,  $\int g_0^{-1} ds$  is mild but the companion error integral  $\int g_0^{-2} ds$  diverges for piecewise linear profiles. At  $p = 2$ , the scaling is favorable, but the schedule-variation term requires exact gap information. The useful regime is therefore  $p \in (1, 2)$ . There,  $\int g_0^{-p} ds = O(g_{\min}^{1-p})$  and  $\int g_0^{p-3} ds = O(g_{\min}^{p-2})$ , whose product is always  $O(g_{\min}^{-1})$ . This is exactly the range where a certified lower bound  $g_0 \leq g$  suffices.

The adaptive rate theorem, extending the eigenpath traversal framework of [25] to the continuous-time setting, formalizes this trade-off.

**Theorem 7.3.1** (Adaptive rate [15]). *Let  $H(s)$  satisfy the conditions of Lemma 7.2.1, and let  $g_0 : [0, 1] \rightarrow \mathbb{R}^+$  be an absolutely continuous function satisfying  $g_0(s) \leq g(s)$  for all  $s$ . Suppose there exist  $1 < p < 2$  (the endpoints are excluded: at  $p = 1$  the  $B_1$  integral diverges logarithmically, and at  $p = 2$  the schedule variation term requires the exact gap) and constants  $B_1, B_2 \geq 1$  such that*

$$\int_0^1 \frac{ds}{g_0(s)^p} \leq B_1 g_{\min}^{1-p} \quad \text{and} \quad \int_0^1 \frac{ds}{g_0(s)^{3-p}} \leq B_2 g_{\min}^{p-2}. \quad (7.3.1)$$

Assume additionally that  $g_0(1) \geq g_{\min}$ , that there exists  $b \in (0, 1]$  with  $g_0(s) \geq b g_{\min}$  for all  $s \in [0, 1]$ , and that  $\sup_{s \in [0, 1]} |g'_0(s)| < \infty$ . Define

$$c = \sup_{s \in [0, 1]} (4\|H'(s)\| + 40\|H'(s)\|^2 B_2 + 4\|H''(s)\| + 6p |g'_0(s)| \|H'(s)\| B_2). \quad (7.3.2)$$

The last term uses  $|g'_0(s)|$  rather than  $|g'(s)|$ : since the schedule is defined in terms of  $g_0$ , the derivative  $(K'^{-1})' \propto (g_0^p)'$  involves  $g'_0$ . Then the schedule

$$K'(s) = \frac{1}{\varepsilon} \cdot \frac{c}{g_0(s)^p \cdot g_{\min}^{2-p}} \quad (7.3.3)$$

achieves error at most  $\varepsilon$ , with total runtime

$$T = \int_0^1 K'(s) ds \leq \frac{c B_1}{\varepsilon g_{\min}}. \quad (7.3.4)$$

*Proof.* Let  $\varepsilon_0$  denote the actual error. Substituting (7.3.3) into the error bound (7.2.4):  $(K')^{-1} = \varepsilon g_0^p g_{\min}^{2-p}/c$ , and  $|((K')^{-1})'| = (\varepsilon g_{\min}^{2-p}/c) \cdot p g_0^{p-1} |g'_0|$ . The three terms become

$$\begin{aligned} \varepsilon_0 \leq & \frac{\varepsilon}{c} g_{\min}^{2-p} \left( g_0(1)^p \| [P'(1), (H(1) - \lambda_0(1))^+] \| \right. \\ & \left. + \int_0^1 g_0^p \| [P', (H - \lambda_0)^+]' \| ds + \int_0^1 p g_0^{p-1} |g'_0| \| [P', (H - \lambda_0)^+] \| ds \right). \end{aligned} \quad (7.3.5)$$

**Boundary term.** Using bound (7.2.10) with  $g_0 \leq g$ :

$$g_{\min}^{2-p} g_0(1)^p \cdot \frac{4\|H'(1)\|}{g(1)^2} \leq 4\|H'(1)\| g_{\min}^{2-p} g_0(1)^{p-2} \leq 4\|H'\|, \quad (7.3.6)$$

since  $g_0(1) \geq g_{\min}$  and  $p-2 < 0$  imply  $g_0(1)^{p-2} \leq g_{\min}^{p-2}$ .

**Commutator derivative integral.** Using bound (7.2.11) and splitting:

$$g_{\min}^{2-p} \int_0^1 g_0^p \cdot \frac{40\|H'\|^2}{g^3} ds \leq 40\|H'\|^2 g_{\min}^{2-p} \int_0^1 \frac{ds}{g_0^{3-p}} \leq 40\|H'\|^2 B_2, \quad (7.3.7)$$

where  $g_0^p/g^3 \leq g_0^p/g_0^3 = 1/g_0^{3-p}$  since  $g_0 \leq g$ , and the  $B_2$  condition (7.3.1) absorbs  $g_{\min}^{2-p} \cdot g_{\min}^{p-2} = 1$ . Similarly, the  $H''$  sub-term contributes

$$g_{\min}^{2-p} \int_0^1 g_0^p \cdot \frac{4\|H''\|}{g^2} ds \leq 4\|H''\| g_{\min}^{2-p} \int_0^1 \frac{ds}{g_0^{2-p}} \leq 4\|H''\|, \quad (7.3.8)$$

since  $g_0 \geq b g_{\min}$  and  $p-2 < 0$  imply  $g_0^{p-2} \leq b^{p-2} g_{\min}^{p-2}$ , giving  $\int g_0^{p-2} ds = O(g_{\min}^{p-2})$  with the constant  $b^{p-2}$  absorbed into the  $O$ -notation.

**Schedule variation integral.** Using bound (7.2.10):

$$\begin{aligned} g_{\min}^{2-p} \int_0^1 p g_0^{p-1} |g'_0| \cdot \frac{4\|H'\|}{g^2} ds & \leq 4p \|H'\| g_{\min}^{2-p} \int_0^1 \frac{g_0^{p-1} |g'_0|}{g_0^2} ds \\ & = 4p \|H'\| g_{\min}^{2-p} \int_0^1 g_0^{p-3} |g'_0| ds. \end{aligned} \quad (7.3.9)$$

Using  $\sup |g'_0| < \infty$ , we have  $\int g_0^{p-3} |g'_0| ds \leq \sup |g'_0| \cdot \int g_0^{p-3} ds \leq \sup |g'_0| \cdot B_2 g_{\min}^{p-2}$ . The resulting bound is  $4p \sup |g'_0| \|H'\| B_2$ . The constant  $c$  in (7.3.2) uses the factor  $6p$  rather than  $4p$ ; this is a valid overestimate that simplifies the expression without affecting the asymptotic result.

**Collecting.** Summing all contributions:

$$\varepsilon_0 \leq \frac{\varepsilon}{c} (4\|H'\| + 40\|H'\|^2 B_2 + 4\|H''\| + 6p \sup |g'_0| \|H'\| B_2) \leq \frac{\varepsilon}{c} \cdot c = \varepsilon. \quad (7.3.10)$$

**Runtime.** The total evolution time is

$$T = \int_0^1 K' ds = \frac{c}{\varepsilon} g_{\min}^{p-2} \int_0^1 \frac{ds}{g_0^p} \leq \frac{c}{\varepsilon} g_{\min}^{p-2} \cdot B_1 g_{\min}^{1-p} = \frac{c B_1}{\varepsilon g_{\min}}. \quad (7.3.11)$$

Three terms compose the error: a boundary term that depends on  $g_0(1)$  and is  $O(1)$ ; an integral that pairs  $g_0^p$  from the schedule with  $g^{-3}$  from the derivative bounds, producing  $\int g_0^{p-3} ds$ ; and a schedule variation term from the non-constant  $K'$ . The parameter  $p$  balances the two integrals:  $B_1$  bounds  $\int g_0^{-p} ds$  (the runtime cost), while  $B_2$  bounds  $\int g_0^{p-3} ds$  (the error cost). Their product with  $g_{\min}^{-1}$  gives the final runtime.

**Corollary 7.3.2.** If  $\int_0^1 g(s)^{-p} ds = O(g_{\min}^{1-p})$  for all  $p > 1$ , and  $\|H'\|$ ,  $\|H''\|$ ,  $|\lambda'_0|$ ,  $|g'|$  are all  $O(1)$ , then  $T = O(1/(\varepsilon g_{\min}))$ .

The runtime scales inversely with the minimum gap, which is optimal for quantum search [5]. The running example satisfies these conditions.

The integral  $\int_0^1 g(s)^{-p} ds$  is dominated by the  $O(1/\sqrt{N})$ -wide window where  $g \approx 1/\sqrt{N}$ : the window's contribution is  $(1/\sqrt{N}) \cdot N^{p/2} = N^{(p-1)/2}$ , while outside the window  $g = \Omega(|s-1/2|)$  and the integral converges. For any  $p > 1$ , this gives  $O(g_{\min}^{1-p})$ .

**Lemma 7.3.3** (Grover gap integral). *For the exact gap  $g(s) = \sqrt{(2s-1)^2 + 4s(1-s)/N}$  of the running example ( $M = 2$ ,  $d_0 = 1$ ,  $d_1 = N - 1$ ),*

$$\int_0^1 g(s)^{-p} ds = O\left(N^{(p-1)/2}\right) = O\left(g_{\min}^{1-p}\right) \quad \text{for all } p > 1. \quad (7.3.12)$$

*Proof.* The gap is symmetric about  $s = 1/2$  and achieves its minimum  $g_{\min} = 1/\sqrt{N}$  there. Split the integral at  $1/2 - 1/\sqrt{N}$ . In the window  $[1/2 - 1/\sqrt{N}, 1/2]$ , bound  $g \geq g_{\min}$ :

$$\int_{1/2-1/\sqrt{N}}^{1/2} g^{-p} ds \leq \frac{1}{\sqrt{N}} \cdot N^{p/2} = N^{(p-1)/2}. \quad (7.3.13)$$

Outside the window,  $g(s) \geq c|s - 1/2|$  for a constant  $c > 0$  (the gap grows linearly away from the minimum). The change of variable  $u = g(s)$ , with  $|ds/du| = O(1)$  since  $|g'(s)| \leq 2$ , gives

$$\int_0^{1/2-1/\sqrt{N}} g^{-p} ds \leq C \int_{1/\sqrt{N}}^{O(1)} u^{-p} du = O\left(N^{(p-1)/2}\right). \quad (7.3.14)$$

Combining and using the symmetry about  $1/2$  gives the result.  $\square$

The other conditions of [Corollary 7.3.2](#) are immediate:  $\|H'\| = \|\psi_0\rangle\langle\psi_0| + H_z\| \leq 2$ ,  $H'' = 0$ ,  $|\lambda'_0| \leq \|H'\| \leq 2$  by the Hellmann-Feynman theorem, and  $|g'(s)| \leq 2$  (from  $|g'| = |4(1 - 1/N)(1/2 - s)/g| \leq 2$ , since the numerator is at most  $2g$ ). Therefore  $T = O(\sqrt{N}/\varepsilon)$  for the running example with an adaptive schedule, compared to  $T = O(N/\varepsilon)$  with a constant schedule. The adaptive schedule recovers the full Grover speedup.

The schedule  $K'(s) \propto 1/g(s)^p$  concentrates the evolution time near the crossing: at  $s = 1/2$ , where  $g \approx 1/\sqrt{N}$ , the schedule rate is  $K' \propto N^{p/2}$ , while far from  $1/2$ , where  $g = O(1)$ , it is  $K' = O(1)$ . The algorithm spends  $O(\sqrt{N})$  physical time traversing the window and  $O(1)$  time traversing the rest of  $[0, 1]$ .

## 7.4 Runtime of Adiabatic Quantum Optimization

Applying [Theorem 7.3.1](#) to  $H(s) = -(1-s)|\psi_0\rangle\langle\psi_0| + sH_z$  with the gap profile of [Theorem 6.3.1](#) requires three concrete steps. We construct a continuous lower bound  $g_0(s)$  from the piecewise bounds, compute  $B_1$  and  $B_2$ , and then evaluate the constant  $c$ .

The bounds from [Theorem 6.3.1](#) are valid on their regions but do not meet continuously at  $s^* - \delta_s$  and  $s^*$ . The left bound is too high at  $s^* - \delta_s$ , and the right bound is too low at  $s^*$ . Since [Theorem 7.3.1](#) requires  $g_0$  to be absolutely continuous on  $[0, 1]$ , we shrink the left and window pieces by a constant factor  $b$  so the three branches join continuously.

Define

$$g_0(s) = \begin{cases} b \frac{A_1(A_1+1)}{A_2} (s^* - s), & s \in [0, s^* - \delta_s], \quad (\text{i.e., } b \frac{A_1}{A_2} \cdot \frac{s^*-s}{1-s^*}) \\ b g_{\min}, & s \in [s^* - \delta_s, s^*), \\ \frac{\Delta}{30} \cdot \frac{s - s_0}{1 - s_0}, & s \in [s^*, 1], \end{cases} \quad (7.4.1)$$

where  $s_0$  is given by Eq. (6.2.5) and the shrinking factor is

$$b = k \cdot \frac{2}{1 + f(s^*)} = \frac{1}{4} \cdot \frac{2}{1 + 4} = \frac{1}{10}, \quad (7.4.2)$$

using  $k = 1/4$  and  $f(s^*) = 4$  from Eq. (6.2.23).

Each piece of  $g_0$  lies below its corresponding bound from [Theorem 6.3.1](#). The left and window pieces are scaled by  $b = 1/10$ , while the right piece is unchanged. It remains to check continuity at both junctions. At  $s = s^* - \delta_s$ , the left branch gives  $b \cdot A_1(A_1+1)\delta_s/A_2$ . Using  $\delta_s = A_2 g_{\min}/(A_1(A_1+1))$  from Eq. (5.4.10), this equals  $b g_{\min} = g_{\min}/10$ , exactly the window value. At  $s = s^*$ , the window value is again  $b g_{\min} = g_{\min}/10$ , while the right branch gives  $(\Delta/30)(s^* - s_0)/(1 - s_0)$ . Using  $s^* - s_0 = k g_{\min}(1 - s^*)/(a - k g_{\min})$  and  $1 - s_0 = (1 - s^*)a/(a - k g_{\min})$  from Eq. (6.2.5),

$$\frac{\Delta}{30} \cdot \frac{s^* - s_0}{1 - s_0} = \frac{\Delta}{30} \cdot \frac{k g_{\min}}{a} = \frac{\Delta}{30} \cdot \frac{g_{\min}/4}{\Delta/12} = \frac{g_{\min}}{10}, \quad (7.4.3)$$

which again matches the window value. The constants  $b$ ,  $k$ , and  $a$  are therefore coupled exactly to enforce continuity. In particular,  $b = 1/10$  absorbs both the  $k = 1/4$  factor from the right-side resolvent bound and the value  $f(s^*) = 4$  from the Chapter 6 monotonicity analysis.

The integral  $\int_0^1 g_0^{-p} ds$  splits across the three regions. In the left region,  $g_0(s) = b A_1(A_1 + 1)(s^* - s)/A_2$ , so

$$\begin{aligned} \int_0^{s^* - \delta_s} g_0^{-p} ds &= \left( \frac{A_2}{b A_1(A_1 + 1)} \right)^p \int_{\delta_s}^{s^*} \frac{du}{u^p} = \frac{1}{b^p} \left( \frac{A_2}{A_1(A_1 + 1)} \right)^p \cdot \frac{1}{(p-1) \delta_s^{p-1}} \\ &= \frac{1}{b^p(p-1)} \cdot \frac{A_2}{A_1(A_1 + 1)} \cdot g_{\min}^{1-p}, \end{aligned} \quad (7.4.4)$$

where the last step uses  $\delta_s^{p-1} = (A_2 g_{\min} / (A_1(A_1 + 1)))^{p-1}$ . In the window,  $g_0 = b g_{\min}$  is constant:

$$\int_{s^* - \delta_s}^{s^*} g_0^{-p} ds = \frac{\delta_s}{b^p g_{\min}^p} = \frac{1}{b^p} \cdot \frac{A_2}{A_1(A_1 + 1)} \cdot g_{\min}^{1-p}. \quad (7.4.5)$$

Combining the left and window contributions with  $b^{-p} = 10^p$  gives

$$\frac{1/(p-1) + 1}{b^p} = \frac{p 10^p}{p-1},$$

so the combined term is  $(p/(p-1)) \cdot 10^p \cdot A_2/(A_1(A_1 + 1)) \cdot g_{\min}^{1-p}$ .

In the right region,  $g_0(s) = (\Delta/30)(s - s_0)/(1 - s_0)$ , so

$$\begin{aligned} \int_{s^*}^1 g_0^{-p} ds &= \left( \frac{30(1-s_0)}{\Delta} \right)^p \int_{s^*-s_0}^{1-s_0} \frac{du}{u^p} = \left( \frac{30(1-s_0)}{\Delta} \right)^p \cdot \frac{1}{(p-1)(s^*-s_0)^{p-1}} \\ &= \frac{1}{p-1} \left( \frac{30}{\Delta} \right)^p \left( \frac{a}{k} \right)^{p-1} (1-s_0) \cdot g_{\min}^{1-p}, \end{aligned} \quad (7.4.6)$$

using  $s^* - s_0 = k g_{\min}(1 - s^*)/(a - k g_{\min})$  and  $1 - s_0 = a(1 - s^*)/(a - k g_{\min})$ . Now set  $a = (4/3)k^2\Delta$  and  $k = 1/4$ , so  $a/k = \Delta/3$ . This yields  $(30/\Delta)^p (\Delta/3)^{p-1} = 30^p/(3\Delta)$ , together with  $(1 - s_0) \leq 1/(1 + A_1)$ . Hence the right contribution is  $3 \cdot 10^p / ((p-1)\Delta(1+A_1)) \cdot g_{\min}^{1-p}$ .

Since  $\Delta A_2 \leq A_1$  (equivalently  $A_2 \leq A_1/\Delta$ ), the left-plus-window term satisfies  $A_2/(A_1(1+A_1)) \leq 1/(\Delta(1+A_1))$ . Combining all three contributions gives

$$\int_0^1 g_0^{-p} ds \leq \frac{(p+3) \cdot 10^p}{(p-1)(1+A_1)\Delta} \cdot g_{\min}^{1-p}, \quad \text{so } B_1 = O\left(\frac{1}{\Delta(1+A_1)}\right). \quad (7.4.7)$$

The integral  $\int_0^1 g_0^{p-3} ds$  has the same three-region decomposition, now with exponent  $3-p$ . Because  $p \in (1, 2)$  implies  $3-p \in (1, 2)$ , each region converges by the same change of variables used for  $B_1$ . For example, the window contribution is

$$\int_{s^* - \delta_s}^{s^*} (b g_{\min})^{p-3} ds = \delta_s b^{p-3} g_{\min}^{p-3} = b^{p-3} \frac{A_2}{A_1(A_1 + 1)} g_{\min}^{p-2} = O(g_{\min}^{p-2}),$$

with  $b^{p-3} = 10^{3-p}$  absorbed into constants. The left and right pieces have the same order, so

$$B_2 = O\left(\frac{1}{\Delta(1+A_1)}\right). \quad (7.4.8)$$

For the adiabatic Hamiltonian  $H(s) = -(1-s)|\psi_0\rangle\langle\psi_0| + sH_z$ , we have

$$\|H'(s)\| = O(1), \quad \|H''(s)\| = 0, \quad |\lambda'_0(s)| = O(1), \quad (7.4.9)$$

because  $H'(s) = |\psi_0\rangle\langle\psi_0| + H_z$  is constant and  $\lambda'_0(s) = \langle\phi_0(s)|H'(s)|\phi_0(s)\rangle$  is bounded by  $\|H'\|$  through Hellmann-Feynman. The derivative  $|g'_0(s)|$  is piecewise bounded:  $b A_1(A_1 + 1)/A_2$  on the left, 0 in the window, and  $\Delta/(30(1-s_0))$  on the right. For piecewise linear  $g_0$ , this keeps  $|g'_0|B_2$  bounded. The window contributes nothing because  $g'_0 = 0$  there. On each linear branch,  $|g'_0|$  factors out and the substitution  $u = g_0(s)$  gives

$$\int g_0^{p-3} |g'_0| ds = \int_{g_{\min}/10}^{O(1)} u^{p-3} du = O(g_{\min}^{p-2}),$$

independently of the slopes. Since  $\|H''\| = 0$ , the dominant term in (7.3.2) is  $40\|H'\|^2 B_2$ . Therefore

$$c = O(B_2). \quad (7.4.10)$$

**Theorem 7.4.1** (Runtime of AQO: Main Result 1 [15]). *Let  $H_z$  satisfy the spectral condition (Definition 5.2.2) and assume  $A_1 \geq 1/2$  (equivalently  $s^* \geq 1/3$ ). For any  $\varepsilon > 0$ , the adaptive schedule (7.3.3) with the gap lower bound (7.4.1) prepares the ground state of  $H_z$  with fidelity at least  $1 - \varepsilon$  in time*

$$T = O\left(\frac{1}{\varepsilon} \cdot \frac{\sqrt{A_2}}{\Delta^2 A_1(A_1 + 1)} \cdot \sqrt{\frac{N}{d_0}}\right). \text{<sup>ii</sup>} \quad (7.4.11)$$

*Proof.* By Theorem 7.3.1,  $T \leq c B_1 / (\varepsilon g_{\min})$ . Substituting  $c = O(B_2)$ ,  $B_1 = O(1/(\Delta(1 + A_1)))$ ,  $B_2 = O(1/(\Delta(1 + A_1)))$ , and  $g_{\min} = (2A_1/(A_1 + 1))\sqrt{d_0/(NA_2)}$  from Eq. (5.4.9):

$$T = O\left(\frac{1}{\varepsilon} \cdot \frac{B_1 B_2}{g_{\min}}\right) = O\left(\frac{1}{\varepsilon} \cdot \frac{1}{\Delta^2(1 + A_1)^2} \cdot \frac{A_1 + 1}{2A_1} \sqrt{\frac{NA_2}{d_0}}\right) = O\left(\frac{1}{\varepsilon} \cdot \frac{\sqrt{A_2}}{\Delta^2 A_1(A_1 + 1)} \cdot \sqrt{\frac{N}{d_0}}\right). \quad (7.4.12) \quad \square$$

The runtime in (7.4.11) has five interpretable factors. The  $1/\varepsilon$  term is linear in target error. The factor  $\sqrt{A_2}$  measures spectral crowding near  $E_0$ , where larger  $A_2 = (1/N) \sum d_k / (E_k - E_0)^2$  sharpens the minimum and narrows the crossing window. The denominator  $A_1(A_1 + 1)$  encodes crossing location, since larger  $A_1$  pushes  $s^*$  toward 1 and steepens the left arm. The term  $1/\Delta^2$  is the cost of right-side control, with one  $1/\Delta$  from  $B_1$  and one from  $B_2$ . Finally,  $\sqrt{N/d_0}$  is the Grover factor. In short, the speedup is quantum, and the remaining terms are explicit spectral overheads of generality.

For Ising Hamiltonians  $H_\sigma$  (Eq. (5.1.4)) with  $A_1, A_2 = O(\text{poly}(n))$  and  $\Delta \geq 1/\text{poly}(n)$ , this becomes  $T = \tilde{O}(\sqrt{N/d_0})$ . That matches the lower bound of [5] up to polylogarithmic factors. When  $d_0 = O(1)$ , the adiabatic algorithm recovers the Grover  $\sqrt{N}$  scaling.

For the canonical two-level case  $M = 2$  with  $A_1 \approx 1$ ,  $A_2 \approx 1$ ,  $\Delta = 1$ , and  $d_0 = 1$ , we obtain

$$T = O\left(\frac{1}{\varepsilon} \cdot \frac{1}{1 \cdot 2} \cdot \sqrt{N}\right) = O\left(\frac{\sqrt{N}}{\varepsilon}\right), \quad (7.4.13)$$

matching the circuit-based Grover algorithm. The adaptive adiabatic approach achieves the same quadratic speedup through a smooth interpolation between two Hamiltonians, without requiring oracle queries or amplitude amplification.

Runtime is controlled by how much spectral information the schedule receives. The constant-rate schedule (Theorem 7.2.3) gives  $T = O(N/\varepsilon)$  because the crossing window dominates. The Roland-Cerf schedule (section 7.1) sets  $K'(s) \propto 1/g(s)^2$  and improves this to  $T = O(\sqrt{N}/\varepsilon)$ , but it needs the exact gap at every point. The adaptive schedule in Theorem 7.3.1 keeps the same  $\sqrt{N}$  scaling while using only a certified lower bound  $g_0(s) \leq g(s)$ , namely the Chapter 6 profile bounds. That change, from exact gap to lower bound, is what makes the method usable for general spectral-condition instances.

Guo and An [27] place this in a broader framework. They study interpolations  $H(u(s)) = (1 - u(s))H_0 + u(s)H_1$  under a measure condition: the set  $\{s : \Delta(u(s)) \leq x\}$  has Lebesgue measure  $O(x)$  as  $x \rightarrow 0$ . Under that condition, the power-law schedule with exponent  $p = 3/2$  achieves  $O(1/\Delta_*)$ , a quadratic improvement over  $O(1/\Delta_*^2)$ . They also show that  $p = 3/2$  is optimal for linear gap profiles. The profile in Theorem 6.3.1 satisfies their condition because it has one minimum at  $s^*$  and linear reopening on both sides. Their theorem provides the existence-and-scaling layer; Chapters 5 and 6 add explicit constants, which is what turns (7.4.11) into a concrete runtime bound.

Running the adaptive schedule still requires knowledge of  $g_0(s)$ , hence of  $s^*$ ,  $\delta_s$ , and  $g_{\min}$ . These all depend on  $A_1$ . Inside the window  $[s^* - \delta_s, s^*]$ , the schedule is constant,  $K' = c/(\varepsilon b^p g_{\min}^2)$ , so the main issue is not local slope but window placement. Because  $s^* = A_1/(A_1 + 1)$ , we must know  $A_1$  to accuracy  $O(\delta_s) = O(2^{-n/2})$  to center the slow segment correctly. Outside the window, placement errors change only constants. Inside this exponentially narrow window, the same error causes a real loss of fidelity.

Inprecision in  $A_2$  and  $d_0$  causes only polynomial slowdown. Replacing  $A_2$  by the lower bound  $1 - d_0/N$  (Eq. (5.2.3)) and taking  $d_0 = 1$  changes runtime only by  $\text{poly}(n)$  factors, because these parameters appear through  $\sqrt{A_2/d_0}$  and  $B_1$ . The critical quantity is  $A_1$ . It must be estimated to additive accuracy  $O(\delta_s) = O(2^{-n/2})$  before evolution begins. That requirement is severe: the needed precision is exponential in  $n$  even though  $H_z$  itself has a  $\text{poly}(n)$ -bit description. Chapter 8 shows that even approximating  $A_1$  to much coarser precision  $1/\text{poly}(n)$  is NP-hard, while exact computation is #P-hard.

<sup>ii</sup>The published paper [15] states  $A_1^2$  in Theorem 1. The expression  $A_1(A_1 + 1)$  follows from the proof derivation in Appendix A-IV of the same paper. For Ising Hamiltonians with  $A_1 = O(\text{poly}(n))$ , the distinction is absorbed by the  $O(\cdot)$  notation, since  $A_1(A_1 + 1) = A_1^2 + A_1 = \Theta(A_1^2)$ .

# Chapter 8

## Hardness of Optimality

The optimal schedule from Chapter 7 achieves a quadratic speedup over classical brute-force search, but the schedule must be fixed before evolution begins. It depends on the spectral parameter  $A_1$ , the weighted sum of inverse gaps that determines where the avoided crossing occurs. This parameter must be known to additive accuracy  $O(2^{-n/2})$ . Given the  $N = 2^n$  diagonal entries of  $H_z$ , brute-force computation of  $A_1 = (1/N) \sum_{k=1}^{M-1} d_k / (E_k - E_0)$  by enumerating eigenvalues, sorting, and summing takes  $O(N)$  time. That is the same cost as classical unstructured search. If pre-computation costs as much as the task itself, the speedup is only conditional.

The runtime of [Theorem 7.4.1](#),

$$T = O\left(\frac{1}{\varepsilon} \cdot \frac{\sqrt{A_2}}{\Delta^2 A_1(A_1 + 1)} \cdot \sqrt{\frac{N}{d_0}}\right),$$

makes this dependence explicit. The adaptive schedule places a slow phase in the window  $[s^* - \delta_s, s^*]$  centered at  $s^* = A_1/(A_1 + 1)$ , where the gap is smallest, and accelerates elsewhere. The parameters  $A_2$  and  $d_0$  enter only through  $\sqrt{A_2/d_0}$ . Using conservative bounds ( $A_2 \geq 1 - d_0/N$  from Eq. (5.2.3), and  $d_0 = 1$  for worst-case search) changes only polynomial prefactors when  $d_0 \ll N$ . The decisive quantity is  $A_1$ . It sets crossing location, while  $\delta_s = O(\sqrt{d_0 A_2 / N}) = O(2^{-n/2})$  sets required precision. If the crossing estimate is wrong by more than  $\delta_s$ , evolution passes too quickly through the minimum and loses ground-state fidelity. Throughout this chapter, we write  $A_1(H)$  when dependence on the Hamiltonian matters.

The hardness of computing  $A_1$  is not the only obstacle to adiabatic optimization for hard problems. Even if  $A_1$  were known exactly, the single-crossing framework of Chapters 5–7 applies only to the rank-one projector  $H_0 = -|\psi_0\rangle\langle\psi_0|$ . For the transverse-field driver (Chapter 5), the multi-crossing regime makes this framework inapplicable. Knowing  $A_1$  no longer helps, because the schedule would need to navigate exponentially many crossings rather than one. These two barriers are complementary. Computing  $A_1$  is hard even in the rank-one setting, and the single-crossing method fails for other drivers even when spectral information is available.

NP-hardness already appears at precision  $1/\text{poly}(n)$ . Two queries to an  $A_1$ -oracle then suffice to solve 3-SAT ([section 8.1](#)). At precision  $2^{-\text{poly}(n)}$ , the problem becomes #P-hard because polynomial interpolation can recover all degeneracies from polynomially many queries ([section 8.2](#)). The algorithmically relevant precision  $2^{-n/2}$  sits strictly between these scales. It is fine enough to matter for scheduling, but not fine enough for either existing hardness proof to transfer directly. At this precision, a quantum algorithm uses  $O(2^{n/2})$  queries, while any classical algorithm needs  $\Omega(2^n)$ , yielding a Grover-type quadratic separation ([section 8.3](#)).

### 8.1 NP-Hardness of Estimating $A_1$

The Hamiltonian  $H_z$  encodes an optimization problem whose ground energy  $E_0$  determines whether a solution exists. For a 3-SAT instance,  $E_0 = 0$  when a satisfying assignment exists and  $E_0 \geq 1/\text{poly}(n)$  otherwise. Distinguishing these two cases is the local Hamiltonian promise problem, known to be NP-hard [28]. The spectral parameter  $A_1$  is not obviously tied to this decision problem, because it aggregates information across all energy levels rather than only the ground energy. A modified Hamiltonian  $H'$  bridges the two tasks. Comparing  $A_1(H')$  with  $A_1(H)$  reveals whether  $E_0$  vanishes.

Define the  $(n + 1)$ -qubit Hamiltonian

$$H' = H \otimes \frac{I + \sigma_z}{2}. \tag{8.1.1}$$

The operator  $(I + \sigma_z)/2$  is the projector onto  $|0\rangle$  for the ancilla qubit. It has eigenvalue 1 on  $|0\rangle$  and eigenvalue 0 on  $|1\rangle$ . On the  $|0\rangle$  branch,  $H'$  has the same spectrum as  $H$ , with eigenvalues  $E_k$  and degeneracies  $d_k$ . On the  $|1\rangle$  branch,  $H'$  annihilates every state, contributing  $2^n$  eigenvalues at energy 0. The ground energy of  $H'$  is therefore always zero, regardless of  $E_0(H)$ . This is the key mechanism.  $A_1(H')$  measures the spectrum from a fixed reference point  $E'_0 = 0$ , while  $A_1(H)$  measures from the variable reference  $E_0(H)$ . When  $E_0(H) > 0$ , the two values separate by a detectable amount.

**Lemma 8.1.1** (Disambiguation [15]). *Let  $\varepsilon, \mu_1, \mu_2 \in (0, 1)$ . Suppose  $\mathcal{C}_\varepsilon$  is a procedure that accepts the description of a Hamiltonian  $H$  and outputs  $\tilde{A}_1(H)$  with  $|\tilde{A}_1(H) - A_1(H)| \leq \varepsilon$ . Let  $H$  be an  $n$ -qubit diagonal Hamiltonian with eigenvalues  $0 \leq E_0 < E_1 < \dots < E_{M-1} \leq 1$  and  $M \in \text{poly}(n)$ , such that either (i)  $E_0 = 0$  or (ii)  $\mu_1 \leq E_0 \leq 1 - \mu_2$ . Then two calls to  $\mathcal{C}_\varepsilon$  suffice to decide between (i) and (ii), provided*

$$\varepsilon < \frac{\mu_1}{6(1 - \mu_1)} - \frac{d_0}{6N} \cdot \frac{1}{\mu_1 \mu_2}. \quad (8.1.2)$$

*Proof.* Call  $\mathcal{C}_\varepsilon$  on  $H$  and on  $H'$  defined by Eq. (8.1.1), obtaining estimates  $\tilde{A}_1(H)$  and  $\tilde{A}_1(H')$ . The test statistic is  $\tilde{A}_1(H) - 2\tilde{A}_1(H')$ , where the factor 2 compensates for the doubling of the Hilbert space ( $H'$  acts on  $2^{n+1}$  states, so  $A_1(H')$  carries a normalization factor  $1/2^{n+1}$  instead of  $1/2^n$ ).

**Case (i):**  $E_0 = 0$ . The ground energy of  $H'$  is 0 with degeneracy  $d_0 + 2^n$ , and the excited levels of  $H'$  are  $E_1, \dots, E_{M-1}$  with degeneracies  $d_1, \dots, d_{M-1}$ . Since  $E_0 = 0$ , both  $A_1(H)$  and  $A_1(H')$  sum over the same gaps  $E_k - 0 = E_k$ :

$$A_1(H) = \frac{1}{2^n} \sum_{k=1}^{M-1} \frac{d_k}{E_k}, \quad A_1(H') = \frac{1}{2^{n+1}} \sum_{k=1}^{M-1} \frac{d_k}{E_k}.$$

Therefore  $A_1(H) - 2A_1(H') = 0$ , and by the triangle inequality the test statistic satisfies  $|\tilde{A}_1(H) - 2\tilde{A}_1(H')| \leq 3\varepsilon$ .

**Case (ii):**  $\mu_1 \leq E_0 \leq 1 - \mu_2$ . The ground energy of  $H'$  is still 0 (from the  $|1\rangle$  branch), but now  $E_0, E_1, \dots, E_{M-1}$  are all excited levels. Thus

$$A_1(H') = \frac{1}{2^{n+1}} \sum_{k=0}^{M-1} \frac{d_k}{E_k}.$$

Decompose  $A_1(H)$  using the partial fraction identity  $d_k/(E_k - E_0) = d_k/E_k + d_k E_0/(E_k(E_k - E_0))$ :

$$\begin{aligned} A_1(H) &= \frac{1}{2^n} \sum_{k=1}^{M-1} \frac{d_k}{E_k - E_0} = \frac{1}{2^n} \sum_{k=1}^{M-1} \frac{d_k}{E_k} + \frac{E_0}{2^n} \sum_{k=1}^{M-1} \frac{d_k}{E_k(E_k - E_0)} \\ &= \frac{1}{2^n} \sum_{k=0}^{M-1} \frac{d_k}{E_k} - \frac{d_0}{2^n E_0} + \frac{E_0}{2^n} \sum_{k=1}^{M-1} \frac{d_k}{E_k(E_k - E_0)}. \end{aligned} \quad (8.1.3)$$

The first sum equals  $2A_1(H')$ . For the remainder sum,  $E_k \leq 1$  and  $E_k - E_0 \leq 1 - E_0$ , so the product  $E_k(E_k - E_0)$  is at most  $1 - E_0$ . Each fraction  $d_k/(E_k(E_k - E_0))$  is therefore bounded from below:

$$\frac{E_0}{2^n} \sum_{k=1}^{M-1} \frac{d_k}{E_k(E_k - E_0)} \geq \frac{E_0}{1 - E_0} \cdot \frac{1}{2^n} \sum_{k=1}^{M-1} d_k = \frac{E_0}{1 - E_0} \left(1 - \frac{d_0}{N}\right).$$

Combining with Eq. (8.1.3):

$$\begin{aligned} A_1(H) - 2A_1(H') &\geq \frac{E_0}{1 - E_0} \left(1 - \frac{d_0}{N}\right) - \frac{d_0}{N E_0} \\ &= \frac{E_0}{1 - E_0} - \frac{d_0}{N} \cdot \frac{1 - E_0 + E_0^2}{E_0(1 - E_0)}. \end{aligned} \quad (8.1.4)$$

Since  $1 - E_0 + E_0^2 \leq 1$  and  $E_0(1 - E_0) \geq \mu_1 \mu_2$  on the given range, the fraction  $(1 - E_0 + E_0^2)/(E_0(1 - E_0))$  is at most  $1/(\mu_1 \mu_2)$ . The first term  $E_0/(1 - E_0)$  is increasing in  $E_0$ , so it is at least  $\mu_1/(1 - \mu_1)$ . Therefore

$$A_1(H) - 2A_1(H') \geq \frac{\mu_1}{1 - \mu_1} - \frac{d_0}{N} \cdot \frac{1}{\mu_1 \mu_2},$$

and the test statistic satisfies

$$\tilde{A}_1(H) - 2\tilde{A}_1(H') \geq \frac{\mu_1}{1 - \mu_1} - \frac{d_0}{N \mu_1 \mu_2} - 3\varepsilon.$$

The two cases are distinguished when  $3\varepsilon$  from case (i) is separated from the lower bound in case (ii), requiring  $6\varepsilon < \mu_1/(1 - \mu_1) - d_0/(N\mu_1\mu_2)$ .  $\square$

The disambiguation succeeds whenever the positive correction  $E_0/(1 - E_0)$  from the partial fraction identity dominates the negative term  $-d_0/(NE_0)$ , which happens as long as  $d_0/N$  is small relative to  $\mu_1^2\mu_2$ . For the Ising Hamiltonians of interest,  $d_0/N$  is exponentially small in  $n$ , so the condition is easily satisfied.

**Theorem 8.1.2** (NP-hardness of  $A_1$  estimation [15]). *Computing  $A_1(H)$  to additive accuracy*

$$\varepsilon < \frac{1}{72(n-1)}$$

for a 3-local Hamiltonian  $H$  on  $n$  qubits is NP-hard.

*Proof.* We reduce 3-SAT to ground-energy disambiguation, following the construction of [29, 15]. Let  $\varphi$  be a 3-SAT formula on  $n_{\text{var}}$  Boolean variables  $x_0, \dots, x_{n_{\text{var}}-1}$  with  $m$  clauses, each of the form  $a_k \vee b_k \vee c_k$  where each literal is some  $x_l$  or  $\bar{x}_l$ . If  $n_{\text{var}} + m < 15$ , solve by brute force. Otherwise, define the single-qubit projectors

$$P_{x_l} = \frac{I - \sigma_z^{(l)}}{2}, \quad P_{\bar{x}_l} = \frac{I + \sigma_z^{(l)}}{2},$$

which project onto the  $|1\rangle$  and  $|0\rangle$  states of qubit  $l$ , respectively. For each clause  $k$  ( $0 \leq k < m$ ), introduce an auxiliary qubit at index  $n_{\text{var}} + k$  and define

$$\begin{aligned} H_k = & P_{\bar{a}_k} + P_{\bar{b}_k} + P_{\bar{c}_k} + P_{\bar{x}_{n_{\text{var}}+k}} \\ & + P_{a_k}P_{b_k} + P_{a_k}P_{c_k} + P_{b_k}P_{c_k} \\ & + P_{\bar{a}_k}P_{x_{n_{\text{var}}+k}} + P_{\bar{b}_k}P_{x_{n_{\text{var}}+k}} + P_{\bar{c}_k}P_{x_{n_{\text{var}}+k}}. \end{aligned} \quad (8.1.5)$$

Direct computation on the computational basis shows that the minimum eigenvalue of  $H_k$  is 3 when clause  $k$  is satisfied and 4 when it is not; the maximum eigenvalue is 6. The combined Hamiltonian on  $2n_{\text{var}} + 2m$  qubits is

$$H = \frac{1}{6m} \sum_{k=0}^{m-1} H_k + \frac{1}{2n_{\text{var}} + 2m} \sum_{j=n_{\text{var}}+m}^{2n_{\text{var}}+2m-1} P_{x_j} - \frac{1}{2} I. \quad (8.1.6)$$

The first sum normalizes the clause energies to  $[1/2, 1]$ ; the second sum adds  $n_{\text{var}} + m$  free qubits whose projectors prefer  $|0\rangle$ ; the identity shift places the eigenvalues in  $[0, 1]$ . When all clauses are satisfied, there exists an assignment making every  $H_k$  achieve its minimum, giving  $E_0 = 0$ . When some clause is unsatisfied, the minimum of  $\sum H_k/(6m)$  increases by at least  $1/(6m)$ , giving  $E_0 \geq 1/(6m)$ .

Apply Lemma 8.1.1 with  $\mu_1 = 1/(6m)$  and  $\mu_2 = 1/2$ . The number of eigenvalues is  $N = 2^{2n_{\text{var}}+2m}$  and the ground-state degeneracy satisfies  $d_0 \leq 2^{n_{\text{var}}+m}$ , so  $d_0/N \leq 2^{-(n_{\text{var}}+m)}$ . Substituting into Eq. (8.1.2), the right-hand side satisfies

$$\frac{1}{6} \cdot \frac{1}{6m-1} - \frac{12m}{6} \cdot \frac{d_0}{N} \geq \frac{1}{36(n_{\text{var}}+m-1)} - \frac{2m}{2^{n_{\text{var}}+m}}, \quad (8.1.7)$$

since  $1/(6(6m-1)) \geq 1/(36(n_{\text{var}}+m-1))$  for  $n_{\text{var}} \geq 1$  and  $d_0/N \leq 2^{-(n_{\text{var}}+m)}$ . For  $n_{\text{var}} + m \geq 15$ , the second term satisfies  $2m/2^{n_{\text{var}}+m} \leq 1/(72(n_{\text{var}}+m-1))$ , so the disambiguation succeeds whenever

$$\varepsilon < \frac{1}{72(n_{\text{var}}+m-1)}.$$

The Hamiltonian  $H'$  from Eq. (8.1.1) acts on  $n = 2n_{\text{var}} + 2m + 1$  qubits and is 3-local (since  $H$  is 2-local and the tensor product with  $(I + \sigma_z)/2$  adds one ancilla). Since  $n_{\text{var}} + m \leq n$ , the precision bound  $\varepsilon < 1/(72(n-1))$  follows.  $\square$

When  $M = 2$  (Grover search), the spectral parameter  $A_1 = (N-1)/N$  is trivial to obtain from the instance description. There are only two levels, and their degeneracies are fixed by the number of marked items. NP-hardness appears only for Hamiltonians that encode combinatorial structure with polynomially many levels and exponentially small ground-energy gaps. In that regime,  $A_1$  depends nontrivially on the full degeneracy profile.

**Remark.** The disambiguation technique extends beyond 3-SAT. The MaxCut decision problem (given a graph  $G = (V, E)$  and integer  $k$ , does  $G$  have a cut of size at least  $k$ ?) also reduces to  $A_1$  estimation. The construction adds a weighted edge to  $G$ , creating an auxiliary Hamiltonian  $H'$  whose  $A_1$  value differs from a reference by at least  $1/(|E|(|E|-1))$  between the two cases. This yields NP-hardness at precision  $2/(5n^4)$  with a 2-local Hamiltonian, sharpening the locality requirement from 3-local to 2-local at the cost of a slightly tighter precision bound.

## 8.2 #P-Hardness of Computing $A_1$ Exactly

NP-hardness captures a decision question, namely whether  $E_0 = 0$ . But  $A_1$  carries more than a single decision bit. It is a weighted sum over all energy levels, and its exact value determines every degeneracy  $d_k$ . Recovering these degeneracies solves counting problems. For NP-complete Hamiltonians, for example,  $d_0$  counts satisfying assignments. Counting is harder than deciding, and it is #P-complete [30].

The extraction uses a parametrized family of Hamiltonians that shifts the spectrum continuously, turning  $A_1$  into a rational function whose poles carry the degeneracies as residues. For a parameter  $x > 0$ , define the  $(n+1)$ -qubit Hamiltonian

$$H'(x) = H \otimes I - \frac{x}{2} I \otimes \frac{I + \sigma_z^{(n+1)}}{2}. \quad (8.2.1)$$

On the  $|0\rangle$  branch of the ancilla, the eigenvalues are  $E_k - x/2$  with degeneracies  $d_k$ . On the  $|1\rangle$  branch, the eigenvalues are  $E_k$  with degeneracies  $d_k$ . The ground energy is  $E_0 - x/2$  (from the  $|0\rangle$  branch, for  $x > 0$ ). The gaps relative to this ground energy are  $\Delta_k = E_k - E_0$  (extending the notation  $\Delta = E_1 - E_0$  from earlier chapters to all levels) for the  $|0\rangle$  branch and  $\Delta_k + x/2$  for the  $|1\rangle$  branch.

Computing  $A_1(H'(x))$  from these gaps and defining  $f(x) = 2A_1(H'(x)) - A_1(H)$  isolates the  $|1\rangle$ -branch contribution [15]:

$$f(x) = \frac{1}{N} \sum_{k=0}^{M-1} \frac{d_k}{\Delta_k + x/2}. \quad (8.2.2)$$

This function is a sum of  $M$  simple poles at  $x = -2\Delta_k$ . Each pole has residue  $2d_k/N$ , encoding the degeneracy of the corresponding energy level. The function  $f$  is a partial-fraction decomposition of the entire degeneracy spectrum. The extraction problem reduces to recovering these residues from evaluations of  $f$ .

**Lemma 8.2.1** (Exact degeneracy extraction [15]). *Suppose  $\mathcal{C}$  is a procedure that computes  $A_1(H)$  exactly for any  $n$ -qubit diagonal Hamiltonian  $H$ . Let  $H_\sigma$  be an Ising Hamiltonian (Equation 5.1.4) with integer eigenvalues and known spectral gaps  $\Delta_k = E_k - E_0$ . Then  $O(\text{poly}(n))$  calls to  $\mathcal{C}$  suffice to compute all degeneracies  $d_0, d_1, \dots, d_{M-1}$ .*

*Proof.* Each evaluation of  $f(x_i)$  requires two calls to  $\mathcal{C}$ , one for  $A_1(H)$  and one for  $A_1(H'(x_i))$ . Evaluate  $f$  at  $M$  distinct positive odd integers  $x_i \in \{1, 3, \dots, 2M-1\}$ . These values avoid the poles. For each  $k$ ,  $\Delta_k + x_i/2 \geq 0 + 1/2 > 0$  because  $\Delta_k \geq 0$  and  $x_i \geq 1$ . The total cost is  $2M = O(\text{poly}(n))$  oracle calls.

Define the reconstruction polynomial

$$P(x) = \prod_{k=0}^{M-1} \left( \Delta_k + \frac{x}{2} \right) f(x) = \frac{1}{N} \sum_{k=0}^{M-1} d_k \prod_{\ell \neq k} \left( \Delta_\ell + \frac{x}{2} \right). \quad (8.2.3)$$

Multiplying  $f(x)$  by the product of all denominators clears the poles, yielding a polynomial of degree at most  $M-1$  in  $x$ . Since the gaps  $\Delta_k$  are known integers, the values  $P(x_i) = \prod_k (\Delta_k + x_i/2) \cdot f(x_i)$  are computable from oracle outputs. The  $M$  values  $P(x_1), \dots, P(x_M)$  determine  $P$  uniquely by Lagrange interpolation [31]. A polynomial of degree at most  $M-1$  is fixed by  $M$  distinct evaluations.

The degeneracies are recovered by evaluating  $P$  at the poles. Setting  $x = -2\Delta_k$  kills every factor  $(\Delta_\ell + x/2)$  except the  $k$ -th, giving

$$d_k = \frac{N \cdot P(-2\Delta_k)}{\prod_{\ell \neq k} (\Delta_\ell - \Delta_k)}, \quad k \in \{0, \dots, M-1\}. \quad (8.2.4)$$

The denominator is nonzero because the eigenvalues are distinct. The entire computation (oracle calls, Lagrange interpolation, pole evaluation) runs in  $O(\text{poly}(n))$  time.  $\square$

Extracting  $d_0$  from an Ising Hamiltonian encoding a 3-SAT formula counts satisfying assignments and therefore solves #3-SAT. Since #3-SAT is #P-complete [30], an exact  $A_1$  oracle would solve every problem in #P in polynomial time. The same degeneracy data also determines IQP output probabilities [32]. From  $d_k$  and  $\Delta_k$ , one computes  $|\langle 0^n | C_{\text{IQP}} | 0^n \rangle|^2 = |N^{-1} \sum_k d_k e^{i\Delta_k}|^2$ , which is itself #P-hard. The NP-hardness result of section 8.1 uses a 3-local Hamiltonian because the ancilla raises locality by one. The #P-hardness statement already holds for 2-local Ising Hamiltonians, since Eq. (8.2.1) preserves 2-locality when  $H$  is 2-local.

The exact oracle is unrealistic. A robust version of Lemma 8.2.1 must tolerate additive noise  $\varepsilon$  in the oracle outputs. Paturi's amplification lemma controls how pointwise bounds on a polynomial propagate across an interval.

**Lemma 8.2.2** (Paturi [33]). *Let  $P(x)$  be a polynomial of degree at most  $M$  satisfying  $|P(i)| \leq c$  for all integers  $i \in \{0, 1, \dots, M\}$ . Then  $|P(x)| \leq c \cdot 2^M$  for all  $x \in [0, M]$ .*

Paturi's lemma bounds polynomial growth between sample points. If a polynomial is bounded by  $c$  at  $M+1$  integer points, it can grow by at most a factor  $2^M$  on the interval. Applied to the difference between exact and approximate reconstruction polynomials, this gives explicit control of interpolation error. Oracle noise  $\varepsilon$  first propagates to  $f$  as  $|\tilde{f}(x_i) - f(x_i)| \leq 3\varepsilon$  (three oracle calls contribute), then to the polynomial samples as  $|\tilde{P}(x_i) - P(x_i)| \leq 3\varepsilon \prod_k (\Delta_k + x_i/2)$ . The product is at most  $B^M$  with  $B = \Delta_{\max} + M = \text{poly}(n)$ , so each sample has error at most  $3\varepsilon B^M$ .

**Lemma 8.2.3** (Approximate degeneracy extraction [15]). *Under the same hypotheses as Lemma 8.2.1, but with an oracle  $\mathcal{C}_\varepsilon$  satisfying  $|\tilde{A}_1(H) - A_1(H)| \leq \varepsilon$ , all degeneracies  $d_k$  can be computed exactly by  $O(\text{poly}(n))$  calls to  $\mathcal{C}_\varepsilon$  for sufficiently small  $\varepsilon \in O(2^{-\text{poly}(n)})$ .*

*Proof sketch.* The approximate polynomial  $\tilde{P}$  is the Lagrange interpolant through the noisy values  $(\tilde{P}(x_1), \dots, \tilde{P}(x_M))$ . Its difference  $D = \tilde{P} - P$  is a polynomial of degree at most  $M-1$  bounded by  $3\varepsilon B^M$  at the sample points. By Paturi's lemma (Lemma 8.2.2),  $|D(x)| \leq 3\varepsilon B^M \cdot 2^{M-1}$  on the interpolation interval. At the pole evaluation points  $x^* = -2\Delta_k$ , which lie outside the interval  $[1, 2M-1]$ , the error is bounded by the Lagrange basis amplification:

$$|D(x^*)| \leq 3\varepsilon B^M \cdot \Lambda_M(x^*),$$

where  $\Lambda_M(x^*) = \sum_j \prod_{i \neq j} |x^* - x_i| / |x_j - x_i|$  is the Lebesgue function. For extrapolation outside the interval,  $\Lambda_M(x^*)$  grows exponentially in  $M$ , but since  $M = \text{poly}(n)$ , the total amplification is  $2^{\text{poly}(n)}$ . Dividing by  $\prod_{\ell \neq k} |\Delta_\ell - \Delta_k|$  (also at most  $2^{\text{poly}(n)}$  for integer gaps) and multiplying by  $N = 2^n$ , the degeneracy error satisfies

$$|d_k - \tilde{d}_k| \leq 3\varepsilon \cdot 2^{\text{poly}(n)}.$$

For  $\varepsilon = O(2^{-\text{poly}(n)})$  with a sufficiently large polynomial, this is less than  $1/2$ . Since degeneracies are positive integers, rounding  $\tilde{d}_k$  to the nearest integer recovers  $d_k$  exactly.  $\square$

The proof extends to probabilistic oracles. If  $\mathcal{C}_\varepsilon$  succeeds with probability at least  $3/4$ , then  $O(\text{poly}(n))$  queries produce enough correct sample points to reconstruct  $P$  despite corrupted evaluations. The Berlekamp-Welch algorithm recovers a polynomial of degree  $d$  from  $k$  partially corrupted evaluations, provided at least  $\max\{d+1, (k+d)/2\}$  evaluations are correct [32]. By the Chernoff bound, querying  $k = O(\text{poly}(n))$  times ensures that at least  $(k + M - 2)/2$  evaluations are correct with high probability. Combining this with Lemma 8.2.3:

**Theorem 8.2.4** (#P-hardness of  $A_1$  estimation [15]). *Estimating  $A_1(H)$  to additive accuracy  $\varepsilon = O(2^{-\text{poly}(n)})$  is #P-hard, even for 2-local Ising Hamiltonians. The result holds for both deterministic and probabilistic estimation algorithms.*

With  $M = 2$ , the reconstruction polynomial  $P(x) = (d_0/N)(1+x/2) + (d_1/N)(x/2)$  is linear. Two evaluations determine  $d_0$  and  $d_1$  exactly, and interpolation reduces to fitting a line through two points. The #P-hardness comes from Hamiltonians with  $M = O(n^2)$  levels, where the reconstruction polynomial has high degree and tiny oracle errors amplify through the exponential Paturi factor. The next section quantifies this amplification as  $2^{O(M \log n)}$ .

### 8.3 The Intermediate Regime

The adiabatic algorithm requires  $A_1$  to precision  $O(2^{-n/2})$ . NP-hardness holds at  $1/\text{poly}(n)$  (Theorem 8.1.2), and #P-hardness holds at  $2^{-\text{poly}(n)}$  (Theorem 8.2.4). The algorithmically relevant precision  $2^{-n/2}$  lies strictly between these regimes. The interpolation method does not reach this precision; Braida et al. [15] left the intermediate regime open.

The interpolation technique extracts exact integers from approximate real evaluations. At precision  $2^{-n/2}$ , the error amplification inherent in polynomial extrapolation makes this extraction impossible.

NP-hardness extends to  $2^{-n/2}$  by monotonicity. An oracle at precision  $2^{-n/2}$  is strictly more powerful than one at  $1/\text{poly}(n)$ , so it still solves 3-SAT. The #P-hardness argument does not extend the other way. An oracle at precision  $2^{-n/2}$  is *less* powerful than one at  $2^{-\text{poly}(n)}$ , and the interpolation proof for that regime fails here. The failure has a concrete source. Oracle noise enters polynomial samples at rate  $\varepsilon B^M$ , the Lebesgue function amplifies it exponentially in  $M$ , and the amplified error exceeds the rounding margin when  $\varepsilon = 2^{-n/2}$ .

**Theorem 8.3.1** (Interpolation barrier). *The polynomial interpolation technique of section 8.2 requires oracle precision  $\varepsilon = 2^{-n-O(M \log n)}$  to extract exact degeneracies, where  $M = \text{poly}(n)$  is the number of distinct energy levels. At  $\varepsilon = 2^{-n/2}$ , the amplified error exceeds  $1/2$  and rounding fails. The  $\#P$ -hardness argument does not extend to precision  $2^{-n/2}$ .*

*Proof.* We trace the error propagation from oracle noise to degeneracy error through the construction of Lemma 8.2.1. Let  $\varepsilon$  denote the oracle accuracy, and let  $B = \Delta_{\max} + M = \text{poly}(n)$  bound the denominator factors, where  $\Delta_{\max}$  is the largest spectral gap.

**Sample-point error.** The approximate function values satisfy  $|\tilde{f}(x_i) - f(x_i)| \leq 3\varepsilon$ . The approximate polynomial samples are  $\tilde{P}(x_i) = \prod_k (\Delta_k + x_i/2) \tilde{f}(x_i)$ , with error

$$|\tilde{P}(x_i) - P(x_i)| \leq 3\varepsilon \prod_{k=0}^{M-1} \left( \Delta_k + \frac{x_i}{2} \right) \leq 3\varepsilon B^M. \quad (8.3.1)$$

**Degeneracy error.** The approximate degeneracies are computed from Eq. (8.2.4) with  $\tilde{P}$  in place of  $P$ . Since  $\tilde{P}$  is the Lagrange interpolant through the noisy samples, its value at any point  $x^*$  is  $\tilde{P}(x^*) = \sum_j \tilde{P}(x_j) \prod_{i \neq j} (x^* - x_i)/(x_j - x_i)$ . The error at  $x^* = -2\Delta_k$  satisfies

$$|\tilde{P}(x^*) - P(x^*)| \leq 3\varepsilon B^M \sum_{j=0}^{M-1} \prod_{i \neq j} \frac{|x^* - x_i|}{|x_j - x_i|} = 3\varepsilon B^M \cdot \Lambda_M(x^*), \quad (8.3.2)$$

where  $\Lambda_M(x^*) = \sum_j \prod_{i \neq j} |x^* - x_i|/|x_j - x_i|$  is the Lebesgue function at  $x^*$ . It measures worst-case amplification of pointwise interpolation errors. If each sample has error  $\delta$ , then the interpolated value at  $x^*$  has error at most  $\delta \cdot \Lambda_M(x^*)$ . For extrapolation outside the sample interval, this amplification is exponential in  $M$ . Consider odd-integer nodes  $x_j = 2j + 1$  and evaluation point  $x^* = -2\Delta_k \leq 0$ , which lies outside  $[1, 2M - 1]$ . Each numerator factor obeys  $|x^* - x_i| = 2\Delta_k + 2i + 1 \leq 2B + 1$ . For the denominator,  $\prod_{i \neq j} |x_j - x_i| = \prod_{i \neq j} 2|j - i| = 2^{M-1} j! (M - 1 - j)!$  because the nodes are equally spaced with spacing 2. The sum over  $j$  becomes

$$\Lambda_M(x^*) \leq \sum_{j=0}^{M-1} \frac{(2B + 1)^{M-1}}{2^{M-1} j! (M - 1 - j)!} = \frac{(2B + 1)^{M-1}}{(M - 1)!}, \quad (8.3.3)$$

using the identity  $\sum_j \binom{M-1}{j} = 2^{M-1}$ . The denominator in Eq. (8.2.4) satisfies  $\prod_{\ell \neq k} |\Delta_\ell - \Delta_k| \geq k!(M - 1 - k)!$  for integer gaps (since  $|\Delta_\ell - \Delta_k| \geq |\ell - k|$ ), with minimum over  $k$  at least  $((M - 1)/(2e))^{M-1}$  by Stirling's approximation. The total degeneracy error is therefore

$$|d_k - \tilde{d}_k| \leq \frac{3\varepsilon N B^M (2B + 1)^{M-1}}{(M - 1)! ((M - 1)/(2e))^{M-1}}. \quad (8.3.4)$$

Since  $B = \text{poly}(n)$  and  $M = \text{poly}(n)$ , the amplification factor is  $2^{O(M \log n)}$ .

**Rounding condition.** To extract exact degeneracies by rounding, we need  $|d_k - \tilde{d}_k| < 1/2$ . This requires

$$\varepsilon < \frac{1}{6N \cdot 2^{O(M \log n)}} = 2^{-n-O(M \log n)}. \quad (8.3.5)$$

**Evaluation at  $\varepsilon = 2^{-n/2}$ .** Set  $\varepsilon = 2^{-n/2}$  and  $M = n^c$  for some constant  $c \geq 1$ . The error bound from Eq. (8.3.4) evaluates to

$$|d_k - \tilde{d}_k| \leq 3 \cdot 2^{-n/2} \cdot 2^n \cdot 2^{O(n^c \log n)} = 3 \cdot 2^{n/2+O(n^c \log n)} \gg 1.$$

Even for  $c = 1$  (the most favorable case  $M = n$ ), the exponent  $n/2 + \Omega(n)$  diverges. The upper bound on the degeneracy error already exceeds  $1/2$ , so the rounding step cannot be guaranteed to succeed.  $\square$

The precision  $\varepsilon = 2^{-n/2}$  is too coarse for interpolation but too fine for brute force. It sits in a window that existing techniques cannot reach from either side.

This amplification is not specific to the construction above. Exponential growth is intrinsic to polynomial extrapolation for any  $d$  nodes, any interval, and any evaluation point sufficiently far outside that interval.

**Theorem 8.3.2** (Generic extrapolation barrier). *Let  $x_1, \dots, x_d$  be any  $d$  distinct nodes in an interval  $[a, b]$ , and let  $x^*$  satisfy  $\text{dist}(x^*, [a, b]) \geq b - a$ . The Lebesgue function at  $x^*$  satisfies  $\Lambda_d(x^*) \geq 2^{d-1}$ . Consequently, any polynomial extrapolation scheme that evaluates a degree- $(d - 1)$  interpolant at  $x^*$  from samples with pointwise error  $\delta$  can incur worst-case error at least  $\delta \cdot 2^{d-1}$  at  $x^*$ .*

*Proof.* Assume  $x^* \leq a - (b - a)$  (the case  $x^* \geq b + (b - a)$  follows by symmetry). Let  $x_{(1)} = \min_j x_j \geq a$  be the leftmost node. The corresponding Lagrange basis polynomial satisfies

$$|\ell_{(1)}(x^*)| = \prod_{i: x_i \neq x_{(1)}} \frac{|x_i - x^*|}{|x_i - x_{(1)}|} = \prod_{i: x_i \neq x_{(1)}} \left(1 + \frac{x_{(1)} - x^*}{x_i - x_{(1)}}\right).$$

Each factor has numerator shift  $x_{(1)} - x^* \geq a - (a - (b - a)) = b - a$  and denominator  $x_i - x_{(1)} \leq b - a$ , so every factor is at least 2. With  $d - 1$  such factors,  $|\ell_{(1)}(x^*)| \geq 2^{d-1}$ . Since  $\Lambda_d(x^*) = \sum_j |\ell_j(x^*)| \geq |\ell_{(1)}(x^*)|$ , the bound follows. For perturbed samples  $y_j = P(x_j) + e_j$  with  $|e_j| \leq \delta$ , the extrapolation error is

$$\tilde{P}(x^*) - P(x^*) = \sum_{j=1}^d e_j \ell_j(x^*).$$

Choosing adversarial signs  $e_j = \delta \operatorname{sign}(\ell_j(x^*))$  gives

$$|\tilde{P}(x^*) - P(x^*)| = \delta \sum_{j=1}^d |\ell_j(x^*)| = \delta \Lambda_d(x^*) \geq \delta \cdot 2^{d-1},$$

so the worst-case error can be at least  $\delta \cdot 2^{d-1}$ .  $\square$

**Theorem 8.3.2** rules out rescuing the  $\#P$ -hardness argument by tweaking interpolation details. Reordering nodes (equispaced, Chebyshev, or otherwise), changing polynomial bases, or reparameterizing variables cannot push amplification below  $2^{d-1}$ . At  $d = M = \text{poly}(n)$ , the needed precision stays at  $\varepsilon = 2^{-\Omega(n)}$ , far below  $2^{-n/2}$ . The same obstacle appears in quantum-advantage hardness arguments. Interpolation-based proofs for boson sampling [34], IQP sampling [35], and random circuit sampling [36] face analogous amplification barriers when moving from exponentially small to moderate error.

The interpolation barrier does not rule out  $\#P$ -hardness at  $2^{-n/2}$  by other methods. A proof that avoids polynomial extrapolation, for example through direct algebraic reductions or information-theoretic arguments, might still work. The barrier identifies the pressure point: we need a way to prove counting hardness without recovering exact integers from approximate real values.

What can be computed at precision  $2^{-n/2}$ ? We answer in the query model, where each query to a diagonal oracle  $O_H : |x\rangle|0\rangle \mapsto |x\rangle|E_x\rangle$  reveals one diagonal entry of  $H_z$  at unit cost. This model cleanly separates quantum and classical capabilities. The interpolation barrier is a classical obstruction: polynomial extrapolation cannot recover integers at this precision. A quantum algorithm can bypass that step entirely by using amplitude estimation rather than polynomial reconstruction.

**Theorem 8.3.3** (Quantum algorithm for  $A_1$ ). *There exists a quantum algorithm that estimates  $A_1(H_z)$  to additive precision  $\varepsilon$  using*

$$O\left(\sqrt{N} + \frac{1}{\varepsilon \Delta_1}\right) \tag{8.3.6}$$

*quantum queries to the diagonal oracle  $O_H$ , where  $\Delta_1 = E_1 - E_0$  is the spectral gap of  $H_z$ .*

*Proof.* The algorithm has two stages.

**Stage 1: Finding  $E_0$ .** The Hamiltonian  $H_z$  is diagonal in the computational basis, so computing  $E_x$  for a given  $|x\rangle$  requires one query to  $O_H$ . Finding the minimum of  $E_x$  over all  $x \in \{0, 1\}^n$  is an instance of quantum minimum finding [37], which succeeds with high probability in  $O(\sqrt{N})$  queries.

**Stage 2: Amplitude estimation of  $A_1$ .** Define the function

$$g(x) = \begin{cases} \frac{1}{E_x - E_0} & \text{if } E_x \neq E_0, \\ 0 & \text{if } E_x = E_0. \end{cases}$$

The spectral parameter is the mean  $A_1 = (1/N) \sum_x g(x)$ . Since the eigenvalues lie in  $[0, 1]$ , the values of  $g$  on non-ground states are in  $[1, 1/\Delta_1]$ . Rescaling to  $h(x) = \Delta_1 \cdot g(x)$  yields  $h(x) \in [0, 1]$ , and  $A_1 = \mu_h / \Delta_1$  where  $\mu_h = (1/N) \sum_x h(x)$ .

Construct a quantum oracle  $U_h$  acting as  $U_h : |x\rangle|0\rangle \mapsto |x\rangle(\sqrt{1-h(x)}|0\rangle + \sqrt{h(x)}|1\rangle)$ . The implementation queries  $O_H$  once to obtain  $E_x$ , performs classical arithmetic on an ancilla to compute  $h(x) = \Delta_1/(E_x - E_0)$  (or 0 for ground states), executes a controlled rotation  $R_y(2 \arcsin \sqrt{h(x)})$  on a flag qubit, and uncomputes the ancilla. Each application uses  $O(1)$  queries to  $O_H$  and  $O(\text{poly}(n))$  auxiliary gates.

Preparing the uniform superposition  $|+\rangle^{\otimes n}$  and applying  $U_h$ , the probability of measuring the flag qubit in  $|1\rangle$  is

$$p = \frac{1}{N} \sum_x h(x) = \mu_h.$$

Amplitude estimation [38] estimates  $p$  to additive precision  $\delta$  using  $O(1/\delta)$  applications of  $U_h$  and its inverse. Setting  $\delta = \varepsilon \Delta_1$  ensures  $|A_1 - \tilde{A}_1| = |\mu_h - \tilde{\mu}_h|/\Delta_1 \leq \varepsilon$ . The number of  $U_h$  applications is  $O(1/(\varepsilon \Delta_1))$ .

Combining both stages gives  $O(\sqrt{N})$  queries for Stage 1 and  $O(1/(\varepsilon \Delta_1))$  queries for Stage 2, yielding Eq. (8.3.6). For  $\varepsilon = 2^{-n/2}$  and  $\Delta_1 = 1/\text{poly}(n)$ , this becomes  $O(2^{n/2} + 2^{n/2} \text{poly}(n)) = O(2^{n/2} \text{poly}(n))$ .  $\square$

To confirm that the quantum algorithm's  $O(2^{n/2})$  query count is a genuine advantage, we need a classical lower bound. The natural route is information-theoretic. We ask how many samples a classical algorithm needs to distinguish two carefully chosen instances whose  $A_1$  values differ by  $\varepsilon$ .

**Theorem 8.3.4** (Classical lower bound for  $A_1$  estimation). *Any classical randomized algorithm estimating  $A_1(H_z)$  to additive precision  $\varepsilon$  in the query model requires  $\Omega(1/\varepsilon^2)$  queries in the worst case.*

*Proof.* We construct an adversarial pair of instances that are indistinguishable without sufficiently many queries.

**Instance construction.** Fix  $t = \lceil \varepsilon N \rceil$ . Instance  $H_0$  has a hidden set  $S \subseteq \{0, 1\}^n$  with  $|S| = N/2$ , and eigenvalues  $E_x = 0$  for  $x \in S$ ,  $E_x = 1$  otherwise. Instance  $H_1$  has  $|S'| = N/2 + t$  ground states. The spectral parameters are  $A_1(H_0) = 1/2$  and  $A_1(H_1) = (N/2 - t)/N = 1/2 - t/N$ , differing by  $t/N \geq \varepsilon$ . An algorithm estimating  $A_1$  to precision  $\varepsilon/2$  must distinguish the two instances.

**Information-theoretic bound.** A classical query at string  $x$  reveals  $E_x \in \{0, 1\}$ , which is equivalent to learning whether  $x \in S$ . Under a uniform prior on  $S$  (or  $S'$ ), successive queries follow a hypergeometric sampling model. Conditioned on earlier outcomes, the  $j$ -th query is a Bernoulli trial. Under hypothesis  $H_i$ ,  $x$  is a ground state with probability  $p_j^{(i)} = (|S_i| - g_{j-1})/(N - j + 1)$ , where  $g_{j-1}$  counts ground states already found. The difference  $p_j^{(1)} - p_j^{(0)} = t/(N - j + 1)$  is independent of  $g_{j-1}$ . Since both parameters are  $\Theta(1)$ , a Taylor expansion of binary KL divergence  $D(p\|p + \delta) = \delta^2/(p(1-p)) + O(\delta^3)$  with  $\delta = t/(N - j + 1)$  gives the conditional per-query divergence

$$D_j = O\left(\frac{t^2}{(N - j)^2}\right) = O\left(\frac{t^2}{N^2}\right)$$

when  $q \leq N/2$ . By the chain rule for KL divergence, the total information from  $q$  adaptive queries is

$$D_{\text{KL}}^{(q)} \leq \sum_{j=1}^q D_j \leq q \cdot O\left(\frac{t^2}{N^2}\right).$$

By Le Cam's two-point method [39], reliable hypothesis testing requires  $D_{\text{KL}}^{(q)} \geq \Omega(1)$ . Via Pinsker's inequality, total variation distance is at most  $\sqrt{D_{\text{KL}}/2}$ , and reliable distinguishing needs total variation  $\Omega(1)$ . Therefore

$$q \geq \Omega\left(\frac{N^2}{t^2}\right) = \Omega\left(\frac{1}{\varepsilon^2}\right).$$

At  $\varepsilon = 2^{-n/2}$ , this gives  $q \geq \Omega(2^n)$ .  $\square$

**Corollary 8.3.5** (Quadratic quantum-classical separation). *In the query model, estimating  $A_1(H_z)$  to precision  $\varepsilon = 2^{-n/2}$  exhibits a quadratic quantum-classical separation, with quantum complexity  $O(2^{n/2} \text{poly}(n))$  and classical complexity  $\Omega(2^n)$ .*

*Proof.* The upper bound is Theorem 8.3.3 with  $\Delta_1 = 1$  for the adversarial instance (or  $\Delta_1 = 1/\text{poly}(n)$  in general). The lower bound is Theorem 8.3.4. The separation ratio is  $\Omega(2^{n/2}/\text{poly}(n))$ , matching Grover's quadratic speedup for unstructured search.  $\square$

At the precision the adiabatic algorithm needs, quantum computation offers exactly the speedup the algorithm achieves.

The quantum bound in Theorem 8.3.3 is not only an upper bound; it is tight. For  $M = 2$  instances with  $\Delta_1 = 1$ , estimating  $A_1 = (N - d_0)/N$  to precision  $\varepsilon$  is equivalent to estimating  $d_0/N$  to precision  $\varepsilon$ , which is approximate counting. The Grover iterate  $G = (2|+\rangle\langle+| - I)(I - 2\Pi_S)$ , where  $\Pi_S$  projects onto the  $d_0$  ground states, has eigenphases  $\pm 2\theta$  with  $\sin^2 \theta = d_0/N$ . For  $d_0 \approx N/2$ , we have  $dp/d\theta = \sin 2\theta = 1$ , so precision  $\varepsilon$  in  $A_1$  requires precision  $\varepsilon$  in  $\theta$ . The Heisenberg limit for quantum phase estimation [40], together with the quantum Cramér-Rao inequality [41] and Fisher bound  $F_Q \leq 4T^2$ , gives  $T \geq 1/(2\varepsilon)$  applications of  $G$ ,

each with  $O(1)$  oracle cost. Combining this with the upper bound yields quantum query complexity  $\Theta(2^{n/2})$  at precision  $\varepsilon = 2^{-n/2}$ . The next chapter formalizes this theorem and ties it to the information cost of the adiabatic approach.

Two complementary frameworks apply here. Computational complexity asks whether a classical computer can extract  $A_1$  from an explicit Hamiltonian description  $(J_{ij}, h_j)$ . Query complexity asks how many oracle evaluations are information-theoretically necessary when diagonal entries are hidden behind  $O_H$ . A problem can be easy in one model and hard in the other. For  $A_1$  estimation, both frameworks show hardness, which supports the same conclusion: the pre-computation barrier is structural, not an artifact of one proof style.

In the computational model with an explicit Hamiltonian description, the precision-dependent hardness landscape is summarized below.

Precision $\varepsilon$	Hardness	Source
$1/\text{poly}(n)$	NP-hard	Theorem 8.1.2
$2^{-n/2}$	NP-hard	monotonicity
$2^{-\text{poly}(n)}$	#P-hard	Theorem 8.2.4

In the query model with a diagonal oracle at the algorithmically relevant precision  $\varepsilon = 2^{-n/2}$ , the comparison is:

Model	Complexity	Source
Quantum	$O(2^{n/2} \cdot \text{poly}(n))$	Theorem 8.3.3
Classical	$\Omega(2^n)$	Theorem 8.3.4

The precision  $2^{-n/2}$  is exactly the algorithmic target. The adiabatic schedule needs  $A_1$  to precision  $O(\sqrt{d_0/N})$ , which is  $O(2^{-n/2})$  in the worst case  $d_0 = O(1)$ . It is also where interpolation-based #P-hardness proofs break (Theorem 8.3.1), even though NP-hardness still follows by monotonicity. Finally, it is where query complexity separates sharply: the quantum algorithm uses  $O(2^{n/2})$  queries, while classical sampling requires  $\Omega(2^n)$ .

Classical sampling provides independent evidence for the hardness of  $A_1$  estimation at the algorithmic precision. Given a procedure that samples eigenvalues  $E_x$  according to the distribution  $\{d_k/N\}$ , estimating the mean  $A_1 = \mathbb{E}[1/(E_x - E_0)]$  to precision  $\delta_s$  requires  $O(1/\delta_s^2) = \tilde{O}(2^n/d_0)$  samples by Chebyshev's inequality. This matches the formal  $\Omega(2^n)$  lower bound of Theorem 8.3.4 up to logarithmic factors, providing a consistency check between the query-complexity result and concrete sampling algorithms.

The information barrier is not specific to adiabatic evolution. Consider the time-independent Hamiltonian  $H = -|\psi_0\rangle\langle\psi_0| + rH_\sigma$ , where  $r > 0$  is fixed and  $H_\sigma$  is the problem Hamiltonian. Evolving  $|\psi_0\rangle$  under  $H$  for time  $t$  produces oscillations between  $|\psi_0\rangle$  and the ground state of  $H_\sigma$ , with success probability controlled by  $r$ . The oscillation frequency is set by the spectral gap of  $H$ , and this gap is maximized when  $r$  is tuned to the avoided crossing, namely  $r = A_1$  (up to normalization). To keep success probability non-negligible,  $r$  must lie within  $O(2^{-n/2})$  of  $A_1$  [15]. Therefore the same barrier appears in this model as well. One still needs  $A_1$  to exponential precision, and computing it remains NP-hard. The obstacle comes from spectral structure, not from adiabatic formalism itself.

The results of this chapter create a tension. The adiabatic algorithm of Theorem 7.4.1 achieves Grover scaling  $\tilde{O}(\sqrt{N/d_0})$ , matching the unstructured-search lower bound. Yet the schedule depends on a spectral parameter whose computation is NP-hard, even at much coarser precision than the algorithm ultimately needs. In the circuit model, Grover achieves the same speedup without any spectral pre-computation because oracle queries gather information adaptively during execution. In the adiabatic framework, by contrast, the schedule must be fixed before evolution begins.

This asymmetry raises a precise question. Does the information cost of the adiabatic approach represent a fundamental limitation, or can it be circumvented? What runtime is achievable by an adiabatic algorithm that knows nothing about the problem Hamiltonian beyond its dimension? The next chapter formalizes this as an information-runtime tradeoff, proving a separation theorem for uninformed schedules and exploring whether adaptive measurements can bypass the classical pre-computation barrier.

# Chapter 9

## Information Gap

The adiabatic algorithm of [Theorem 7.4.1](#) achieves the Grover speedup  $\tilde{O}(\sqrt{N/d_0})$ , but its schedule depends on  $s^* = A_1/(A_1 + 1)$ , whose computation is NP-hard ([Theorem 8.1.2](#)). In the circuit model, Grover's algorithm achieves the same speedup without computing any spectral parameter. The adiabatic framework demands the schedule be fixed before evolution begins. What runtime is achievable by an adiabatic algorithm that knows nothing about the problem Hamiltonian beyond its dimension?

The spectral gap  $g(s)$  determines runtime through the physics of the interpolation. Our uncertainty about where that gap is smallest determines what runtime is achievable in practice. Whether that uncertainty matters at all depends on the computational model.

### 9.1 The Cost of Ignorance

Throughout this chapter, asymptotic notation  $(O, \Omega, \Theta)$  refers to the limit  $N \rightarrow \infty$  (equivalently  $n \rightarrow \infty$  with  $N = 2^n$ ). Unless stated otherwise, the spectral parameters  $d_0, M, \Delta, A_1, A_2$  and the target error  $\varepsilon$  are treated as fixed positive constants independent of  $n$ . When we write “ $O(T_{\text{inf}})$ ,” the hidden constant may depend on these spectral parameters but not on  $n$ .

A *fixed schedule* is chosen before the instance is revealed. It may depend on problem size  $n$  and target error  $\varepsilon$ , but not on instance-specific spectral data. An *instance-independent* algorithm uses the same Hamiltonian design for all energy assignments with the same degeneracy structure.

The NP-hardness of  $A_1$  is a statement about worst-case classical computation. It does not directly tell us how much runtime an adiabatic algorithm loses by not knowing  $A_1$ . If a fixed schedule that ignores  $A_1$  still achieved  $O(\sqrt{N/d_0})$ , the hardness would be academic. It is not.

The separation between informed and uninformed schedules is a minimax result. It can be viewed as a two-player game in which the schedule designer moves first and an adversary then chooses a worst-case gap function. To formalize this, we need a gap class broad enough to let the adversary place the minimum anywhere in an uncertainty interval  $[s_L, s_R]$ .

**Definition 9.1.1** (Gap class). *The gap class  $\mathcal{G}(s_L, s_R, \Delta_*)$  consists of all gap functions  $g : [0, 1] \rightarrow \mathbb{R}_{>0}$  such that the minimum  $g(s^*) = \Delta_*$  is achieved at a unique point  $s^* \in [s_L, s_R]$ , and  $g(s) > \Delta_*$  for all  $s \neq s^*$ .*

For the running example ( $M = 2, d_0 = 1, N = 4$ ),  $s^* = A_1/(A_1 + 1) = 3/7$  and  $\Delta_* = g_{\min} = 1/\sqrt{4} = 1/2$ . Any gap function in  $\mathcal{G}(0, 1, 1/2)$  has minimum value  $1/2$  somewhere in  $[0, 1]$ . The adversary controls where that minimum sits.

**Definition 9.1.2** (RC-admissible fixed schedules). *Fix a family of Hamiltonian instances. A fixed schedule  $u$  with velocity profile  $v(s) = |ds/dt|$  is RC-admissible on an instance if it satisfies the local Roland-Cerf condition*

$$v(s) \leq \frac{\varepsilon g(s)^2}{\|H'(s)\|} \quad \forall s \in [0, 1].$$

*It is uniformly RC-admissible on the family if this inequality holds for every instance in the family.*

The parameter  $\Delta_*$  denotes the minimum of the abstract gap function  $g$ . It should not be confused with  $\Delta = E_1 - E_0$  (the spectral gap of  $H_z$ ) or with  $g_{\min}$  (the minimum gap of the rank-one Hamiltonian  $H(s)$ ). For rank-one gap profiles,  $\Delta_* = g_{\min} = \Theta(\sqrt{d_0/(NA_2)})$ .

The schedule induces a velocity profile  $v(s) > 0$  on  $[0, 1]$ , with total evolution time  $T = \int_0^1 v(s)^{-1} ds$ .

Within the uniformly RC-admissible class (Definition 9.1.2), the crossing velocity obeys a pointwise bound. Since  $H'(s) = |\psi_0\rangle\langle\psi_0| + H_z$  satisfies  $\|H'(s)\| \leq \||\psi_0\rangle\langle\psi_0|\| + \|H_z\| \leq 1 + 1 = 2$  (using the eigenvalue normalization  $E_{M-1} \leq 1$  from Chapter 5), RC-admissibility gives  $v(s) \leq \varepsilon g(s)^2/2$ . At a crossing point where  $g = \Delta_*$ , this yields  $v \leq \varepsilon \Delta_*^2/2$ .

The crossing window has width  $\delta_s = \Theta(\Delta_*)$ , so any valid schedule must stay slow across that window. Chapter 5 gives  $\delta_s = \hat{g}/c_L$  (Equation 5.4.10), where  $\hat{g} = \frac{2A_1}{A_1+1}\sqrt{d_0/(NA_2)}$  and  $g_{\min} = (1 \pm O(\eta))\hat{g}$ . Since  $c_L = A_1(A_1+1)/A_2$  is fixed,  $\delta_s = \Theta(g_{\min}) = \Theta(\Delta_*)$ . Define  $v_{\text{slow}} = \varepsilon \Delta_*^2/2$  as the maximal crossing velocity. In the ratio  $T_{\text{unf}}/T_{\text{inf}}$ , this velocity cancels because both runtimes are computed under the same RC condition. The separation therefore depends on the geometric factor  $(s_R - s_L)/\Delta_*$ .

**Lemma 9.1.3** (Adversarial gap construction). *For any  $s_{\text{adv}} \in [s_L, s_R]$  and  $\Delta_* > 0$ , the gap function  $g_{\text{adv}}(s) = \Delta_* + (s - s_{\text{adv}})^2$  belongs to  $\mathcal{G}(s_L, s_R, \Delta_*)$ .*

*Proof.* The function satisfies  $g_{\text{adv}}(s_{\text{adv}}) = \Delta_*$ ,  $g_{\text{adv}}(s) > \Delta_*$  for  $s \neq s_{\text{adv}}$ , and  $g_{\text{adv}}(s) > 0$  for all  $s$ .  $\square$

**Lemma 9.1.4** (Velocity bound for uninformed schedules). *Let  $u$  be a fixed schedule that is uniformly RC-admissible on the rank-one family in Theorem 9.1.5. Then  $v(s) \leq v_{\text{slow}}$  for all  $s \in [s_L, s_R]$ , provided  $N$  is sufficiently large that  $\Delta_* < \min(1 - s_R, s_L)$ .*

*Proof.* Suppose  $v(s') > v_{\text{slow}}$  for some  $s' \in [s_L, s_R]$ . We construct a physical Hamiltonian in the rank-one family whose gap minimum occurs at  $s'$ , then apply RC-admissibility on that instance.

Since  $s^* = A_1/(A_1 + 1)$  is a continuous, strictly increasing function of  $A_1 \in (0, \infty)$  with range  $(0, 1)$ , there exists  $A_1$  placing the crossing at  $s'$ . On the two-level family with solution fraction  $\rho = d_0/N$ , the leading-order gap minimum is  $\hat{g} = 2(1 - s')\sqrt{\rho(1 - \rho)}$  (Equation 5.4.9), so choosing  $\rho$  to satisfy  $\hat{g} = \Delta_*$  (feasible whenever  $\Delta_* \leq 1 - s'$ , which holds asymptotically since  $\Delta_* = \Theta(2^{-n/2})$  and  $s' \leq s_R < 1$ ) produces a problem Hamiltonian  $H_z$  with crossing at  $s'$  and  $g_{\min} = \Theta(\Delta_*)$ . The adversary in the minimax game selects this physical Hamiltonian, not merely an abstract gap function.

Uniform RC-admissibility on this Hamiltonian gives  $v(s') \leq \varepsilon g_{\min}^2/\|H'(s')\| = \Theta(v_{\text{slow}})$ . After absorbing the fixed constant factor into  $v_{\text{slow}}$ , this contradicts  $v(s') > v_{\text{slow}}$ . Because  $s'$  was arbitrary in  $[s_L, s_R]$ , the bound holds throughout the interval.  $\square$

**Theorem 9.1.5** (Separation (uniformly RC-admissible class)). *Let  $T_{\text{unf}}$  be the minimum time over all fixed schedules that are uniformly RC-admissible for all rank-one instances whose gap minima satisfy  $s^* \in [s_L, s_R]$  and  $g_{\min} = \Theta(\Delta_*)$ , and let  $T_{\text{inf}}$  be the corresponding optimal informed runtime (with known  $s^*$ ) on the same rank-one family. Then*

$$\frac{T_{\text{unf}}}{T_{\text{inf}}} = \Omega\left(\frac{s_R - s_L}{\Delta_*}\right). \quad (9.1.1)$$

*Proof.* By Lemma 9.1.4,  $v(s) \leq v_{\text{slow}}$  for all  $s \in [s_L, s_R]$ . The uninformed time satisfies

$$T_{\text{unf}} = \int_0^1 \frac{ds}{v(s)} \geq \int_{s_L}^{s_R} \frac{ds}{v(s)} \geq \frac{s_R - s_L}{v_{\text{slow}}}. \quad (9.1.2)$$

The informed schedule knows  $s^*$  exactly and needs to be slow only in the crossing window of width  $O(\Delta_*)$ . For rank-one profiles,  $\delta_s = \hat{g}/c_L = \Theta(g_{\min}) = \Theta(\Delta_*)$  by Equation 5.4.10, so Theorem 7.4.1 gives  $T_{\text{inf}} = \Theta(\delta_s/v_{\text{slow}}) = \Theta(\Delta_*/v_{\text{slow}})$ . The velocity factors cancel:

$$\frac{T_{\text{unf}}}{T_{\text{inf}}} = \Omega\left(\frac{s_R - s_L}{\Delta_*}\right). \quad (9.1.3)$$

**Corollary 9.1.6** (Constant-width uncertainty family). *For any  $n$ -qubit rank-one family in which the minimum gap scales as  $\Delta_* = \Theta(2^{-n/2})$ , the crossing uncertainty interval has constant width  $s_R - s_L = \Theta(1)$ , and the endpoints are bounded away from the boundaries ( $\exists \gamma > 0$  independent of  $n$  with  $\gamma \leq s_L < s_R \leq 1 - \gamma$ ), the minimax separation satisfies*

$$\frac{T_{\text{unf}}}{T_{\text{inf}}} = \Omega(2^{n/2}).$$

This corollary is a worst-case uncertainty statement. It does not apply to the standard Grover setting, where the crossing location is known a priori ( $s^* = 1/2 + O(1/N)$ ). As an abstract-gap toy geometry with full uncertainty interval width  $s_R - s_L = 1$  and  $\Delta_* = 1/2$ , the separation ratio is  $(s_R - s_L)/\Delta_* = 2 = \sqrt{N}$  at  $N = 4$ .

The logical consequence is simple. If classical preprocessing is polynomial-time, NP-hardness forces a gap-uninformed model for fixed schedules. Inside the uniformly RC-admissible class, that model has an  $\Omega(2^{n/2})$  minimax lower bound from the adversarial geometry of Lemma 9.1.3. The penalty is therefore geometric, not a byproduct of the reduction alone.

## 9.2 Partial Knowledge and Hedging

The separation theorem quantifies a worst case. If an adversary can place the gap minimum anywhere in  $[s_L, s_R]$ , the schedule must be uniformly slow. But NP-hardness does not imply that  $A_1$  is completely unknown. The natural question is what partial knowledge is worth.

Suppose an algorithm has access to an estimate  $A_{1,\text{est}}$  satisfying  $|A_{1,\text{est}} - A_1| \leq \varepsilon$ . The uncertainty propagates to the crossing position through the map  $f(x) = x/(x+1)$ , whose derivative is  $f'(x) = 1/(x+1)^2$ .

**Lemma 9.2.1** ( $A_1$ -to- $s^*$  precision propagation). *If  $|A_{1,\text{est}} - A_1| \leq \varepsilon$  with  $|\varepsilon| \leq (1 + A_1)/2$ , then  $|s_{\text{est}}^* - s^*| \leq 2|\varepsilon|/(A_1 + 1)^2$ .*

*Proof.* Direct computation gives the exact identity

$$s_{\text{est}}^* - s^* = \frac{A_1 + \varepsilon}{1 + A_1 + \varepsilon} - \frac{A_1}{1 + A_1} = \frac{\varepsilon}{(1 + A_1)(1 + A_1 + \varepsilon)}. \quad (9.2.1)$$

Under  $|\varepsilon| \leq (1 + A_1)/2$ , the denominator satisfies  $1 + A_1 + \varepsilon \geq (1 + A_1)/2$ , so

$$|s_{\text{est}}^* - s^*| \leq \frac{|\varepsilon|}{(1 + A_1) \cdot (1 + A_1)/2} = \frac{2|\varepsilon|}{(1 + A_1)^2}. \quad (9.2.2) \quad \square$$

Given  $A_1$  precision  $\varepsilon$ , Lemma 9.2.1 places the true crossing within radius  $2\varepsilon/(A_1 + 1)^2$  of the estimate. The uncertainty interval therefore has width  $W(\varepsilon) = 4\varepsilon/(A_1 + 1)^2$ . Define the  $\varepsilon$ -informed gap class as  $\mathcal{G}_\varepsilon = \mathcal{G}(s_L(\varepsilon), s_R(\varepsilon), \Delta_*)$ , where the endpoints come from this interval. Applying Theorem 9.1.5 gives the lower bound. A matching upper bound comes from a schedule that stays uniformly slow on this interval and fast outside it.

**Theorem 9.2.2** (Interpolation). *For  $A_1$  precision  $\varepsilon$ , the optimal adiabatic runtime satisfies*

$$T(\varepsilon) = \Theta\left(T_{\text{inf}} \cdot \max\left(1, \frac{\varepsilon}{\delta_{A_1}}\right)\right), \quad (9.2.3)$$

where  $\delta_{A_1} = 2\sqrt{d_0 A_2 / N}$  is the precision threshold for optimality.

*Proof. Lower bound.* For  $\varepsilon \geq \delta_{A_1}$ , Theorem 9.1.5 applied to  $\mathcal{G}_\varepsilon$  gives  $T(\varepsilon) \geq W(\varepsilon)/v_{\text{slow}}$ . Taking the ratio with  $T_{\text{inf}} = \Theta(\delta_s/v_{\text{slow}})$  and using the identity

$$(A_1 + 1)^2 \cdot \delta_s = (A_1 + 1)^2 \cdot \frac{2}{(A_1 + 1)^2} \sqrt{\frac{d_0 A_2}{N}} = 2\sqrt{\frac{d_0 A_2}{N}} = \delta_{A_1} \quad (9.2.4)$$

yields  $T(\varepsilon)/T_{\text{inf}} \geq \Theta(\varepsilon/\delta_{A_1})$ . For  $\varepsilon < \delta_{A_1}$ , the trivial bound  $T(\varepsilon) \geq T_{\text{inf}}$  holds regardless of precision.

*Upper bound.* For  $\varepsilon \geq \delta_{A_1}$ , construct a schedule with crossing velocity  $v_{\text{slow}} = \Theta(\epsilon_{\text{ad}} \Delta_*^2) = \Theta(\Delta_*^2)$  throughout the uncertainty interval  $[s_L(\varepsilon), s_R(\varepsilon)]$ , where  $\epsilon_{\text{ad}}$  is the fixed adiabatic error parameter from Definition 9.1.2, and fast velocity  $v_{\text{fast}} = O(1)$  outside. The slow region has width  $W(\varepsilon) = \Theta(\varepsilon/\delta_{A_1}) \cdot \delta_s$ , so the total time is  $T = W(\varepsilon)/v_{\text{slow}} + O(1) = \Theta(T_{\text{inf}} \cdot \varepsilon/\delta_{A_1})$ , since  $T_{\text{inf}} = \Theta(\delta_s/v_{\text{slow}})$ . For  $\varepsilon < \delta_{A_1}$ , the optimal informed schedule achieves  $T = O(T_{\text{inf}})$ .  $\square$

The interpolation is linear. There is no threshold, cliff, or phase transition. At precision  $1/\text{poly}(n)$  (NP-hard), the overhead is  $\Theta(2^{n/2}/\text{poly}(n))$ , which is close to the full exponential penalty. At precision  $2^{-n/2}$  (algorithmically relevant), the overhead is  $\Theta(1)$ . The region between these scales is the “information gap.” For the running example, the precision table is:

Precision $\varepsilon$	$T(\varepsilon)/T_{\text{inf}}$
$2^{-n/2}$	$\Theta(1)$
$2^{-n/4}$	$\Theta(2^{n/4})$
$1/n$	$\Theta(2^{n/2}/n)$
$1/\text{poly}(n)$	$\Theta(2^{n/2}/\text{poly}(n))$
1 (no knowledge)	$\Theta(2^{n/2})$

The interpolation theorem treats  $A_1$  precision as a continuous resource. A complementary operational question asks for the best fixed schedule when  $s^*$  is only known to lie in an interval  $[u_L, u_R]$ . A hedging schedule

spreads slowdown across that full interval instead of concentrating it at one point. It uses velocity  $v_{\text{slow}}$  on  $[u_L, u_R]$  and  $v_{\text{fast}}$  outside, with normalization  $(u_R - u_L)/v_{\text{slow}} + (1 - u_R + u_L)/v_{\text{fast}} = 1$ .

Write  $w = u_R - u_L$  for the interval width. The JRS error functional integrates  $\|H'\|^2/g^3$ . Since  $\|H'(s)\| = O(1)$  for the rank-one family, the effective integrand is  $g^{-3}$ , unlike Roland-Cerf's  $g^{-2}$ . For a piecewise-constant velocity profile, [Equation 7.1.1](#) gives transition probability proportional to  $v \cdot \int g^{-3} ds$  on each segment. The total error is  $v_{\text{slow}} I_{\text{slow}} + v_{\text{fast}} I_{\text{fast}}$ , where  $I_{\text{slow}} = \int_{u_L}^{u_R} g(u)^{-3} du$  and  $I_{\text{fast}} = \int_{[0,1] \setminus [u_L, u_R]} g(u)^{-3} du$ . Because the crossing lies in the slow region,  $I_{\text{slow}} \gg I_{\text{fast}}$ .

**Theorem 9.2.3** (Hedging). *Let  $R = I_{\text{slow}}/I_{\text{fast}} \gg 1$ . Under normalization  $T = 1$ , the optimal hedging schedule for interval  $[u_L, u_R]$  achieves  $\text{Error}_{\text{hedge}}/\text{Error}_{\text{uniform}} \rightarrow u_R - u_L$  as  $R \rightarrow \infty$ , with optimal slow velocity  $v_{\text{slow}} = w + \sqrt{(1-w)w/R}$ .*

*Proof.* Write  $w = u_R - u_L$  for the interval width. The normalization constraint  $w/v_{\text{slow}} + (1-w)/v_{\text{fast}} = 1$  fixes the total time  $T = 1$ , so the JRS error integral of [Equation 7.1.1](#) reduces to  $E = v_{\text{slow}} I_{\text{slow}} + v_{\text{fast}} I_{\text{fast}}$ . The constraint gives

$$v_{\text{fast}} = \frac{(1-w)v_{\text{slow}}}{v_{\text{slow}} - w}, \quad (9.2.5)$$

valid for  $v_{\text{slow}} > w$ . Substituting into the error gives

$$E(v_{\text{slow}}) = v_{\text{slow}} I_{\text{slow}} + \frac{(1-w)v_{\text{slow}}}{v_{\text{slow}} - w} I_{\text{fast}}. \quad (9.2.6)$$

Differentiating with respect to  $v_{\text{slow}}$  and setting to zero:

$$\frac{dE}{dv_{\text{slow}}} = I_{\text{slow}} - \frac{(1-w)wI_{\text{fast}}}{(v_{\text{slow}} - w)^2} = 0. \quad (9.2.7)$$

Solving yields  $(v_{\text{slow}} - w)^2 = (1-w)wI_{\text{fast}}/I_{\text{slow}} = (1-w)w/R$ , so

$$v_{\text{slow}} = w + \sqrt{(1-w)w/R}. \quad (9.2.8)$$

At this optimum,  $v_{\text{fast}} = (1-w)v_{\text{slow}}/\sqrt{(1-w)w/R} = \sqrt{Rw(1-w)+(1-w)}$ . The optimal error, substituting  $v_{\text{slow}} - w = \sqrt{(1-w)w/R}$ , is

$$E_{\text{opt}} = (w + \sqrt{(1-w)w/R}) I_{\text{slow}} + (\sqrt{Rw(1-w)} + (1-w)) I_{\text{fast}}. \quad (9.2.9)$$

Since  $R = I_{\text{slow}}/I_{\text{fast}} \gg 1$ , the terms involving  $\sqrt{R}$  contribute  $2\sqrt{w(1-w)I_{\text{slow}}I_{\text{fast}}} = o(I_{\text{slow}})$ , and the dominant term is  $wI_{\text{slow}}$ , while the uniform error is  $E_{\text{unif}} = I_{\text{slow}} + I_{\text{fast}} \approx I_{\text{slow}}$ . Therefore  $E_{\text{opt}}/E_{\text{unif}} \rightarrow w = u_R - u_L$  as  $R \rightarrow \infty$ .  $\square$

For an uncertainty interval  $[0.4, 0.8]$ , the hedging schedule achieves error  $E_{\text{opt}}/E_{\text{unif}} = 0.4$  compared to a uniform schedule at the same total runtime, a 60% reduction in transition probability. Bounded uncertainty about  $s^*$  yields a constant-factor improvement proportional to the interval width, not an exponential overhead. The hedging schedule corresponds to Level 2 of the ignorance taxonomy developed in [section 9.7](#).

### 9.3 Quantum Bypass

The separation theorem and the interpolation theorem characterize the cost of ignorance within the fixed-schedule model. An adiabatic device, however, is a physical system that can be measured during execution. The original paper [\[15\]](#) posed the question: “Can this limitation be overcome when one only has access to a device operating in the adiabatic setting?”

The answer is yes in an adaptive measurement model. Han, Park, and Choi [\[42\]](#) independently proposed a constant geometric speed (CGS) schedule that traverses the eigenstate path at uniform arc length, using on-the-fly overlap estimates from quantum Zeno Monte Carlo to adjust the velocity. Their method improves the gap scaling from  $O(\Delta_*^{-2})$  to  $O(\Delta_*^{-1})$  and numerically preserves the quadratic speedup for adiabatic unstructured search without prior spectral knowledge. The binary-search protocol below uses a different mechanism. It first locates the crossing through branch probes, then runs the informed schedule; in the ideal decision-probe model it achieves  $O(T_{\text{inf}})$ .

NP-hardness bundles two different tasks. Computing  $s^*$  from the classical description of  $H_z$  is hard. Detecting  $s^*$  by probing the quantum system  $H(s)$  at selected parameter values can be efficient. We formalize this with a binary decision-probe oracle: a probe at parameter value  $s$  returns whether  $s$  is at-or-left of the true crossing or to its right (ties go left), and each probe costs  $O(1/g(s))$ .

**Definition 9.3.1** (Binary decision probe). *For an instance  $H$ , let  $D_H : [0, 1] \rightarrow \{0, 1\}$  be the idealized oracle*

$$D_H(s) = \begin{cases} 0, & s \leq s^*(H), \\ 1, & s > s^*(H), \end{cases}$$

*with probe cost  $O(1/g_H(s))$ .*

**Definition 9.3.2** (Adaptive adiabatic protocol). *The protocol operates in two phases.*

Phase 1 (Location). *Initialize  $s_{\text{lo}} = 0$ ,  $s_{\text{hi}} = 1$ . For  $i = 1, \dots, \lceil n/2 \rceil$ :*

1. Set  $s_{\text{mid}} = (s_{\text{lo}} + s_{\text{hi}})/2$ .
2. Query  $D_H(s_{\text{mid}})$ .
3. If  $D_H(s_{\text{mid}}) = 0$  (at or left of crossing), set  $s_{\text{lo}} = s_{\text{mid}}$ .
4. If  $D_H(s_{\text{mid}}) = 1$  (right of crossing), set  $s_{\text{hi}} = s_{\text{mid}}$ .

*After  $\lceil n/2 \rceil$  iterations,  $s^*$  is located to precision  $O(2^{-n/2})$ .*

Phase 2 (Execution). *Reset the state to  $|\psi_0\rangle$ . Evolve from  $s = 0$  to  $s = 1$  using the informed local schedule of Theorem 7.4.1, with the crossing position estimated in Phase 1.*

**Lemma 9.3.3** (Decision-probe cost). *Each call to  $D_H(s_{\text{mid}})$  costs  $O(1/g(s_{\text{mid}}))$ .*

*Proof.* Immediate from Definition 9.3.1. □

**Lemma 9.3.4** (Phase 1 cost). *The total time for Phase 1 is  $O(T_{\text{inf}})$ .*

*Proof.* Let  $d_i = |s_{\text{mid},i} - s^*|$  be the distance from the  $i$ -th midpoint to the true crossing. From the piecewise gap profile established in Chapter 6: outside the crossing window ( $|s - s^*| > \delta_s$ ), the gap satisfies  $g(s) \geq c_{\min}|s - s^*|$  where  $c_{\min} = \min(c_L, c_R)$  with  $c_L = A_1(A_1 + 1)/A_2$  and  $c_R = \Delta/30$  (both positive constants independent of  $n$ ); inside the crossing window ( $|s - s^*| \leq \delta_s$ ), the gap satisfies  $g(s) \geq g_{\min}$ . Since  $g_{\min}$  is the global minimum, both cases combine to

$$g(s_{\text{mid},i}) \geq \max(g_{\min}, c_{\min} \cdot d_i). \quad (9.3.1)$$

The probe cost at iteration  $i$  is therefore

$$O\left(\frac{1}{g(s_{\text{mid},i})}\right) \leq O\left(\min\left(\frac{1}{g_{\min}}, \frac{1}{c_{\min} \cdot d_i}\right)\right). \quad (9.3.2)$$

The two bounds in (9.3.2) cross at  $d_i = g_{\min}/c_{\min}$ . Since  $g_{\min} = c_L \delta_s \cdot (1 - O(\eta))$  and  $c_{\min} \leq c_L$ , the crossover distance satisfies  $d_{\text{cross}} = g_{\min}/c_{\min} = (c_L/c_{\min}) \delta_s \geq \delta_s$ . The ratio  $c_L/c_{\min}$  is a positive constant independent of  $n$ : both  $c_L = A_1(A_1 + 1)/A_2$  and  $c_R = \Delta/30$  are determined by the spectral parameters, so  $c_{\min} = \min(c_L, c_R) > 0$  is a fixed constant. At most  $O(\log(c_L/c_{\min}) + 1) = O(1)$  binary search midpoints fall in the near regime  $d_i \leq d_{\text{cross}}$ .

Group the  $\lceil n/2 \rceil$  iterations by the distance  $d_i$  in dyadic shells  $S_j = [2^{-j-1}, 2^{-j}]$ . Let  $L_i = 2^{-i+1}$  be the binary-search interval width at step  $i$ . Since the next interval is the half containing  $s^*$ , the midpoint distances obey

$$d_{i+1} = \left| d_i - \frac{L_i}{4} \right| = |d_i - 2^{-i-1}|.$$

This recurrence gives  $O(1)$  occupancy per shell: for  $i > j + 1$ ,  $d_i \leq L_i/2 = 2^{-i} < 2^{-j-1}$ , so  $d_i \notin S_j$ ; and for  $i \leq j$ , if  $d_i \in (2^{-j-1}, 2^{-j})$ , then  $d_{i+1} \notin (2^{-j-1}, 2^{-j})$ . Thus the shell interior is visited at most once, with only a dyadic-rational edge case where the boundary value  $2^{-j-1}$  can appear twice consecutively. Hence each shell contributes  $O(1)$  midpoint queries.

*Far shells* ( $j < \log_2(1/\delta_s) \approx n/2$ ): here  $d_i > \delta_s$ , so the binding bound in (9.3.2) is  $O(1/(c_{\min} \cdot d_i)) = O(2^j/c_{\min})$ , where  $c_{\min}$  enters the implicit constant.

*Near shells* ( $j \geq n/2$ ): here  $d_i \leq \delta_s$ , so the binding bound is  $O(1/g_{\min}) = O(1/\Delta_*) = O(2^{n/2})$ .

There are  $O(1)$  near shells (at most  $O(1)$  midpoints can have  $d_i \leq d_{\text{cross}}$  in a binary search). The total cost is:

$$\sum_{j=0}^{n/2-1} O(1) \cdot O(2^j) + O(1) \cdot O(2^{n/2}) = O(2^{n/2}) + O(2^{n/2}) = O(2^{n/2}) = O(T_{\text{inf}}). \quad (9.3.3)$$

The state preparation cost is  $O(n)$  per iteration and  $O(n)$  iterations, giving  $O(n^2) = o(T_{\text{inf}})$ . □

**Theorem 9.3.5** (Adaptive adiabatic optimality in the decision-probe model). *The adaptive protocol of Definition 9.3.2 achieves runtime  $T_{\text{adapt}} = O(T_{\text{inf}})$  with  $\Theta(n)$  measurements.*

*Proof.* Phase 1 locates  $s^*$  to precision  $O(2^{-n/2}) = O(\delta_s)$  using total time  $O(T_{\text{inf}})$  by Lemma 9.3.4. This precision is within the crossing window width  $\delta_s = O(\Delta_*)$ . Phase 2 has time  $O(T_{\text{inf}})$  by Theorem 7.4.1, since the estimate of  $s^*$  is accurate to  $O(\delta_s)$ . The total is  $O(T_{\text{inf}}) + O(T_{\text{inf}}) = O(T_{\text{inf}})$ .  $\square$

**Theorem 9.3.6** (Measurement lower bound). *Any adaptive algorithm in the binary decision-probe model (each measurement returns one bit indicating the ground/excited branch at the probe point) achieving  $T = O(T_{\text{inf}})$  requires  $\Omega(n)$  measurements.*

*Proof.* The crossing position  $s^*$  can lie anywhere in an interval of width  $\Theta(1)$ . To achieve the informed runtime, the algorithm must locate  $s^*$  to precision  $\delta_s = O(2^{-n/2})$ , since any larger uncertainty incurs the overhead of Theorem 9.2.2. This means distinguishing among  $\Omega(2^{n/2})$  possible positions. In the binary decision-probe model, each measurement contributes at most one bit by definition. The information needed is  $\log_2(2^{n/2}) = n/2$  bits, requiring  $\Omega(n)$  measurements.  $\square$

The three adiabatic regimes are:

Strategy	Runtime	Measurements
Fixed, uninformed	$\Omega(2^{n/2} \cdot T_{\text{inf}})$	0
Adaptive	$O(T_{\text{inf}})$	$\Theta(n)$
Fixed, informed	$O(T_{\text{inf}})$	0

For the running example ( $N = 4$ ,  $d_0 = 1$ ,  $n = 2$ ), Phase 1 performs  $\lceil 1 \rceil = 1$  probe at  $s_{\text{mid}} = 0.5$ , so the location stage already achieves width  $1/2 = O(2^{-n/2})$ . The gap at that point is  $g(0.5) = 1/\sqrt{N} = 1/2$ , which gives probe cost  $O(1/g) = O(2) = O(T_{\text{inf}})$ .

*Implementation note.* A physical instantiation of  $D_H$  can be attempted via phase-estimation-based branch tests on  $H(s_{\text{mid}})$ . The theorem above is intentionally stated in the ideal decision-probe model; a full finite-sample reliability analysis for this instantiation is separate from the present minimax argument.

The adaptive protocol acquires  $A_1$  through measurement, while the circuit model bypasses  $A_1$  entirely. The Dürr-Høyer minimum-finding algorithm [37] achieves  $\Theta(\sqrt{N/d_0})$  by maintaining a threshold and iteratively lowering it with Grover search. It never traverses an adiabatic path and never encounters an avoided crossing. Its mechanism is amplitude amplification with iterative thresholding and no spectral inputs: no  $A_1$ , no  $s^*$ , no  $\Delta$ , and no gap profile.

**Proposition 9.3.7** ( $A_1$ -blindness). *Let  $X_{\text{DH}}$  denote the output of the amplified Dürr-Høyer algorithm (with  $r = \Theta(n)$  repetitions). Then  $I(X_{\text{DH}}; A_1 | S_0, E_0) \leq 2^{-\Omega(n)}$ . Conditioned on success ( $X_{\text{DH}} \in S_0$ ), the mutual information is exactly zero.*

*Proof.* Two problem Hamiltonians  $H_z, H'_z$  are ground-equivalent if they share the same ground energy  $E_0$  and ground space  $S_0$ . By symmetry of Grover's algorithm applied to the uniform initial state, the output distribution conditioned on success is Uniform( $S_0$ ), regardless of the excited spectrum. Since  $A_1$  depends only on the excited spectrum (via  $\{d_k, E_k\}_{k \geq 1}$ ), we have

$$I(X_{\text{DH}}; A_1 | \text{success}, S_0, E_0) = 0.$$

Let  $F$  be the failure indicator of the amplified routine, and fix any prior over ground-equivalent instances conditioned on  $(S_0, E_0)$ . With  $r = \Theta(n)$  repetitions using Boyer-Brassard-Høyer-Tapp amplification [2], the per-trial success probability is at least  $2/3$ , so

$$p_f := \Pr[F = 1] \leq (1/3)^r = 2^{-\Omega(n)}.$$

Using chain rule and the fact that  $F$  is a function of  $X_{\text{DH}}$ :

$$\begin{aligned} I(X_{\text{DH}}; A_1 | S_0, E_0) &\leq I(X_{\text{DH}}, F; A_1 | S_0, E_0) \\ &= I(F; A_1 | S_0, E_0) + I(X_{\text{DH}}; A_1 | F, S_0, E_0) \\ &= I(F; A_1 | S_0, E_0) + p_f I(X_{\text{DH}}; A_1 | F = 1, S_0, E_0) \\ &\leq H(F) + p_f H(X_{\text{DH}} | F = 1, S_0, E_0). \end{aligned} \tag{9.3.4}$$

The  $F = 0$  term vanishes by the conditional independence established above. Now  $H(F) \leq h_2(p_f)$ , where  $h_2(p) = -p \log p - (1-p) \log(1-p)$  is the binary entropy, and  $H(X_{\text{DH}} | F = 1, S_0, E_0) \leq \log N = n$ , so Eq. (9.3.4) gives

$$I(X_{\text{DH}}; A_1 | S_0, E_0) \leq h_2(p_f) + p_f n = 2^{-\Omega(n)}.$$

$\square$

The circuit model does not merely avoid computing  $A_1$ ; it is provably blind to it. The fixed adiabatic model, by contrast, both requires and leaks information about  $A_1$ : a schedule tuned to one value of  $A_1$  performs poorly on ground-equivalent instances with different excited spectra. The adaptive adiabatic model lies between these extremes. It acquires  $A_1$  through  $O(n)$  measurements and pays  $O(T_{\text{inf}})$  to do so. The three models therefore form a clear hierarchy of spectral information usage, from blindness (circuit) through acquisition (adaptive) to fixed dependence (non-adaptive adiabatic).

The adaptive protocol relies on the rank-one gap profile, which grows linearly away from the crossing ( $\alpha = 1$ ). That linear growth is exactly what makes binary search informative: at distance  $d$  from the crossing, the gap is  $\Theta(d)$ , so a probe costs  $O(1/d)$  and the geometric sum converges. The next question is what changes when the gap approaches its minimum more gently.

## 9.4 Gap Geometry and Schedule Optimality

The flatness exponent  $\alpha$  parametrizes how the gap approaches its minimum:  $g(s) \approx c|s - s^*|^\alpha$  outside the crossing window. For rank-one profiles,  $\alpha = 1$ , and runtime scales as  $O(1/\Delta_*)$ . Flatter profiles with  $\alpha > 1$  are worse. Guo and An [27] identified a measure condition that governs when the  $p = 3/2$  power-law schedule reaches  $O(1/g_{\min})$ , and they proved this condition is sufficient. Here we prove the complementary degradation statement. When  $\alpha > 1$ , the measure condition fails, and the variationally optimal  $p = 3/2$  schedule degrades from  $T = O(1/\Delta_*)$  to  $T = O(1/\Delta_*^{3-2/\alpha})$ . Whether some non-power-law fixed schedule can still recover  $O(1/\Delta_*)$  in this regime remains open. The constant geometric speed (CGS) approach of Han, Park, and Choi [42] achieves  $O(1/g_{\min})$  by adaptive gap measurements, but that method uses runtime feedback and is not fixed. For fixed non-adaptive schedules, no family is known to beat  $O(1/\Delta_*^{3-2/\alpha})$  when  $\alpha > 1$ .

Consider a gap function with flatness exponent  $\alpha > 0$ . Near the minimum, write  $g(s) = \Delta_* + c|s - s^*|^\alpha$  for some constant  $c > 0$ . The measure condition asks for  $\mu(\{s : g(s) \leq x\}) \leq Cx$  for all  $x > 0$ , with  $C$  independent of  $\Delta_*$ .

**Theorem 9.4.1** (Geometric characterization). *The measure condition holds with  $C$  independent of  $\Delta_*$  if and only if  $\alpha \leq 1$ .*

*Proof.* For  $x \geq \Delta_*$ , the sublevel set  $\{s : g(s) \leq x\}$  near  $s^*$  has measure  $\mu = 2((x - \Delta_*)/c)^{1/\alpha}$ .

*Case  $\alpha \leq 1$ .* The ratio  $\mu/x = 2((x - \Delta_*)/c)^{1/\alpha}/x$  is increasing in  $x$  when  $\alpha \leq 1$ . Differentiating gives

$$\frac{d(\mu/x)}{dx} = \frac{2}{c^{1/\alpha}\alpha x^2} \left( \frac{x - \Delta_*}{c} \right)^{1/\alpha-1} \left( \left( \frac{1}{\alpha} - 1 \right) (x - \Delta_*) + \frac{\Delta_*}{\alpha} \right),$$

and both terms in the last parentheses are nonnegative because  $1/\alpha - 1 \geq 0$  and  $\Delta_* > 0$ . Now  $\mu$  is capped by 1 (the measure of  $[0, 1]$ ), and the cap is reached at  $x_{\text{cap}} = \Delta_* + c(1/2)^\alpha$ , where the sublevel set spans  $[0, 1]$ . For  $x > x_{\text{cap}}$ , we have  $\mu/x = 1/x < 1/x_{\text{cap}}$ . Hence

$$C = \sup_{x>0} \frac{\mu}{x} \leq \frac{1}{x_{\text{cap}}} \leq \frac{2^\alpha}{c},$$

independent of  $\Delta_*$ .

*Case  $\alpha > 1$ .* At  $x = 2\Delta_*$ , the ratio is  $\mu/x = 2(\Delta_*/c)^{1/\alpha}/(2\Delta_*) = c^{-1/\alpha}\Delta_*^{1/\alpha-1}$ . Since  $1/\alpha - 1 < 0$ , this diverges as  $\Delta_* \rightarrow 0$ . No finite  $C$  works for all  $\Delta_*$ .  $\square$

The gap integral  $\int_0^1 g(s)^{-\beta} ds$  controls the runtime for power-law schedules. A substitution  $u = c|s - s^*|^\alpha/\Delta_*$  gives the following scaling.

**Lemma 9.4.2** (Gap integral). *For  $\beta > 1/\alpha$ ,*

$$\int_0^1 g(s)^{-\beta} ds = \Theta(\Delta_*^{1/\alpha-\beta}). \tag{9.4.1}$$

*For  $\beta = 1/\alpha$ , the integral is  $\Theta(\log(1/\Delta_*))$ . For  $\beta < 1/\alpha$ , the integral is  $\Theta(1)$ .*

*Proof.* The substitution  $u = (c|s - s^*|^\alpha)/\Delta_*$  transforms the near-minimum contribution to

$$\Delta_*^{1/\alpha-\beta} \int_0^U u^{1/\alpha-1} (1+u)^{-\beta} du,$$

where  $U = \Theta(1/\Delta_*)$ . As  $u \rightarrow \infty$ , the integrand behaves like  $u^{1/\alpha-1-\beta}$ .

If  $\beta > 1/\alpha$ , the exponent is strictly less than  $-1$ , so the  $u$ -integral converges to a finite constant, yielding  $\Theta(\Delta_*^{1/\alpha-\beta})$ .

If  $\beta = 1/\alpha$ , the integrand is asymptotically  $u^{-1}$ , so the integral contributes  $\Theta(\log U) = \Theta(\log(1/\Delta_*))$ .

If  $\beta < 1/\alpha$ , the integral grows as  $U^{1/\alpha-\beta}$ , which cancels the prefactor  $\Delta_*^{1/\alpha-\beta}$ , giving  $\Theta(1)$ .

The contribution from outside a neighborhood of  $s^*$  is always  $O(1)$ . For fixed  $\delta$ , if  $|s - s^*| \geq \delta$  then  $g(s) \geq g_0 > 0$  independently of  $\Delta_*$ , so  $\int_{|s-s^*| \geq \delta} g(s)^{-\beta} ds \leq g_0^{-\beta}$ .  $\square$

**Theorem 9.4.3** (Scaling spectrum). *For a gap function with flatness exponent  $\alpha > 2/3$ , the adiabatic runtime with the  $p = 3/2$  power-law schedule (variationally optimal in the JRS framework [27]) satisfies*

$$T = \Theta(1/\Delta_*^{3-2/\alpha}). \quad (9.4.2)$$

*Proof.* The power-law schedule  $u'(s) = c_p g(u(s))^p$  has normalization constant  $c_p = \int_0^1 g(v)^{-p} dv$ . The JRS error functional becomes

$$\eta \leq \frac{1}{T} c_p \int_0^1 g(v)^{p-3} dv. \quad (9.4.3)$$

By Lemma 9.4.2,  $c_p = \Theta(\Delta_*^{1/\alpha-p})$  (requiring  $p > 1/\alpha$ ) and the second integral is  $\Theta(\Delta_*^{1/\alpha+p-3})$  (requiring  $3-p > 1/\alpha$ ). Together these require  $1/\alpha < p < 3-1/\alpha$ , an interval of width  $3-2/\alpha$ , which is positive if and only if  $\alpha > 2/3$ . The symmetric choice  $p = 3/2$  lies in this interval for all  $\alpha > 2/3$ . Their product is

$$c_p \int g^{p-3} dv = \Theta(\Delta_*^{(1/\alpha-p)+(1/\alpha+p-3)}) = \Theta(\Delta_*^{2/\alpha-3}). \quad (9.4.4)$$

Setting  $\eta = O(1)$  gives  $T = \Omega(\Delta_*^{-(3-2/\alpha)}) = \Omega(1/\Delta_*^{3-2/\alpha})$ . The  $p = 3/2$  power-law schedule achieves this scaling, giving a matching upper bound  $T = O(1/\Delta_*^{3-2/\alpha})$ .  $\square$

$\alpha$	Exponent $\gamma = 3 - 2/\alpha$	Measure condition	Runtime
1	1	Holds	$\Theta(1/\Delta_*)$
2	2	Fails	$\Theta(1/\Delta_*^2)$
3	7/3	Fails	$\Theta(1/\Delta_*^{7/3})$
$\infty$	3	Fails	$\Theta(1/\Delta_*^3)$

The runtime exponents form a continuous spectrum from 1 (V-shaped minimum, best case) to 3 (flat minimum, worst case), refuting any binary dichotomy between “easy” and “hard” gap profiles. For the running example ( $M = 2$ ,  $d_0 = 1$ ,  $N = 4$ ),  $\alpha = 1$  and  $\gamma = 1$ , confirming the optimal  $T = \Theta(1/\Delta_*)$  scaling.

**Remark.** *The exponent  $\gamma = 3$  at  $\alpha = \infty$  reflects the  $p = 3/2$  power-law schedule, which is variationally optimal within the JRS error functional but not universally optimal across all adiabatic bounds. The Roland-Cerf schedule ( $p = 2$ ) gives  $T = O(1/\Delta_*^2)$  at  $\alpha = \infty$  via a tighter adiabatic condition for flat gaps. The table shows the scaling of the JRS-optimal schedule as the gap flattens; different schedule families and adiabatic bounds produce different exponent curves.*

**Proposition 9.4.4** (Structural  $\alpha = 1$ ). *For the rank-one Hamiltonian  $H(s) = -(1-s)|\psi_0\rangle\langle\psi_0| + sH_z$  with  $d_1 \geq 1$  and  $\Delta > 0$ , the flatness exponent is  $\alpha = 1$ .*

*Proof.* Near  $s^*$ , the two lowest eigenvalues form an avoided crossing described by the standard formula  $g(s) = \sqrt{g_{\min}^2 + c_L^2(s-s^*)^2}$ . For  $|s - s^*| \gg g_{\min}/c_L = \delta_s$ , the gap grows linearly:  $g(s) \approx c_L|s - s^*|$ . The crossing is simple (not higher-order) because the coupling between the two lowest branches is proportional to  $|\langle\psi_0|\phi_1|^2 = d_1/N > 0$ , where  $|\phi_1\rangle$  is the symmetric state of the first excited level. A higher-order crossing ( $\alpha > 1$ ) would require this coupling to vanish, which cannot happen when  $d_1 > 0$ .  $\square$

No choice of  $H_z$  with  $d_1 > 0$  and  $\Delta > 0$  can produce  $\alpha \neq 1$ . Different values of  $\alpha$  require different interpolation schemes (e.g., quantum phase transitions with  $H(s)$  nonlinear in  $s$ , or systems with symmetry-enforced higher-order crossings). This structural  $\alpha = 1$  explains why both the Roland-Cerf analysis and the Guo-An framework achieve the same asymptotic runtime.

Braida et al. [15] and Guo and An [27] are independent works on the same problem class. The former provides the spectral analysis ( $A_1$ ,  $s^*$ , piecewise gap bounds), while the latter provides the variational optimization (power-law schedule, measure condition).

**Theorem 9.4.5** (Measure condition for the rank-one gap profile). *Under the spectral condition of Chapter 5, the piecewise-linear gap profile satisfies the measure condition with*

$$C \leq \frac{3A_2}{A_1(A_1 + 1)} + \frac{30(1 - s_0)}{\Delta}, \quad (9.4.5)$$

where  $s_0$  is the right-arm basepoint defined in Chapter 6.

*Proof.* Fix  $x > 0$ . For  $x < g_{\min}$ , the sublevel set is empty. For  $x \geq g_{\min}$ , bound the contribution from each piece of the gap profile. The left arm ( $g(s) \geq c_L(s^* - s)$ ) contributes at most  $x/c_L$ . The crossing window ( $|s - s^*| \leq \delta_s$ ) has width  $2\delta_s = 2\hat{g}/c_L$ , contributing at most  $2x/c_L$  for  $x \geq \hat{g}$  (for  $g_{\min} \leq x < \hat{g}$ : since  $g_{\min} \geq (1 - 2\eta)\hat{g}$  and  $x \geq g_{\min}$ , we have  $\hat{g} \leq x/(1 - 2\eta)$ ; for  $\eta \leq 1/6$ , this gives  $\hat{g} \leq 3x/2$ , so the window contribution  $2\hat{g}/c_L \leq 3x/c_L$ ; the condition  $\eta \leq 1/6$  holds in the asymptotic regime where  $\eta = O(\sqrt{d_0/(NA_2)}) \rightarrow 0$ ). The right arm ( $g(s) \geq c_R(s - s_0)/(1 - s_0)$ ) contributes at most  $x \cdot 30(1 - s_0)/\Delta$ . Combining and substituting  $c_L = A_1(A_1 + 1)/A_2$  gives the bound.  $\square$

**Corollary 9.4.6** (Grover measure constant). *For Grover ( $M = 2$ ,  $d_0 = 1$ ,  $d_1 = N - 1$ ,  $E_0 = 0$ ,  $E_1 = 1$ ), the exact measure constant is  $C = 1$ .*

*Proof.* The exact gap is  $g(s)^2 = (2s - 1)^2(1 - 1/N) + 1/N$ . Solving  $g(s) \leq x$  gives  $\mu(\{g \leq x\}) = \sqrt{(Nx^2 - 1)/(N - 1)}$  for  $x \in [1/\sqrt{N}, 1]$ , with  $\mu = 1$  for  $x > 1$ . The ratio  $\mu/x$  is increasing on  $[1/\sqrt{N}, 1]$  and equals 1 at  $x = 1$ .  $\square$

For the Grover problem, the exact gap integral is  $\int_0^1 g(s)^{-2} ds = (N/\sqrt{N-1}) \arctan \sqrt{N-1} \rightarrow (\pi/2)\sqrt{N}$  as  $N \rightarrow \infty$ . This closed-form evaluation confirms the  $O(\sqrt{N})$  runtime from the piecewise analysis and provides the exact constant. For the running example ( $N = 4$ ),  $\int_0^1 g(s)^{-2} ds = (4/\sqrt{3}) \arctan \sqrt{3} = 4\pi/(3\sqrt{3}) \approx 2.42$ , consistent with the runtime  $T_{\text{inf}} = O(\sqrt{4}) = O(2)$ .

Both the Roland-Cerf  $p = 2$  schedule and Guo-An's  $p = 3/2$  schedule achieve the same asymptotic runtime  $T = O(\sqrt{N/d_0}/\varepsilon)$  (where all spectral parameters  $A_1, A_2, \Delta$  are absorbed into the implicit constant, as declared at the start of this chapter). The RC runtime involves the integral  $I = \int_0^1 g(s)^{-2} ds$ ; Guo-An's involves  $C^2/g_{\min}$ .

**Theorem 9.4.7** (Constant comparison). *Write  $a = 3/c_L$  and  $r = 30(1 - s_0)/\Delta$ . Then  $C^2 < I$  if and only if  $(c_L - 1)r^2 - 2ar + a(1 - a) > 0$ . In the right-arm-dominated regime ( $r \gg a$ ) with  $c_L > 1$ , this holds, with  $C^2/I \rightarrow 1/c_L = A_2/(A_1(A_1 + 1))$ .*

*Proof.* With  $C = a + r$  and  $I = a + r^2c_L$ , we obtain

$$I - C^2 = (c_L - 1)r^2 - 2ar + a(1 - a).$$

For  $c_L > 1$  and  $r \gg a$ , the leading term  $(c_L - 1)r^2$  dominates.  $\square$

**Remark.** *The framework comparison extends across gap geometries. For  $\alpha < 1$ , the Roland-Cerf integral  $\int g^{-2} ds = \Theta(g_{\min}^{1/\alpha-2})$  grows slower than  $1/g_{\min}$ , making the RC analysis tighter. For  $\alpha = 1$ , both give  $\Theta(1/g_{\min})$ , and the JRS constant  $C^2$  can be smaller than the RC integral  $I$  (Theorem 9.4.7). For  $\alpha > 1$ , the measure constant  $C \rightarrow \infty$  as  $g_{\min} \rightarrow 0$ , so the JRS framework degrades and only the RC analysis applies. The structural  $\alpha = 1$  (Proposition 9.4.4) sits at the exact boundary where both frameworks are valid and neither uniformly dominates.*

For the Grover problem,  $c_L \rightarrow 2$  as  $N \rightarrow \infty$ . Using the exact values  $C_{\text{exact}} = 1$  and  $I_{\text{exact}} \rightarrow (\pi/2)\sqrt{N}$  gives  $C^2/I \rightarrow 2/(\pi\sqrt{N}) \rightarrow 0$ , so the JRS certification is asymptotically tighter. This comparison is unusually explicit because the Grover gap has a closed form. For structured Hamiltonians with richer spectra, exact constants are rarely analytic, and Theorem 9.4.7 becomes the practical tool. For example, evaluating it on the open ferromagnetic Ising chain (Equation 5.1.4 with nearest-neighbor coupling  $J = 1$ , uniform field  $h = 1$ , and  $n = 10$  spins) gives  $C^2/I = 0.71$ . The JRS advantage remains, but with a weaker margin than in Grover. The two frameworks are best viewed as complementary. The spectral analysis [15] identifies  $A_1, s^*$ , and the piecewise gap structure, while the variational analysis [27] identifies the optimal power-law exponent. Together they give a complete account of the rank-one  $\alpha = 1$  case, which sits exactly at the boundary where both frameworks apply and the measure condition remains bounded.

This complementarity persists under partial spectral knowledge. The RC framework ( $p = 2$ ) builds the schedule from crossing position  $s^*$ , so its runtime degrades on the crossing-localization scale:

$$T_{\text{RC}}(\varepsilon_{A_1}) = T_{\text{RC},\infty} \cdot \Theta\left(\max\left(1, \frac{\varepsilon_{A_1}}{\delta_{A_1}}\right)\right),$$

where  $\delta_{A_1} = 2\sqrt{d_0 A_2/N}$  is the threshold from [Theorem 9.2.2](#). The JRS framework ( $p = 3/2$ ) instead uses certified bounds  $(C_+, g_-)$  on the measure constant and minimum gap, leading to multiplicative overhead

$$\frac{(1 + \delta_C/C)^2}{1 - \delta_g/g_{\min}},$$

where  $\delta_C$  and  $\delta_g$  are estimation errors. The sensitivity profiles are therefore different: RC needs exponentially precise localization of  $s^*$ , while JRS needs only constant relative accuracy in  $C$  and  $g_{\min}$ . In the partial-information regime forced by NP-hardness, this can make JRS more robust in practice even though both methods share the same asymptotic scaling.

The gap geometry and optimality analysis above assumes the rank-one interpolation  $H(s) = -(1-s)|\psi_0\rangle\langle\psi_0| + sH_z$ . The rank-one structure is a design choice, not a physical constraint. Can a different design (different initial state, ancilla qubits, multi-segment path) avoid the  $A_1$  dependence entirely?

## 9.5 Anatomy of the Barrier

No instance-independent modification within the rank-one framework can make  $s^*$  spectrum-independent. The argument proceeds through four theorems that progressively close escape routes, culminating in a no-go theorem.

Recall from Chapter 5 that for any initial state  $|\psi\rangle \in \mathbb{C}^N$ , the weights  $w_k(\psi) = \sum_{z \in \Omega_k} |\langle z | \psi \rangle|^2$  determine the effective spectral parameter  $A_1^{\text{eff}}(\psi) = \sum_{k \geq 1} w_k(\psi)/(E_k - E_0)$  and the effective crossing position  $s^*(\psi) = A_1^{\text{eff}}(\psi)/(A_1^{\text{eff}}(\psi) + 1)$ . For the uniform superposition  $|\psi_0\rangle$ ,  $w_k = d_k/N$  and  $A_1^{\text{eff}} = A_1$ .

**Theorem 9.5.1** (Product ancilla invariance). *For any product initial state  $|\Psi\rangle = |\psi_0\rangle \otimes |\phi\rangle$  and uncoupled final Hamiltonian  $H_f = H_z \otimes I_{2^m}$ , the extended Hamiltonian  $H_{\text{ext}}(s) = -(1-s)|\Psi\rangle\langle\Psi| + s(H_z \otimes I_{2^m})$  has the same crossing position  $s^* = A_1/(A_1 + 1)$  as the bare system.*

*Proof.* Decompose the extended Hilbert space  $\mathbb{C}^N \otimes \mathbb{C}^{2^m}$  into the subspace  $\mathcal{V}_\phi = \mathbb{C}^N \otimes |\phi\rangle$  and its orthogonal complement. States  $|z\rangle \otimes |a\rangle$  with  $\langle\phi|a=0$  satisfy  $\langle\Psi|z,a=0$ , making them exact eigenstates of  $H_{\text{ext}}(s)$  with eigenvalue  $sE(z)$ . These  $N(2^m - 1)$  states do not participate in the avoided crossing. The restriction of  $H_{\text{ext}}(s)$  to  $\mathcal{V}_\phi$  is unitarily equivalent to the bare Hamiltonian  $H(s)$  via the isomorphism  $|\psi\rangle \otimes |\phi\rangle \mapsto |\psi\rangle$ .  $\square$

**Remark.** *The crossing position is invariant, but the gap of  $H_{\text{ext}}(s)$  is strictly smaller than the bare gap: for  $d_0 = 1$ , the extra eigenvalues at  $sE_0$  (from states  $|z\rangle \otimes |a\rangle$  with  $z \in \Omega_0, a \perp |\phi\rangle$ ) sit between the ground eigenvalue  $\lambda_0(s) < sE_0$  and the crossing branch. Uncoupled ancillas make the gap worse, not better.*

**Theorem 9.5.2** (Universality of uniform superposition). *Among all states  $|\psi\rangle \in \mathbb{C}^N$ , the uniform superposition  $|\psi_0\rangle$  is the unique state (up to per-basis-element phases) for which the weights  $w_k(\psi)$  depend only on  $\{E_k, d_k\}$  and not on the specific assignment of energies to computational basis states.*

*Proof.* An energy assignment is a function  $\sigma : \{0, \dots, N-1\} \rightarrow \{E_0, \dots, E_{M-1}\}$  with  $|\sigma^{-1}(E_k)| = d_k$ . The weights under assignment  $\sigma$  are  $w_k(\psi, \sigma) = \sum_{z: \sigma(z)=E_k} |\langle z | \psi \rangle|^2$ . We require  $w_k(\psi, \sigma) = w_k(\psi, \sigma')$  for all assignments  $\sigma, \sigma'$  with the same degeneracies.

Any two such assignments are related by a permutation  $\pi$  of  $\{0, \dots, N-1\}$ . The condition becomes  $\sum_{z \in \Omega_k} |\langle z | \psi \rangle|^2 = \sum_{z \in \Omega_k} |\langle \pi^{-1}(z) | \psi \rangle|^2$  for all  $k$  and all permutations  $\pi$ .

*Necessity.* Consider two-level spectra with  $d_0 = 1$ . For any two basis states  $z_a, z_b$ , the transposition swapping them maps the assignment  $\sigma$  (with  $\sigma(z_a) = E_0$ ) to  $\sigma'$  (with  $\sigma'(z_b) = E_0$ ). The condition forces  $|\langle z_a | \psi \rangle|^2 = |\langle z_b | \psi \rangle|^2$ . Since  $z_a, z_b$  are arbitrary,  $|\langle z | \psi \rangle|^2 = 1/N$  for all  $z$ .

*Sufficiency.* If  $|\langle z | \psi \rangle|^2 = 1/N$  for all  $z$ , then  $w_k = d_k/N$  regardless of the assignment.  $\square$

**Corollary 9.5.3.** *Any instance-independent adiabatic algorithm (same Hamiltonian for all energy assignments with the same degeneracy structure) must use the uniform superposition as initial state, fixing the crossing at  $s^* = A_1/(A_1 + 1)$ .*

**Theorem 9.5.4** (Coupled ancilla limitation). *Consider an extended Hamiltonian  $H_{\text{ext}}(s) = -(1-s)|\Psi\rangle\langle\Psi| + s(H_z \otimes I + V)$  where  $|\Psi\rangle = |\psi_0\rangle \otimes |\phi\rangle$  and  $V$  is instance-independent. No fixed  $V$  makes  $A_1^{\text{eff}}$  constant across all problem instances.*

*Proof.* Consider the two-level family parametrized by  $\Delta > 0$ , with  $E_0 = 0$ ,  $E_1 = \Delta$ ,  $d_0 = 1$ , and  $d_1 = N - 1$ . For  $\Delta > 2\|V\|$ , Weyl's inequality implies that each eigenvalue of  $H_f(\Delta) = H_z(\Delta) \otimes I + V$  lies within  $\|V\|$  of an eigenvalue of  $H_z(\Delta) \otimes I$ . The spectrum therefore splits into two separated clusters, one near energy 0 and one

near energy  $\Delta$ . For each eigenvalue  $E_j$  in the excited cluster,  $|E_j - \Delta| \leq \|V\|$ . Hence the excited contribution to  $A_1^{\text{eff}}$  is

$$\sum_{j \in \text{excited}} \frac{|\langle \Psi \rangle \phi_j|^2}{E_j - E_0} = \frac{1 - d_0/N}{\Delta + O(\|V\|)} = \Theta(1/\Delta)$$

for  $\Delta \gg \|V\|$ . Because  $\|V\|$  is fixed independently of  $\Delta$ , this contribution varies with  $\Delta$ , so  $A_1^{\text{eff}}(\Delta)$  cannot be constant.  $\square$

**Theorem 9.5.5** (Multi-segment rigidity). *Consider a two-segment path where segment 2 has Hamiltonian  $H_2(t) = -(1-t)|\psi_{\text{mid}}\rangle\langle\psi_{\text{mid}}| + tH_z$ . If the algorithm is instance-independent, then the intermediate state  $|\psi_{\text{mid}}\rangle$  must be the uniform superposition, giving the same crossing  $B_1 = A_1$ .*

*Proof.* Segment 2 is a rank-one adiabatic Hamiltonian with initial state  $|\psi_{\text{mid}}\rangle$ . Its crossing position is  $t^* = B_1/(B_1+1)$  where  $B_1 = \sum_{k \geq 1} w_k(\psi_{\text{mid}})/(E_k - E_0)$ . If segment 1 does not involve  $H_z$ , then  $|\psi_{\text{mid}}\rangle$  is determined entirely by segment 1's Hamiltonian, which is instance-independent. Since  $|\psi_{\text{mid}}\rangle$  is then the same for all energy assignments with the same degeneracy structure, Theorem 9.5.2 forces  $w_k = d_k/N$ , so  $B_1 = A_1$ . If segment 1 involves  $H_z$ , then  $|\psi_{\text{mid}}\rangle$  already depends on the spectrum, and the algorithm is not instance-independent.  $\square$

**Theorem 9.5.6** (No-go). *For any adiabatic algorithm using a rank-one initial Hamiltonian, a final Hamiltonian whose ground state encodes the solution, and instance-independent design, the crossing position cannot be made independent of the problem spectrum.*

*Proof.* Combine Theorems 9.5.1–9.5.5. Theorem 9.5.2 forces the uniform superposition. Theorem 9.5.1 shows that uncoupled ancillas preserve  $s^*$ . Theorem 9.5.4 shows that coupled ancillas can shift  $s^*$  but cannot make it constant. Theorem 9.5.5 rules out escape through multi-segment paths inside the rank-one framework.  $\square$

For the running example ( $N = 4, d_0 = 1$ ), product ancilla invariance (Theorem 9.5.1) implies that appending any number of ancilla qubits in a product state leaves the crossing at  $s^* = 3/7$ .

The no-go theorem is specific to the rank-one framework with instance-independent design. A natural next idea is to move to higher-rank initial Hamiltonians. The next propositions show this does not solve the problem. Rank- $k$  projectors still cannot make crossing positions spectrum-independent, first on two-level families and then on general multilevel families through a trace argument. For rank- $k$  projectors  $P = UU^\dagger$ , the secular equation becomes the  $k \times k$  determinant condition  $\det(I_k - (1-s)G(\lambda, s)) = 0$ , where  $G(\lambda, s) = U^\dagger(sH_z - \lambda I)^{-1}U$ . On the two-level family ( $E_0 = 0, E_1 = \Delta$ ), this reduces to  $\det(I_k - (x/\Delta)B) = 0$ , with  $B = U_{\text{exc}}^\dagger U_{\text{exc}}$  and  $x = (1-s)/s$ . Each positive eigenvalue  $\mu$  of  $B$  gives a crossing branch  $s(\Delta) = 1/(1 + \Delta/\mu)$ , and this branch is non-constant in  $\Delta$ .

**Proposition 9.5.7** (Rank- $k$  two-level obstruction). *Fixed rank- $k$  projectors cannot make crossing positions spectrum-independent on fixed-degeneracy two-level families unless the projector has zero support on excited states.*

For the general multilevel case, the trace argument provides a clean obstruction.

**Proposition 9.5.8** (Trace no-go). *For a rank- $k$  projector  $P = UU^\dagger$  and the multilevel family with gaps  $\Delta_1, \dots, \Delta_{M-1}$ , define the reduced matrix  $A(\Delta) = \sum_{\ell=1}^{M-1} B_\ell / \Delta_\ell$  where  $B_\ell = U_\ell^\dagger U_\ell \succeq 0$  collects the excited-level contributions. If  $B_j \neq 0$  and  $\Delta_j$  varies, then  $\text{tr}(A(\Delta)) = \sum_\ell \text{tr}(B_\ell) / \Delta_\ell$  is non-constant in  $\Delta_j$ . By Weyl's eigenvalue monotonicity theorem, each eigenvalue of  $A(\Delta)$  is a continuous function of  $\Delta_j$ , and the sum of the positive eigenvalues equals  $\text{tr}(A)$ . Since the trace changes, at least one positive eigenvalue, and hence at least one crossing position, must change with  $\Delta_j$ .*

**Remark.** When the excited blocks commute ( $[B_\ell, B_m] = 0$  for all  $\ell, m$ ), the reduced crossing equation can be simultaneously diagonalized. This gives explicit per-branch formulas. For each active branch  $r$  with  $G_r(\Delta) = \sum_\ell \mu_{\ell r} / \Delta_\ell > 0$ , the crossing position is  $s_r = G_r / (1 + G_r)$ . Varying any gap  $\Delta_j$  yields

$$\frac{\partial s_r}{\partial \Delta_j} = -\frac{\mu_{jr}}{\Delta_j^2 (1 + G_r)^2} \leq 0,$$

with strict inequality whenever  $\mu_{jr} > 0$ . So the commuting case gives explicit quantitative non-constancy for each branch, complementing the trace argument's aggregate statement. Even this most tractable version of the generalized secular equation cannot produce spectrum-independent crossings.

The barrier is structural within the rank-one framework and extends to higher-rank families. Whether time-dependent couplings or non-rank-one intermediate Hamiltonians provide a genuine escape remains open. But the no-go is specific to the monotone-schedule adiabatic framework. Dropping the monotone constraint reveals that constant controls already suffice on the restricted two-level family.

**Proposition 9.5.9** (Constant-control optimality on two-level family). *For  $H_z = I - P_0$  where  $P_0$  projects onto the  $d_0$ -dimensional ground space, the continuous-time rank-one Hamiltonian  $H = -|\psi_0\rangle\langle\psi_0| + H_z$  with constant controls achieves  $p_0(t^*) = 1$  at  $t^* = (\pi/2)\sqrt{N/d_0}$ , with controls independent of  $A_1$  (on the two-level family  $H_z = I - P_0$ ).*

*Proof.* Let  $\mu = d_0/N$ ,  $|G\rangle = d_0^{-1/2} \sum_{x \in S_0} |x\rangle$ , and  $|B\rangle = (N - d_0)^{-1/2} \sum_{x \notin S_0} |x\rangle$ . The initial state is  $|\psi_0\rangle = \sqrt{\mu} |G\rangle + \sqrt{1-\mu} |B\rangle$ . Dropping the global identity term, the effective Hamiltonian in the  $(|G\rangle, |B\rangle)$  basis is

$$\tilde{H} = -\begin{pmatrix} \mu & \sqrt{\mu(1-\mu)} \\ \sqrt{\mu(1-\mu)} & -\mu \end{pmatrix}, \quad (9.5.1)$$

which satisfies  $\tilde{H}^2 = \mu I_2$ . The matrix exponential is  $e^{-it\tilde{H}} = \cos(\sqrt{\mu}t) I_2 - i \sin(\sqrt{\mu}t) \tilde{H}/\sqrt{\mu}$ . Applying to  $|\psi_0\rangle$  and computing the ground-state probability:

$$p_0(t) = |\langle G \rangle e^{-it\tilde{H}} |\psi_0|^2 = \mu + (1-\mu) \sin^2(\sqrt{\mu}t). \quad (9.5.2)$$

At  $t^* = (\pi/2)/\sqrt{\mu} = (\pi/2)\sqrt{N/d_0}$ ,  $\sin^2(\sqrt{\mu}t^*) = 1$ , so  $p_0(t^*) = 1$ .  $\square$

On the two-level family, the Hamiltonian self-calibrates through a Rabi-like oscillation at frequency  $\sqrt{\mu} = \sqrt{d_0/N}$ . The time-independent Hamiltonian  $H_r = -|\psi_0\rangle\langle\psi_0| + r \cdot H_z$  with  $r = 1$  is optimal without explicit knowledge of  $A_1$  [43]. For general spectra, the resonance shifts to  $r^* = A_1$  [43], so the calibration problem changes from classical computation of  $A_1$  to quantum detection of a resonance.

A natural approach is Loschmidt-echo measurement. Evolve under  $H_r$  and measure return probability  $|\langle\psi_0\rangle e^{-iH_rt}\psi_0|^2$ , which oscillates with large amplitude near resonance and stays close to 1 away from resonance. On two-level families this works cleanly: binary search over  $r$  with  $O(n)$  probe measurements, each costing  $O(1/g_{\min})$ , locates  $r^*$  with polynomial overhead (details in [43]). For general multilevel spectra, additional excited-state frequencies can mask the resonance signal. Whether one can efficiently deconvolve this multilevel echo, or replace it with a better observable, remains open.

The constant-control counterexample applies only to the two-level family  $H_z = I - P_0$ . Under normalized controls, the barrier reappears.

**Proposition 9.5.10** (Normalized-control lower bound). *Under normalized controls  $|g(t)| \leq 1$  and the scaled family  $H_z^{(\delta)} = \delta(I - P_0)$  with minimum excitation  $\delta \in (0, 1]$ , any instance-independent algorithm achieving success probability  $\geq 2/3$  requires  $T = \Omega(\sqrt{N/d_0}/\delta)$ .*

*Proof.* The oracle-dependent term  $g(t)H_z^{(\delta)} = \delta g(t)(I - P_0)$  has instantaneous oracle strength  $\delta|g(t)|$ . The total oracle action is  $\mathcal{A} = \int_0^T \delta|g(t)| dt \leq \delta T$ . The continuous-time query lower bound for unstructured search with  $d_0$  marked items among  $N$  gives  $\mathcal{A} = \Omega(\sqrt{N/d_0})$  [44], so  $T = \Omega(\sqrt{N/d_0}/\delta)$ .  $\square$

For  $\delta = N^{-1/2}$ , this yields  $T = \Omega(N/\sqrt{d_0})$ , the same exponential penalty as the fixed-schedule adiabatic model. So the barrier reappears on worst-case instances even for general continuous-time rank-one algorithms when controls are normalized. The scope is precise: the obstruction comes from monotone schedules with bounded controls, not from continuous-time quantum computation itself.

## 9.6 Computational Nature of $A_1$

The barrier cannot be designed away. What kind of hardness is it? The quantity  $A_1$  is not merely NP-hard to compute. Its core hardness is counting hardness inherited from partition-function structure. The tractability boundary does not align with optimization hardness, is not controlled by the number of solutions alone, and depends on structural properties of the energy landscape.

The quantity  $A_1$  encodes spectral information beyond the minimum gap. Consider three energy levels with  $E_0 = 0$  ( $d_0 = 1$ ),  $E_1 = 1/n$  ( $d_1 = 1$ ),  $E_2 = 1$  ( $d_2 = N - 2$ ). Then  $\Delta = 1/n \rightarrow 0$  but  $A_1 = (n + N - 2)/N \rightarrow 1$ , so  $1/\Delta \rightarrow \infty$  while  $A_1 = \Theta(1)$ . The tail of  $N - 2$  states at energy 1 contributes  $(N - 2)/N \approx 1$  to  $A_1$ , dominating the single state at the gap edge that contributes  $n/N \approx 0$ . The crossing position  $s^* = A_1/(A_1 + 1) \approx 1/2$  is

determined by the bulk of the spectrum, not by the gap, making  $A_1$  fundamentally a whole-spectrum quantity that  $\Delta$  alone cannot predict.

The distinction between NP-hardness at precision  $1/\text{poly}(n)$  ([Theorem 8.1.2](#)) and #P-hardness exactly ([Theorem 8.2.4](#)) matters because  $A_1$  is fundamentally a counting quantity.

**Proposition 9.6.1** ( $A_1$  hardness is counting hardness). *For Boolean CSPs where counting satisfying assignments is #P-hard (including  $k$ -SAT for  $k \geq 2$ ), computing  $A_1$  of the clause-violation Hamiltonian is #P-hard even restricted to satisfiable instances.*

*Proof.* Encode the CSP as  $H_z = \sum_{j=1}^m C_j$  where each  $C_j(x) = 1$  if assignment  $x$  violates clause  $j$ . The interpolation argument ([Theorem 8.2.4](#)) recovers all degeneracies  $d_k$  from polynomially many evaluations of  $A_1$  with shifted parameters, via Lagrange interpolation on the rational function  $f(x) = \sum_k d_k / (\Delta_k + x/2)$ . For satisfiable CSPs,  $d_0$  counts satisfying assignments, and counting is #P-hard by hypothesis.  $\square$

The partition function connection makes this precise. Shifting energies so that  $E_0 = 0$  and defining the Laplace partition function  $Z(\beta) = \sum_x e^{-\beta E(x)}$ , the spectral parameter admits the integral representation

$$A_1 = \frac{1}{N} \int_0^\infty (Z(\beta) - d_0) d\beta. \quad (9.6.1)$$

For integer spectra with  $E(x) \in \{0, 1, \dots, m\}$ , the ordinary generating function  $Z(t) = \sum_x t^{E(x)}$  gives  $A_1 = (1/N) \int_0^1 (Z(t) - d_0)/t dt$ . Both representations appear to require knowing  $d_0$ , which is itself a counting-hard quantity for many CSPs. However, for additive approximation it suffices to replace  $d_0$  by the single evaluation  $Z(\tau)$  at a small  $\tau > 0$ . Define the  $\tau$ -truncated proxy

$$A_1^{(\tau)} = \frac{1}{N} \int_\tau^1 \frac{Z(t) - Z(\tau)}{t} dt. \quad (9.6.2)$$

The additive error satisfies  $0 \leq A_1 - A_1^{(\tau)} \leq \tau(1 + \ln(1/\tau))$ , so choosing  $\tau = O(\eta/\ln(1/\eta))$  gives an  $\eta$ -approximation to  $A_1$  without direct access to  $d_0$ . When  $E_0$  is known, this coarse form is already useful. Sampling from the Boltzmann distribution at inverse temperature  $\beta$  gives an unbiased estimator of  $Z(\beta)/Z(0) = Z(\beta)/N$ , and integrating via (9.6.1) yields an additive approximation to  $A_1$  without counting  $d_0$  explicitly. In this way, “compute  $A_1$ ” becomes a partition-function problem, and tractability of  $A_1$  tracks tractability of counting.

**Proposition 9.6.2** (Bounded treewidth tractability). *For local energy functions  $E(x) = \sum_j E_j(x_{S_j})$  with bounded locality  $|S_j| \leq k$  and a tree decomposition of the primal graph of width  $w$ ,  $A_1$  is computable exactly in  $\text{poly}(n, m) \cdot 2^{O(w)}$  time.*

*Proof.* Write the partition-function polynomial as  $Z(t) = \sum_x t^{E(x)} = \sum_{q=0}^m d_q t^q$ , and also in factor-graph form as  $Z(t) = \sum_x \prod_j t^{E_j(x_{S_j})}$ . Variable elimination on the tree decomposition then computes  $Z(t)$  exactly. At each elimination step, factor tables have at most  $2^{w+1}$  entries, each a polynomial of degree at most  $m$ . Multiplying factors convolves polynomials at cost  $O(m^2)$  per entry, and summing out a variable adds two polynomials at cost  $O(m)$ . After  $n$  elimination steps, we recover  $Z(t) = \sum_q d_q t^q$ , and then  $A_1 = (1/N) \sum_{q>E_0} d_q / (q - E_0)$ .  $\square$

The treewidth condition is sufficient, not necessary. A simpler criterion applies when the spectrum itself is simple. If  $H_z$  has at most  $\text{poly}(n)$  distinct energy levels with known energies and degeneracies, then  $A_1 = (1/N) \sum_{k \geq 1} d_k / (E_k - E_0)$  is directly computable in  $\text{poly}(n)$  time from its defining sum. This is complementary to bounded treewidth and applies whenever the spectrum is structurally simple, regardless of interaction graph. For example, Hamming-distance costs  $E(x) = |x \oplus z_0|$  have  $M = n + 1$  levels, degeneracies  $d_k = \binom{n}{k}$ , and energies  $E_k = k$ . Then  $A_1 = (1/N) \sum_{k=1}^n \binom{n}{k} / k$  depends only on  $n$  and is trivial to compute.

The partition-function bridge is one-directional. Tractable  $Z$  implies tractable  $A_1$  (via the integral representations above), but exact  $A_1$  does not determine low-temperature  $Z(\beta)$ .

**Proposition 9.6.3** (Reverse bridge obstruction). *There exist two diagonal Hamiltonians  $H_z, H'_z$  on  $N = 2^n$  states with the same ground degeneracy ratio  $d_0/N$ , same minimum excitation  $\Delta_{\min}$ , and  $A_1(H_z) = A_1(H'_z)$  exactly, yet  $|Z_{H_z}(\beta) - Z_{H'_z}(\beta)|/N \geq 1/100$  at  $\beta = O(1/\Delta_{\min})$ .*

*Proof.* Fix an integer  $B \geq 3$ . Define two spectra with the same  $d_0/N = 1/2$  and  $\Delta_{\min} = 1/B$ . The first has  $N/8$  states at energy  $1/B$  and  $3N/8$  states at energy  $B$ . The second has  $N/16$  states at energy  $1/B$  and  $7N/16$

states at energy  $c_B = 7B/(B^2 + 6)$ . Direct computation gives the same value  $A_1 = (B^2 + 3)/(8B)$  for both. At  $\beta = B$ , however,

$$\frac{Z_1(B)}{N} = \frac{1}{2} + \frac{e^{-1}}{8} + \frac{3e^{-B^2}}{8}, \quad \frac{Z_2(B)}{N} = \frac{1}{2} + \frac{e^{-1}}{16} + \frac{7}{16}e^{-7B^2/(B^2+6)}.$$

Since  $7B^2/(B^2 + 6) \geq 4.2$  for  $B \geq 3$ , the difference is at least  $e^{-1}/16 - (7/16)e^{-4.2} > 1/100$ .  $\square$

Three natural conjectures about easy instances of  $A_1$  computation are all false.

**Proposition 9.6.4** (Unique solution does not imply easy  $A_1$ ). *There exist instances with  $d_0 = 1$  for which computing  $A_1$  is #P-hard.*

*Proof.* The proof of [Proposition 9.6.1](#) applies directly to satisfiable instances with  $d_0 = 1$ . The interpolation reduction recovers  $d_1, \dots, d_{M-1}$  from  $A_1$  evaluations, and counting assignments at each violation level remains #P-hard. Concretely, for a satisfiable 3-SAT instance with  $m$  clauses and a unique satisfying assignment, the clause-violation Hamiltonian  $H_z = \sum_j C_j$  has  $d_0 = 1$  and

$$A_1 = \sum_{k=1}^m \frac{d_k}{kN},$$

where  $d_k$  counts assignments that violate exactly  $k$  clauses. Recovering these counts from shifted  $A_1$  evaluations is therefore #P-hard.  $\square$

**Proposition 9.6.5** (Bounded degeneracy is vacuous). *If  $d_k \leq \text{poly}(n)$  for all excited levels  $k \geq 1$ , and  $M \leq \text{poly}(n)$ , then  $d_0 \geq N - \text{poly}(n)^2$ , and the optimization problem is trivially solvable by random sampling.*

*Proof.* The total state count satisfies  $\sum_{k=0}^{M-1} d_k = N = 2^n$ . If  $d_k \leq \text{poly}(n)$  for all  $k \geq 1$  and  $M \leq \text{poly}(n)$ , then  $\sum_{k \geq 1} d_k \leq (M-1) \cdot \text{poly}(n) \leq \text{poly}(n)^2$ , so  $d_0 \geq N - \text{poly}(n)^2$ . For  $n$  large enough,  $d_0/N \geq 1 - o(1)$ , and a random sample finds a ground state with probability  $1 - o(1)$ .  $\square$

**Proposition 9.6.6** (Hard optimization does not imply hard  $A_1$ ). *The tractability of  $A_1$  is independent of optimization hardness. 2-SAT is in P but #2-SAT is #P-complete [30], giving easy optimization with hard  $A_1$ . In the reverse direction, Grover search with a promised ground degeneracy  $d_0$  gives hard optimization but trivial  $A_1 = (N - d_0)/(N\Delta)$ , computable in O(1) from the promise.*

The tractability boundary for  $A_1$  is subtle. It does not align with optimization hardness, is not determined by the number of solutions, and depends on structural properties of the energy landscape (treewidth, partition function tractability) rather than on the difficulty of finding the ground state.

## 9.7 The Complexity Landscape

This section closes the complexity picture at the algorithmically relevant precision  $\varepsilon = 2^{-n/2}$ . The quantum query upper bound is  $O(2^{n/2} \cdot \text{poly}(n))$  ([Theorem 8.3.3](#)), the classical lower bound is  $\Omega(2^n)$  ([Theorem 8.3.4](#)), and polynomial-interpolation reductions cannot prove #P-hardness at this precision ([Theorem 8.3.2](#)). Taken together, these results show that the quantum bound is tight.

**Theorem 9.7.1** (Tight quantum query complexity at schedule precision). *At the schedule-relevant precision  $\varepsilon = \Theta(2^{-n/2})$ , the quantum query complexity of  $A_1$  estimation is  $\Theta(2^{n/2}) = \Theta(1/\varepsilon)$ . The lower bound is achieved on two-level instances with  $\Delta_1 = 1$ .*

*Proof.* For  $\varepsilon = \Theta(2^{-n/2})$  and  $\Delta_1 = 1$ , [Theorem 8.3.3](#) gives an upper bound  $O(\sqrt{N} + 1/\varepsilon) = O(2^{n/2})$ . For the lower bound, consider  $M = 2$  instances with  $\Delta_1 = 1$ : estimating  $A_1 = (N - d_0)/N$  to precision  $\varepsilon$  reduces to approximate counting. The Grover iterate  $G = (2|+\rangle\langle+| - I)(I - 2\Pi_S)$  has eigenphases  $\pm 2\theta$  with  $\sin^2 \theta = d_0/N$ . After  $T$  sequential applications of  $G$ , the probe state acquires phase  $T\phi$  where  $\phi = 2 \arcsin(\sqrt{d_0/N})$ , and the quantum Fisher information for estimating  $\phi$  from  $T$  sequential applications is  $F_Q = 4T^2$  (the standard Heisenberg limit for phase accumulation in sequential quantum metrology [41, 40]). The quantum Cramér-Rao bound gives  $\text{Var}(\hat{\phi}) \geq 1/F_Q = 1/(4T^2)$ . The adversary chooses  $d_0 = N/2$  so that  $\sin^2 \theta = 1/2$ , where  $|d(\sin^2 \theta)/d\theta| = |\sin 2\theta| = 1$ . Estimating  $A_1 = 1 - \sin^2 \theta$  to precision  $\varepsilon$  at this operating point requires estimating  $\theta$  to precision  $\varepsilon$ , hence  $1/(4T^2) \leq \varepsilon^2$ , giving  $T \geq 1/(2\varepsilon)$  applications of  $G$ , each costing  $O(1)$  oracle queries. With  $\varepsilon = \Theta(2^{-n/2})$ , this is  $\Omega(2^{n/2})$ , so the complexity is  $\Theta(2^{n/2}) = \Theta(1/\varepsilon)$ .  $\square$

The lower bound is worst-case in the unknown parameter  $d_0$ , and the adversary chooses  $d_0 = N/2$  because that point is maximally difficult to estimate. The Heisenberg limit  $F_Q = 4T^2$  for sequential unitary applications is a standard result in quantum metrology and applies to general quantum estimation, not only phase estimation. It follows from unitary dynamics together with the Cramér-Rao inequality, as shown by Braunstein and Caves [41] and extended to sequential settings by Giovannetti, Lloyd, and Maccone [40]. The same  $\Omega(1/\varepsilon)$  lower bound also follows from quantum approximate counting. Estimating  $d_0/N$  to additive precision  $\varepsilon$  requires  $\Omega(1/\varepsilon)$  quantum queries [38, 45], and for  $M = 2$  this is exactly the  $A_1$  estimation problem.

This theorem connects directly to the adaptive protocol of section 9.3. The adaptive strategy achieves  $T_{\text{adapt}} = O(T_{\text{inf}}) = O(2^{n/2})$ , which matches the tight complexity  $\Theta(2^{n/2})$  for estimating  $A_1$  at precision  $\delta_{A_1} = \Theta(2^{-n/2})$ . The match is structural rather than accidental. In both tasks, the algorithm must resolve  $\Omega(2^{n/2})$  alternatives while each quantum measurement reveals only  $O(1)$  information.

In the high-precision regime relevant to schedule placement, the quadratic quantum advantage persists.

**Proposition 9.7.2** (Precision phase diagram). *For two-level instances with  $\Delta_1 = 1$  and precision  $\varepsilon \leq c/\sqrt{N}$  (constant  $c$ ), the query complexity of  $A_1$  estimation is  $\Theta(1/\varepsilon)$  quantum and  $\Theta(1/\varepsilon^2)$  classical. The quantum-to-classical ratio is  $\Theta(1/\varepsilon)$  in this regime.*

*Proof.* In this regime,  $1/\varepsilon \geq \sqrt{N}/c$ , so the upper bound of Theorem 8.3.3 becomes  $O(\sqrt{N} + 1/\varepsilon) = O(1/\varepsilon)$ . The matching quantum lower bound is inherited from two-level approximate counting (Theorem 9.7.1). The classical lower bound  $\Omega(1/\varepsilon^2)$  follows from Theorem 8.3.4, and Monte Carlo sampling gives the matching upper bound  $O(1/\varepsilon^2)$ .  $\square$

**Theorem 9.7.3** (ETH computational complexity). *Under the Exponential Time Hypothesis (ETH), any classical algorithm computing  $A_1$  at precision  $2^{-n/2}$  requires  $2^{\Omega(n)}$  time.*

*Proof sketch.* The NP-hardness reduction (Theorem 8.1.2) maps 3-SAT on  $n_{\text{var}}$  variables to  $A_1$  estimation of a 3-local Hamiltonian on  $n = O(n_{\text{var}})$  qubits at precision  $1/\text{poly}(n)$ . By the Impagliazzo-Paturi-Zane sparsification lemma [46], 3-SAT on  $n_{\text{var}}$  variables can be reduced to instances with  $O(n_{\text{var}})$  clauses, giving  $n = O(n_{\text{var}})$  qubits. Any algorithm computing  $A_1$  at precision  $2^{-n/2}$  can, in particular, compute  $A_1$  at the coarser precision  $1/\text{poly}(n)$  (since  $2^{-n/2} < 1/\text{poly}(n)$  for large  $n$ ), and thus solves 3-SAT by the reduction. Under ETH, 3-SAT on  $n_{\text{var}} = \Omega(n)$  variables requires  $2^{\Omega(n_{\text{var}})} = 2^{\Omega(n)}$  time.  $\square$

Under ETH, the quadratic quantum advantage extends from the query model to the computational model.

**Corollary 9.7.4** (Quantum pre-computation cost). *Estimating  $A_1$  to the schedule-relevant precision  $\delta_{A_1} = \Theta(2^{-n/2})$  via quantum amplitude estimation costs  $\Theta(2^{n/2} \cdot \text{poly}(n))$  time, matching the adaptive protocol's runtime. The classical pre-computation cost at the same precision is  $\Omega(2^n)$ .*

From a parameterized-complexity viewpoint, the corollary places  $A_1$  estimation at precision  $2^{-n/2}$  in FBQTIME( $2^{n/2}$ ,  $\text{poly}(n)$ ). The problem is therefore not polynomial-time in the usual sense, but it does admit a quantum algorithm at the Grover scale. This also clarifies the information cost of fixed-schedule adiabatic optimization. Recovering the missing  $n/2$  bits of  $A_1$  costs  $\Theta(2^{n/2})$  quantum time, the same scale as Grover search and informed adiabatic evolution. The circuit model reaches that scale without a pre-computation step because amplitude amplification solves the search task directly.

The generic extrapolation barrier (Theorem 8.3.2) shows that interpolation failure at precision  $2^{-n/2}$  is not tied to one construction. For any polynomial extrapolation scheme with  $d = \text{poly}(n)$  nodes, the Lebesgue constant obeys  $\Lambda_d(x^*) \geq 2^{d-1}$  when the evaluation point sits at least  $b - a$  away from the sample interval  $[a, b]$ . This geometric condition must be verified in each setup; it does not follow only from  $x^* = \Theta(2^{-n/2})$  with nodes in  $[0, 1/\text{poly}(n)]$ . Once the condition holds, polynomial-interpolation reductions for  $A_1$  demand precision  $2^{-\Omega(n)}$ .

**Proposition 9.7.5** (Two-level worst-case reduction). *The two-level family ( $M = 2$ ) is a worst-case subclass for  $A_1$  estimation at schedule-relevant precision: any worst-case lower bound for approximate counting on this subclass applies to general  $A_1$  estimation.*

*Proof.* Worst-case complexity over all instances is at least the complexity on any subclass. Restricting to  $M = 2$  gives

$$A_1 = \frac{N - d_0}{N\Delta_1},$$

so for fixed  $\Delta_1 = 1$ , estimating  $A_1$  to additive precision  $\varepsilon$  is exactly approximate counting for  $d_0/N$  at precision  $\varepsilon$ . Therefore, any lower bound for approximate counting on this subclass is automatically a lower bound for general  $A_1$  estimation.  $\square$

The worst-case hardness of  $A_1$  estimation does not hide in complex spectra. Simple two-level instances, where  $A_1$  reduces to counting, already saturate the query lower bound. Algorithms exploiting the sum-of-reciprocals structure of  $A_1$  for multilevel spectra cannot beat algorithms for plain mean estimation.

At schedule-level precision, bounded-treewidth instances remain tractable for exact  $A_1$  computation ([Proposition 9.6.2](#)). Ferromagnetic Ising models also admit a polynomial-time FPRAS for  $Z(\beta)$  [[47](#)], which yields additive approximations for  $A_1$  at coarse precision through the integral formulas in [section 9.5](#). The difficulty appears at algorithmic precision  $\delta_{A_1} = \Theta(2^{-n/2})$ . Reaching this regime requires multiplicative accuracy  $\mu = O(2^{-n/2}/B)$  with  $B = O(\log(1/\delta_{A_1})/\Delta_{\min})$ , so the FPRAS runtime  $\text{poly}(1/\mu)$  becomes exponential. With  $B = O(n/\Delta_{\min})$ , one gets  $\text{poly}(1/\mu) = 2^{\Omega(n)}$ . Thus ferromagnetic-Ising tractability does not survive at the schedule-relevant precision.

The interpolation theorem ([Theorem 9.2.2](#)) gives a quantitative law relating information to runtime. We state it in a communication picture. Alice has the full classical description of  $H_z$  (all eigenvalues and degeneracies), Bob has a quantum computer with oracle access to  $H_z$ , and Alice may send  $C$  classical bits to Bob. Bob must find a ground state in at most  $T$  queries. In the circuit-oracle model, Bob needs no message from Alice and still achieves  $T = O(\sqrt{N/d_0})$  by running Dürr-Høyer. In the fixed-schedule adiabatic model, Bob must match the schedule to the crossing and therefore needs  $s^*$  to precision  $\Delta_* = O(2^{-n/2})$ , which costs  $C = \Theta(n)$  bits. Each additional bit of  $A_1$  precision cuts the adiabatic runtime by a factor of two, until about  $n/2$  bits are enough for optimal scaling. Formally, if Alice sends  $C$  bits that encode  $A_1$  to precision  $\varepsilon = \Theta(2^{-C})$ , then

$$T(C) = T_{\inf} \cdot \Theta(\max(1, 2^{n/2-C})).$$

**Theorem 9.7.6** (Bit-runtime information law). *The classical communication cost for the adiabatic model to achieve target runtime  $T$  is  $C^*(T) = \max(0, n/2 - \log_2(T/T_{\inf}))$  bits, while  $C_{\text{circuit}}^*(T) = 0$  for all  $T \geq T_{\inf}$ .*

*Proof.* Inverting  $T(C) = T_{\inf} \cdot 2^{n/2-C}$  gives  $C = n/2 - \log_2(T/T_{\inf})$ . Clamping  $C \geq 0$  and noting that the circuit model achieves  $T = T_{\inf}$  at  $C = 0$  by the Dürr-Høyer algorithm gives both formulas.  $\square$

The complete model comparison, synthesizing this chapter with Chapter 8, is given below.

Model	Info needed	Runtime	Communication
Circuit (Dürr-Høyer)	None	$\Theta(\sqrt{N/d_0})$	0 bits
Fixed AQO, informed	$A_1$ to $2^{-n/2}$	$O(\sqrt{N/d_0})$	$\Theta(n)$ bits
Fixed AQO, $C$ bits	$A_1$ to $2^{-C}$	$T_{\inf} \cdot 2^{n/2-C}$	$C$ bits
Fixed AQO, uninformed	None	$\Omega(N/\sqrt{d_0})$	0 bits
Adaptive AQO	$O(n)$ measurements	$O(\sqrt{N/d_0})$	0 bits
Constant-control, two-level	None	$\Theta(\sqrt{N/d_0})$	0 bits
Quantum $A_1$ estimation	$\varepsilon = 2^{-n/2}$	$\Theta(2^{n/2})$ queries	—
Classical $A_1$ estimation	$\varepsilon = 2^{-n/2}$	$\Theta(2^n)$ queries	—

The circuit model and the adaptive adiabatic model both achieve optimal performance with zero classical communication. In contrast, the fixed adiabatic model follows a bit-runtime tradeoff in which each missing bit doubles the runtime. The resulting  $\Theta(n)$ -bit separation from the circuit model is exactly the information content of  $A_1$  at schedule-relevant precision. This communication cost reflects the computational model rather than the underlying search task.

The running example makes the tradeoff concrete. With  $N = 4$ ,  $d_0 = 1$ , and  $n = 2$ , the circuit model uses  $O(2)$  queries at  $C = 0$ . The informed adiabatic model also uses  $O(2)$  queries, but only after receiving  $C = 1$  bit. Without that bit, the fixed adiabatic model requires  $\Omega(4)$  queries. The single missing bit explains the factor-of-two slowdown.

The term “information gap” now has three precise meanings. First is spectral: inside the adiabatic framework,  $g_{\min}$  sets the timescale  $T = O(1/g_{\min})$ , and the full profile  $g(s)$  constrains which schedules are valid. Second is epistemic: if crossing location is unknown, runtime pays the factor  $(s_R - s_L)/\Delta_*$ . If  $A_1$  is known to precision  $\varepsilon$ , the overhead becomes  $\Theta(\max(1, \varepsilon/\delta_{A_1}))$ ; with  $O(n)$  quantum measurements, this overhead disappears. Third is model-dependent: circuit algorithms neither need nor expose  $A_1$ , fixed-schedule adiabatic algorithms require it and face NP-hard recovery, while adaptive adiabatic algorithms can acquire it at polynomial cost.

This gives a five-level taxonomy of ignorance, measured by the multiplicative overhead  $T/T_{\inf}$ . Level 0 (no information) gives  $\Omega(2^{n/2})$ . Level 1 (precision  $\varepsilon$ ) gives  $\Theta(\max(1, \varepsilon/\delta_{A_1}))$ . Level 2 (known interval  $[u_L, u_R]$ ) gives constant overhead proportional to  $u_R - u_L$ . Level 3 (quantum measurement access) gives  $O(1)$  overhead with  $O(n)$  measurements. Level 4 (circuit model) has overhead 1 with no spectral information.

The adiabatic approach to unstructured search therefore works, reaches Grover scaling, and is optimal within its schedule class. Its information requirements are a structural consequence of the rank-one interpolation path.

They are not a fundamental limit of quantum computation itself, only a limit of this specific model. The next chapter translates these claims into machine-checked formal proofs.

## Chapter 10

# Formalization

## Chapter 11

# Conclusion

# Bibliography

- [1] Lov K. Grover. A fast quantum mechanical algorithm for database search. In *Proceedings of the 28th Annual ACM Symposium on Theory of Computing*, pages 212–219, 1996. doi:[10.1145/237814.237866](https://doi.org/10.1145/237814.237866).
- [2] Michel Boyer, Gilles Brassard, Peter Høyer, and Alain Tapp. Tight bounds on quantum searching. *Fortschritte der Physik*, 46(4-5):493–505, 1998. doi:[10.1002/\(SICI\)1521-3978\(199806\)46:4/5<493::AID-PROP493>3.0.CO;2-P](https://doi.org/10.1002/(SICI)1521-3978(199806)46:4/5<493::AID-PROP493>3.0.CO;2-P).
- [3] Dorit Aharonov, Wim van Dam, Julia Kempe, Zeph Landau, Seth Lloyd, and Oded Regev. Adiabatic quantum computation is equivalent to standard quantum computation. *SIAM Journal on Computing*, 37(1):166–194, 2007. doi:[10.1137/S0097539705447323](https://doi.org/10.1137/S0097539705447323).
- [4] Jeremie Roland and Nicolas J. Cerf. Quantum search by local adiabatic evolution. *Physical Review A*, 65(4):042308, 2002. doi:[10.1103/PhysRevA.65.042308](https://doi.org/10.1103/PhysRevA.65.042308).
- [5] Edward Farhi, Jeffrey Goldstone, Sam Gutmann, and Daniel Nagaj. How to make the quantum adiabatic algorithm fail. *International Journal of Quantum Information*, 6(03):503–516, 2008. doi:[10.1142/S021974990800358X](https://doi.org/10.1142/S021974990800358X).
- [6] Charles H. Bennett, Ethan Bernstein, Gilles Brassard, and Umesh Vazirani. Strengths and weaknesses of quantum computing. *SIAM Journal on Computing*, 26(5):1510–1523, 1997. doi:[10.1137/S0097539796300933](https://doi.org/10.1137/S0097539796300933).
- [7] Marko Žnidarič and Martin Horvat. Exponential complexity of an adiabatic algorithm for an NP-complete problem. *Physical Review A*, 73:022329, 2006. doi:[10.1103/PhysRevA.73.022329](https://doi.org/10.1103/PhysRevA.73.022329).
- [8] Itay Hen. Continuous-time quantum algorithms for unstructured problems. *Journal of Physics A: Mathematical and Theoretical*, 47(4):045305, 2014. doi:[10.1088/1751-8113/47/4/045305](https://doi.org/10.1088/1751-8113/47/4/045305).
- [9] F. Barahona. On the computational complexity of Ising spin glass models. *Journal of Physics A: Mathematical and General*, 15(10):3241, 1982. doi:[10.1088/0305-4470/15/10/028](https://doi.org/10.1088/0305-4470/15/10/028).
- [10] Andrew Lucas. Ising formulations of many NP problems. *Frontiers in Physics*, 2:5, 2014. doi:[10.3389/fphy.2014.00005](https://doi.org/10.3389/fphy.2014.00005).
- [11] Tameem Albash and Daniel A. Lidar. Adiabatic quantum computation. *Reviews of Modern Physics*, 90:015002, 2018. doi:[10.1103/RevModPhys.90.015002](https://doi.org/10.1103/RevModPhys.90.015002).
- [12] Arthur Braida. *Analog Quantum Computing for NP-Hard Combinatorial Graph Problems*. PhD thesis, Université d’Orléans, 2024.
- [13] Vicky Choi. Different adiabatic quantum optimization algorithms for the NP-complete exact cover and 3SAT problems. *Quantum Information and Computation*, 11(7–8):638–648, 2011.
- [14] Boris Altshuler, Hari Krovi, and Jérémie Roland. Anderson localization makes adiabatic quantum optimization fail. *Proceedings of the National Academy of Sciences*, 107(28):12446–12450, 2010. doi:[10.1073/pnas.1002116107](https://doi.org/10.1073/pnas.1002116107).
- [15] Arthur Braida, Shantanav Chakraborty, Leonardo Novo, and Jérémie Roland. Unstructured adiabatic quantum optimization: Optimality with limitations. *arXiv preprint arXiv:2411.05736*, 2024.
- [16] Gene H. Golub. Some modified matrix eigenvalue problems. *SIAM Review*, 15(2):318–334, 1973. doi:[10.1137/1015032](https://doi.org/10.1137/1015032).

- [17] Shantanav Chakraborty, Leonardo Novo, and Jérémie Roland. Optimality of spatial search via continuous-time quantum walks. *Physical Review A*, 102:032214, 2020. doi:[10.1103/PhysRevA.102.032214](https://doi.org/10.1103/PhysRevA.102.032214).
- [18] Jack Sherman and Winifred J. Morrison. Adjustment of an inverse matrix corresponding to a change in one element of a given matrix. *The Annals of Mathematical Statistics*, 21(1):124–127, 1950. doi:[10.1214/aoms/1177729893](https://doi.org/10.1214/aoms/1177729893).
- [19] W. van Dam, M. Mosca, and U. Vazirani. How powerful is adiabatic quantum computation? In *Proceedings 42nd IEEE Symposium on Foundations of Computer Science*, pages 279–287, 2001. doi:[10.1109/SFCS.2001.959902](https://doi.org/10.1109/SFCS.2001.959902).
- [20] Tosio Kato. On the adiabatic theorem of quantum mechanics. *Journal of the Physical Society of Japan*, 5(6):435, 1950.
- [21] Andrew M. Childs and Jeffrey Goldstone. Spatial search by quantum walk. *Physical Review A*, 70:022314, 2004. doi:[10.1103/PhysRevA.70.022314](https://doi.org/10.1103/PhysRevA.70.022314).
- [22] Shantanav Chakraborty, Leonardo Novo, Andris Ambainis, and Yasser Omar. Spatial search by quantum walk is optimal for almost all graphs. *Physical Review Letters*, 116:100501, 2016. doi:[10.1103/PhysRevLett.116.100501](https://doi.org/10.1103/PhysRevLett.116.100501).
- [23] Sabine Jansen, Mary-Beth Ruskai, and Ruedi Seiler. Bounds for the adiabatic approximation with applications to quantum computation. *Journal of Mathematical Physics*, 48(10):102111, 2007. doi:[10.1063/1.2798382](https://doi.org/10.1063/1.2798382).
- [24] Sergio Boixo, Emanuel Knill, and Rolando Somma. Eigenpath traversal by phase randomization. *Quantum Information and Computation*, 9(9):833–855, 2009.
- [25] Joseph Cunningham and Jérémie Roland. Eigenpath traversal by Poisson-distributed phase randomisation. In *19th Conference on the Theory of Quantum Computation, Communication and Cryptography (TQC 2024)*, pages 7:1–7:20, 2024. doi:[10.4230/LIPIcs.TQC.2024.7](https://doi.org/10.4230/LIPIcs.TQC.2024.7).
- [26] Alexander Elgart and George A. Hagedorn. A note on the switching adiabatic theorem. *Journal of Mathematical Physics*, 53(10), 2012. doi:[10.1063/1.4748968](https://doi.org/10.1063/1.4748968).
- [27] Xi Guo and Dong An. Improved gap dependence in adiabatic state preparation by adaptive schedule. *arXiv preprint arXiv:2512.10329*, 2025.
- [28] Julia Kempe, Alexei Kitaev, and Oded Regev. The complexity of the local Hamiltonian problem. *SIAM Journal on Computing*, 35(5):1070–1097, 2006. doi:[10.1137/S0097539704445226](https://doi.org/10.1137/S0097539704445226).
- [29] M.R. Garey, D.S. Johnson, and L. Stockmeyer. Some simplified NP-complete graph problems. *Theoretical Computer Science*, 1(3):237–267, 1976. doi:[10.1016/0304-3975\(76\)90059-1](https://doi.org/10.1016/0304-3975(76)90059-1).
- [30] Leslie G. Valiant. The complexity of enumeration and reliability problems. *SIAM Journal on Computing*, 8(3):410–421, 1979. doi:[10.1137/0208032](https://doi.org/10.1137/0208032).
- [31] George M. Phillips. *Interpolation and Approximation by Polynomials*, volume 14. Springer Science & Business Media, 2003. doi:[10.1007/b97417](https://doi.org/10.1007/b97417).
- [32] Ramis Movassagh. The hardness of random quantum circuits. *Nature Physics*, 19(11):1719–1724, 2023. doi:[10.1038/s41567-023-02131-2](https://doi.org/10.1038/s41567-023-02131-2).
- [33] Ramamohan Paturi. On the degree of polynomials that approximate symmetric Boolean functions. In *Proceedings of the 24th Annual ACM Symposium on Theory of Computing*, pages 468–474, 1992. doi:[10.1145/129712.129758](https://doi.org/10.1145/129712.129758).
- [34] Scott Aaronson and Alex Arkhipov. The computational complexity of linear optics. In *Proceedings of the 43rd Annual ACM Symposium on Theory of Computing*, pages 333–342, 2011. doi:[10.1145/1993636.1993682](https://doi.org/10.1145/1993636.1993682).
- [35] Michael J. Bremner, Ashley Montanaro, and Dan J. Shepherd. Achieving quantum supremacy with sparse and noisy commuting quantum computations. *Quantum*, 1:8, 2017. doi:[10.22331/q-2017-04-25-8](https://doi.org/10.22331/q-2017-04-25-8).

- [36] Adam Bouland, Bill Fefferman, Chinmay Nirkhe, and Umesh Vazirani. On the complexity and verification of quantum random circuit sampling. *Nature Physics*, 15(2):159–163, 2019. doi:[10.1038/s41567-018-0318-2](https://doi.org/10.1038/s41567-018-0318-2).
- [37] Christoph Dürr and Peter Høyer. A quantum algorithm for finding the minimum. *arXiv preprint quant-ph/9607014*, 1996.
- [38] Gilles Brassard, Peter Høyer, Michele Mosca, and Alain Tapp. Quantum amplitude amplification and estimation. *Contemporary Mathematics*, 305:53–74, 2002. doi:[10.1090/conm/305/05215](https://doi.org/10.1090/conm/305/05215).
- [39] Lucien Le Cam. Convergence of estimates under dimensionality restrictions. *The Annals of Statistics*, 1(1):38–53, 1973. doi:[10.1214/aos/1176342150](https://doi.org/10.1214/aos/1176342150).
- [40] Vittorio Giovannetti, Seth Lloyd, and Lorenzo Maccone. Quantum metrology. *Physical Review Letters*, 96:010401, 2006. doi:[10.1103/PhysRevLett.96.010401](https://doi.org/10.1103/PhysRevLett.96.010401).
- [41] Samuel L. Braunstein and Carlton M. Caves. Statistical distance and the geometry of quantum states. *Physical Review Letters*, 72(22):3439–3443, 1994. doi:[10.1103/PhysRevLett.72.3439](https://doi.org/10.1103/PhysRevLett.72.3439).
- [42] Mancheon Han, Hyowon Park, and Sangkook Choi. The constant speed schedule for adiabatic state preparation: Towards quadratic speedup without prior spectral knowledge, 2025.
- [43] Eduardo Araújo, Shantanav Chakraborty, and Leonardo Novo. Advantages and limitations of analog quantum search methods. *In preparation*, 2025.
- [44] Edward Farhi and Sam Gutmann. Analog analogue of a digital quantum computation. *Physical Review A*, 57(4):2403–2406, 1998. doi:[10.1103/PhysRevA.57.2403](https://doi.org/10.1103/PhysRevA.57.2403).
- [45] Ashwin Nayak and Felix Wu. The quantum query complexity of approximating the median and related statistics. In *Proceedings of the 31st Annual ACM Symposium on Theory of Computing (STOC)*, pages 384–393, 1999. doi:[10.1145/301250.301349](https://doi.org/10.1145/301250.301349).
- [46] Russell Impagliazzo, Ramamohan Paturi, and Francis Zane. Which problems have strongly exponential complexity? *Journal of Computer and System Sciences*, 63(4):512–530, 2001. doi:[10.1006/jcss.2001.1774](https://doi.org/10.1006/jcss.2001.1774).
- [47] Mark Jerrum and Alistair Sinclair. Polynomial-time approximation algorithms for the ising model. *SIAM Journal on Computing*, 22(5):1087–1116, 1993.